UNIVERSIDADE DE LISBOA

FACULDADE DE CIÊNCIAS

DEPARTAMENTO DE QUÍMICA E BIOQUÍMICA

Calcium signalling modulation in astrocytes by adenosine receptors

Andreia Marisa Cruz e Silva

Mestrado em Bioquímica

Área de especialização em Bioquímica Médica

2011

UNIVERSIDADE DE LISBOA

FACULDADE DE CIÊNCIAS

DEPARTAMENTO DE QUÍMICA E BIOQUÍMICA

Calcium signalling modulation in astrocytes by adenosine receptors

Andreia Marisa Cruz e Silva

Tese de mestrado orientada por:

Professora Doutora Ana M. Sebastião

Doutor Pedro A. Lima

Mestrado em Bioquímica

Área de especialização em Bioquímica Médica

2011

O trabalho experimental descrito nesta tese foi realizado no Instituto de Farmacologia e Neurociências, Faculdade de Medicina de Lisboa e Unidade de Neurociências, Instituto de Medicina Molecular.

Resumo

O modelo de sinapse actualmente aceite considera que para o processo de comunicação neuronal contribuem não só os neurónios pré- e pós-sináptico mas também um elemento peri-sináptico, os astrócitos. Estes constituem a população de células mais abundante no cérebro, formando juntamente com a micróglia e os oligodendrócitos a rede de células da glia. Presentemente, sabe-se que os astrócitos não são meros elementos passivos, comunicando activamente com as outras células através do seu mecanismo de excitabilidade que usa iões de cálcio (Ca^{2+}) como mensageiro interno para desencadear a gliotransmissão. Este fenómeno é despoletado pela activação de receptores membranares e consiste na libertação de gliotransmissores (GT) como o glutamato, ATP e D-serina. A libertação de GT parece exercer uma função com características em certa medida semelhantes à libertação de neurotransmissores (NT) pelos neurónios.

Esta conversa dinâmica e bidireccional entre neurónios e astrócitos depende da libertação de NT e GT que são reconhecidos por ambos os tipos de células. Desta forma, a libertação de NT do terminal pré-sináptico afecta o terminal pós-sináptico mas também os astrócitos envolventes, induzindo um aumento nos seus níveis intracelulares de Ca^{2+} $[Ca^{2+}]_i$. Em resposta, os astrócitos libertam GT, por um mecanismo não complemente elucidado, afectando novamente o terminal pós-sináptico e ainda a libertação de NT do terminal pré-sináptico. Através destes mecanismos, os astrócitos modulam a excitabilidade neuronal e a transmissão sináptica, havendo evidências de que também modulam fenómenos como a potenciação de longa duração que está intimamente ligada à memória e aprendizagem.

As purinas, nomeadamente o ATP e a adenosina, modulam a gliotransmissão, regulando a transmissão sináptica e a comunicação neurónio-astrócito. O ATP desencadeia a sinalização por Ca^{2+}, sendo um dos agentes dos primeiros eventos no processo de gliotransmissão em astrócitos. O aumento da $[Ca^{2+}]_i$ mediado pelo ATP deve-se à activação de receptores metabotrópicos (P2YR), que levam à libertação de Ca^{2+} dos compartimentos intracelulares via fosfolipase C (PLC) e inositol (1,4,5)-trifosfato (IP_3), e de

receptores ionotrópicos (P2XR), que medeiam a entrada directa de Ca^{2+} do exterior da célula.

O ATP é convertido extracelularmente em adenosina e ambas as purinas se acumulam simultânea ou sequencialmente, estando os seus níveis aumentados em situações patológicas. Os receptores para o ATP (metabotrópicos P2YR e ionotrópicos P2XR) e para a adenosina (metabotrópicos A_1R, $A_{2A}R$, $A_{2B}R$ e A_3R) são coexpressos nos astrócitos, o que sugere uma possível interacção entre estas duas famílias de receptores. Da família dos receptores de ATP, o $P2Y_1R$ exerce um papel preponderante no desencadear da gliotransmissão. Sabe-se que a adenosina modula a sinalização de Ca^{2+} desencadeada por neurotransmissores e neuromoduladores como o glutamato e ATP, no entanto, não se compreende completamente quais os receptores de adenosina envolvidos neste processo. É de salientar ainda que os receptores A_1 estão negativamente acoplados ao AMP cíclico (cAMP) através de uma proteína G_i inibitória, diminuindo a libertação de GT. Os receptores A_{2A} estão positivamente acoplados ao cAMP através de uma proteína G_s estimuladora, potenciando a libertação de GT.

Estudos anteriores mostram que a adenosina modula diferencialmente a internalização de GABA em astrócitos corticais através dos seus receptores membranares de alta afinidade A_1 e A_{2A}. É de salientar que esta modulação depende da cooperação entre os receptores A_1 e A_{2A}.

O principal objectivo deste trabalho é avaliar o papel dos receptores de adenosina, em particular do A_{2A}, na modulação da sinalização por Ca^{2+}. Pretende-se também explorar a possível cooperação entre os receptores A_1 e A_{2A} de adenosina no efeito modulatório.

As respostas de Ca^{2+} em astrócitos corticais primários foram estudas pela técnica de imagiologia de Ca^{2+}, usando um microscópio invertido de epifluorescência. O fluoróforo escolhido foi o Fura-2AM que é altamente sensível ao Ca^{2+}, ligando este ião de forma estável e reversível. Trata-se de um fluorocromo raciométrico, uma vez, que sofre um desvio no comprimento de onda do pico de absorvência quando ligado ao Ca^{2+}, de 380 (F380) para 340 (F340) nm. O rácio F340/F380 é usado para avaliar as variações da $[Ca^{2+}]_i$. A internalização do fluoróforo processa-se durante 45 minutos a 37^{o}C e ocorre de forma

passiva devido aos grupos AM que atribuem carga global negativa. Já dentro da célula, os grupos AM são clivados por enzimas e o fluoróforo fica retido no interior da célula.

As células foram local e brevemente (0,2 segundos) estimuladas com 10 μM ATP, a 22 ^{o}C, e a amplitude das respostas foi medida na presença de diferentes fármacos. Foi usado um análogo estável da adenosina, 2-cloroadenosina (CADO), um agonista e um antagonista selectivos para o receptor A_{2A}, CGS 21680 e SCH 58261, respectivamente, e um antagonista selectivo para o receptor A_1, DPCPX. No protocolo desenvolvido e optimizado no decurso do projecto, as células foram estimuladas de 5 em 5 minutos e obteve-se respostas para a situação controlo, apenas com tampão HEPES no meio, de seguida na presença do fármaco, que é mantido no meio de perfusão no mínimo durante 15-20 minutos, seguindo-se finalmente a lavagem com tampão HEPES ou com uma mistura de agonista/antagonista do receptor. Como controlo interno, foi ainda obtida a resposta máxima da célula a um estímulo supramáximo, 100 μM ATP.

O desenvolvimento deste protocolo dependeu da optimização de uma serie de parâmetros como o período de intervalo entre estimulações, a concentração de ATP usada como estimulo, a duração de cada estimulação, a temperatura da incubação com o fluoróforo e a temperatura de perfusão usada durante toda o registo de sinais de Ca^{2+}.

As culturas primárias foram caracterizadas quanto às populações de células presentes, astrócitos, neurónios e micróglia, pela técnica de imunocitoquímica, recorrendo a anticorpos que marcam especificamente estas células. Detectou-se ainda a presença dos receptores de ATP, $P2Y_1$, e de adenosina, A_1 e A_{2A}, pela técnica de western blot, aplicando anticorpos específicos para estas proteínas.

Observei que a estimulação breve com 10 μM ATP (0,2 segundos) induz um transiente de Ca^{2+} rápido. A estimulação prolongada (≥ 20 segundos) com ATP induz uma resposta de Ca^{2+} bifásica, constituída por um pico inicial, seguindo-se um patamar na resposta. Segundo outros autores, o pico inicial é mediado por receptores P2Y e o patamar por receptores P2X. O envolvimento dos receptores P2Y no pico inicial foi comprovado na presença de baixa concentração de Ca^{2+} extracelular.

O análogo estável da adenosina que apresenta afinidade semelhante para os receptores A_1 e A_{2A}, 1 μM CADO, potenciou marcadamente a resposta de Ca^{2+} desencadeada pelo ATP (aumento da resposta: 3,19 ± 0,30 vezes, n=72 células). O agonista selectivo para o receptor A_{2A}, 30nM CGS 21680, imitou este efeito (2,92 ± 0,32 vezes, n=80 células). Estes efeitos foram completamente revertidos após remoção do agonista do meio de perfusão. O parâmetro 'aumento da resposta' é o rácio entre a amplitude da resposta ao ATP na presença do fármaco e a amplitude da resposta na ausência de fármaco. Foi ainda calculado o parâmetro 'resposta controlo/resposta máxima', tendo observado uma relação inversa entre os valores de aumento de resposta e resposta controlo/resposta máxima. Desta forma, as células que apresentam uma menor resposta controlo em relação à resposta máxima, determinada na presença de 100 μM ATP, sofrem um aumento mais elevado induzido pelos agonistas, CADO e CGS 21680. Tal variabilidade de respostas mostra que estamos perante uma população de células heterogéneas.

Para estudar a possível cooperação e/ou interacção entre os receptores A_1 e A_{2A}, foram usados antagonistas específicos para estes receptores de forma a testar se revertiam a potenciação induzida pelos agonistas. Verifiquei que os antagonistas, 50 nM SCH 58261 e 50 nM DPCPX, por si só, não induziam variação apreciável na resposta de Ca^{2+}. Surpreendentemente, a potenciação induzida pelo CADO (agonista não-selectivo A_1 e A_{2A}) e pelo CGS 21680 (agonista selectivo A_{2A}) foi completamente revertida não só pelo antagonista específico do receptor A_{2A}, SCH 58261, mas também pelo antagonista específico do receptor A_1, DPCPX. Tais resultados mostram que a activação de ambos os receptores, A_1 e A_{2A}, é fundamental para que o efeito modulatório se verifique, sugerindo a cooperação entre estes receptores.

A caracterização das culturas primárias pela técnica de imunocitoquímica mostrou que estas são constituídas maioritariamente por astrócitos (> 90%) e alguma micróglia. Desta forma, pode-se afirmar que estamos perante culturas primárias enriquecidas em astrócitos. A introdução de um passo extra de agitação ao dia 6 de cultura, antes de replaquear as células, permite obter culturas com uma maior percentagem de astrócitos (> 95%) em relação à micróglia.

Recorrendo à técnica de western blot foi possível detectar a presença dos receptores de ATP, $P2Y_1$, e de adenosina, A_1 na cultura enriquecida em astrócitos. No entanto, usando esta técnica, não foi possível detectar os receptores A_{2A} de adenosina. Uma vez, que a presença de receptores A_{2A} já foi observada anteriormente em astrócitos corticais e que pela técnica de imagiologia de Ca^{2+}, aqui aplicada, foram obtidas respostas a fármacos específicos para estes receptores, pode-se afirmar que estes receptores estão presentes nas culturas primárias usadas neste estudo. Provavelmente a sua densidade será baixa e desta forma difícil de quantificar por western blot.

Os resultados aqui apresentados permitem concluir que a adenosina, através da activação de receptores A_{2A}, facilita a sinalização por Ca^{2+} induzida pelo ATP, em astrócitos corticais. Mais ainda, a cooperação entre os receptores A_1 e A_{2A}, parece ser essencial para a modulação observada.

O envolvimento de receptores A_{2A} na modulação da sinalização de Ca^{2+} aqui demonstrado contrapõe resultados anteriores nos quais outros autores mostraram que estes receptores não tinham qualquer efeito sobre a modulação das respostas de Ca^{2+}. Esses autores mostraram ainda que os receptores A_{2B} de adenosina medeiam a modulação da sinalização por Ca^{2+}. No entanto, no trabalho anterior foram usadas concentrações de fármacos não selectivas para os receptores correspondentes, o que poderá justificar as diferenças nos resultados obtidos.

Os resultados aqui apresentados estão de acordo com o modelo tetramérico - A_1-A_1-A_{2A}-A_{2A} - de receptores de adenosina proposto para a modulação diferencial da internalização de GABA pela adenosina, em astrócitos corticais. Os resultados aqui obtidos apoiam um cenário semelhante para a modulação da sinalização de Ca^{2+} pela adenosina com possíveis implicações na libertação de GT. Trata-se por isso de um novo mecanismo de modulação sináptica indirecto que é provavelmente mediado pela cooperação dos receptores A_1 e A_{2A} de adenosina, permitindo uma regulação apertada e uma transição suave entre os estados inibitório e potenciador.

Abstract

Purines, namely ATP and adenosine, modulate gliotransmission, regulating synaptic transmission and ultimately neuron-astrocyte communication. ATP triggers the signalling of free calcium ions (Ca^{2+}), which is the substrate for gliotransmission, in astrocytes. ATP is extracellularly converted into adenosine and both purines can be accumulated simultaneously or sequentially, acting on a plethora of membrane astrocytic receptors. Adenosine modulates GABA uptake in cortical astrocytes through A_1 (A_1R) and A_{2A} ($A_{2A}R$) receptors. Most importantly, this modulation is dependent on tight A_1R-$A_{2A}R$ cooperation. Therefore, the aim of this project was to evaluate the role of adenosine receptors, mainly $A_{2A}R$, in Ca^{2+} signalling modulation and also to explore the possible cross-talk between A_1R and $A_{2A}R$ in this modulation.

Ca^{2+} responses of cortical primary astrocytes were studied by Ca^{2+} imaging technique using Fura-2AM, at 22^{o}C. Cells were locally and briefly (0.2 seconds) stimulated with 10μM ATP and the amplitude of fluorescence signals was measured in the presence of different drugs. Cultures were further characterized by immunocytochemistry and western blot techniques.

A stable adenosine analogue, 2-Chloroadenosine (1 μM), markedly enhanced ATP-induced Ca^{2+} responses (fold increase: 3.19 ± 0.30, n=72 cells). An $A_{2A}R$ selective agonist, CGS 21680 (30nM), mimicked this effect (2.92 ± 0.32, n=80 cells). The potentiation mediated by both agonists was not only completely reverted by an $A_{2A}R$ selective antagonist, SCH 58261 (50nM), but also by an A_1R selective antagonist, DPCPX (50nM).

Primary enriched astrocytic cultures are constituted mainly by astrocytes (> 90%) and microglial cells. The presence of ATP, $P2Y_1R$, and adenosine, A_1R, but not $A_{2A}R$ could be demonstrated for primary astrocytic cultures. Nevertheless, selective agonists and antagonist used in Ca^{2+} imaging have proven the presence of functional $A_{2A}R$.

It is concluded that adenosine, through $A_{2A}R$ activation, potentiates ATP-induced Ca^{2+} signalling in astrocytes. Furthermore, A_1R-$A_{2A}R$ cooperation seems to be required for this modulation.

Index

Abbreviation List

A_1R A_1 adenosine receptor

$A_{2A}R$ A_{2A} adenosine receptor

AC adenylate cyclase

ADO adenosine

ADOR adenosine receptors

ADA adenosine deaminase

ADP adenosine 5'-diphosphate

AMP adenosine 5'-monophosphate

AMPAR 2-amino-3-(5-methyl-3-oxo-1,2- oxazol-4-yl)propanoic acid receptor

ATP adenosine 5'-triphosphate

BAPTA 1,2-bis(o-aminophenoxy)ethane-N,N,N',N'-tetraacetic acid

Ca^{2+} free calcium ion

$[Ca^{2+}]_i$ intracellular free calcium ion concentration

CADO 2-chloro-adenosine

cAMP cyclic adenosine 5'-monophosphate

CGS 21680 4-[2-[[6-amino-9-(N-ethyl-β-Dribofuranuronamidosyl)-9H-purinyl]amino]ethyl]benzenepropanoic acid hydrochloride

DIC days in culture

DMEM Dulbecco's Modified Eagle's Medium

DPCPX 8-cyclopentyl-1,3-dipropylxanthine

EGTA ethyleneglycol bis(β-aminoethylester)-N,N,N',N'-tetraacetate

F340 fluorescence at 340 nm

F380 fluorescence at 380 nm

F340/F380 fluorescence ratio at 340 nm over 380 nm

FBS Fetal Bovine Serum

Frest resting fluorescence

Fmax maximal fluorescence

Fmin minimum fluorescence

Fura-2AM Fura-2 acetoxymethyl Ester

Fzero zero fluorescence (autofluorescence)

GT gliotransmitter

IP_3 inositol triphosphate

Kd dissociation constant

NMDAR *N*-methyl *D*-aspartate receptor

NT neurotransmitter

LTP long-term potentiation

LTD long-term depression

P2YR P2Y (ATP) receptor

P2XR P2X (ATP) receptor

PBS phosphate buffered saline

PFA paraformaldehyde

PKA protein kinase A

PKC protein kinase C

PLC phospholipase C

RT room temperature (22^{o}C)

SCH 58261 (2-(2-furanyl)-7-(2-phenylethyl)-7H-pyrazolo[4,3-e][1,2,4]triazolo[1,5-c]pyrimidin-5-amine

1 Introduction

1.1 Astrocytes

More than 150 years ago, in 1856, Rudolf Virchow introduced the concept of neuroglia as connective material that supports the true nerve cells, neurons (Kettenmann & Verkhratsky, 2008). The word glia, Greek for 'glue', was used to designate cells that bring neurons together. This idea persisted throughout the 20th century, as astrocytes were shown to be electrically nonexcitable, in contrast to neurons. This paradigm has only begun to change in the last two decades with the emerging of calcium imaging techniques and the discovery of astrocytic calcium ion (Ca^{2+}) excitable mechanism (Agulhon *et al.*, 2008).

The word astrocyte was introduced in 1893, by Michael von Lenhossek, to designate glial cells with a stellate morphology (reviewed by Matyash & Kettenmann (2010)). Prior to that there was no differentiation between astrocytes, microglial cells and oligodendrocytes, which constitute the glial cell family.

Astrocytes are the most abundant cell population in the brain and currently they are no longer seen as mere supportive elements. Throughout the years different roles were proposed for astrocytes. Camillo Golgi suggested that astrocytes provide metabolic support to neurons. Followed by the acknowledgement that astrocytes control blood flow, homeostasis of the extracellular milieu and synaptogenesis (Kettenmann & Ransom, 2005). Very recently, astrocytes were recognized as active elements in cell communication, which are intimately involved in control of brain function. Glial regulation of neuronal communication had already been proposed by Carl Ludwig Schleich, in 1898 (see Kettenmann & Verkhratsky (2008)), but back then astrocytes were not envisioned as integral elements of important brain functions.

The word astrocyte is normally used as a general designation, but it actually refers to cells from the central nervous system since there are other specialized astrocytes. They are the Bergmann glia, in cerebellum and Müller cells, in retina (Newman, 2003).

Presently, astrocytes are known to express a plethora of membrane receptors, which recognize neurotransmitters that modulate astrocytic functions. Furthermore, astrocytes themselves release a number of signalling molecules to influence other cells and also transmit messages through the glial web of connections (reviewed by Hamilton & Attwell (2010)). Astrocytes also take up neurotransmitters, such as glutamate and GABA, regulating their extracellular levels. Consequently, these cells modulate synaptic activity and plasticity (reviewed by Perea & Araque (2010)), a characteristic that was for a long period of time only related to neurons.

In pathological situations astrocytes undergo reactive gliosis, characterized by proliferation and cellular hypertrophy, forming the glial scar that isolates the lesion site, avoiding axon regrowth but also secondary damage (James & Butt, 2002).

1.1.1 Type-I and Type-II astrocytes

In the 19th century, it was already recognized that astrocytes are a heterogeneous cell population divided into two classes, protoplasmic (Type-I) and fibrous (Type-II) (reviewed by Matyash & Kettenmann (2010)). The terms protoplasmic and fibrous were introduced by Andriezen (1893) and Kölliker (1889), respectively, and are related to cell morphology.

Type-I astrocytes are found mostly in grey matter. Their large projections enwrap synapses and express neurotransmitter receptors, transporters and ion channels. Type-II astrocytes are more abundant in white matter and present numerous fine finger-like projections that form points of contact with nodes of Ranvier of the neuronal network. They also express ion channels and transporters, and probably neurotransmitter receptors. Other than morphological differences, namely, functional differences between these two types of cells are not well understood (Matyash & Kettenmann, 2010).

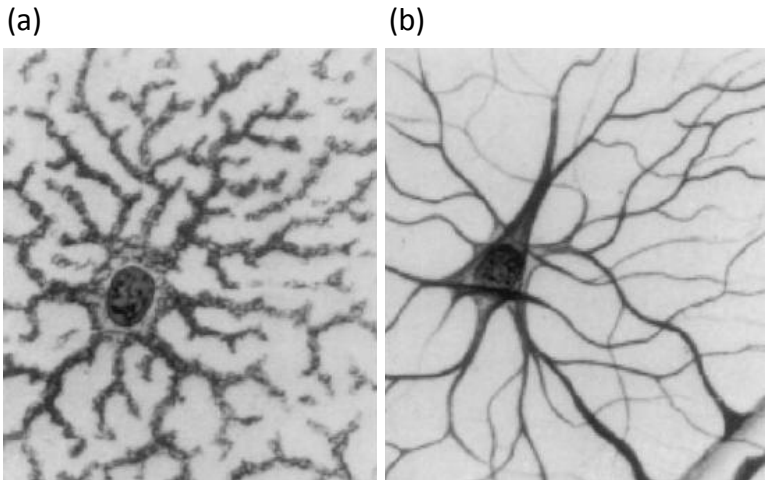

Figure 1.1 - An earliest illustration of (a) protoplasmic (b) fibrous astrocytes in central nervous system by Del Rio-Hortega from 1920. Image from Verkhrtsky *et al.* (1998).

1.2 Tripartite Signalling

For the past two decades, evidences have been accumulated showing that astrocytes have an active role in the brain, "listening" and "talking" to synapses. Recently, this dynamic two-way conversation between astrocytes and neurons at the synapse led to the postulation of a new concept, the tripartite synapse, in opposition to the previous bipartite paradigm. The term tripartite signaling was first introduced by Alfonso Araque and considers that communication at synaptic level involves pre- and post-synaptic neuronal elements as well as peri-synaptic elements, the astrocytes (Araque *et al.*, 1999).

In the early 1990s, astrocytes were first found to respond to membrane receptor activation with an increase in intracellular Ca^{2+} levels ($[Ca^{2+}]_i$) (Salm & McCarthy, 1990). Around the same time, independent works showed that extracellular stimuli, such as glutamate, evoked an intracellular Ca^{2+} rise in astrocytes, followed by a Ca^{2+} wave throughout the glial network (Cornell-Bell *et al.*, 1990; Charles *et al.*, 1991; Porter & McCarthy, 1996). In the same decade, other research groups demonstrated that Ca^{2+} responses in astrocytes induced a similar Ca^{2+} rise in nearby neurons (Nedergaard, 1994;

Parpura *et al.*, 1994; Pasti *et al.*, 1997). These were the first steps to unveil the complex bidirectional communication between neurons and astrocytes.

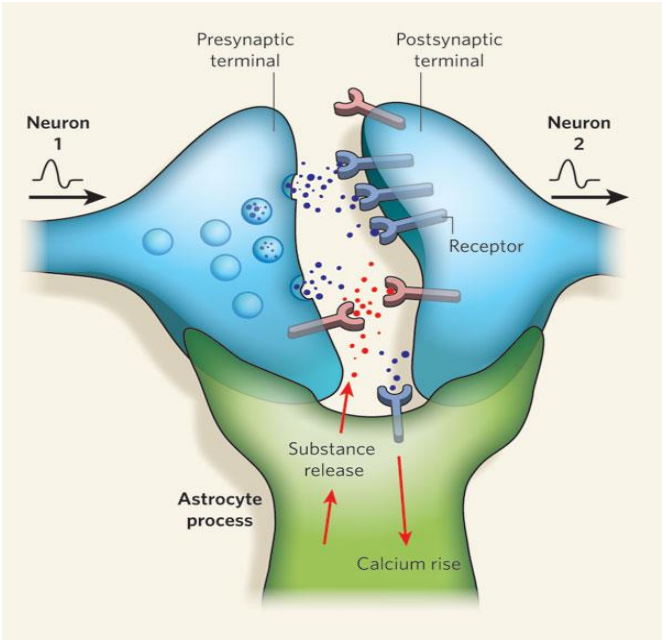

Figure 1.2 - Release of neurotransmitter from the pre-synaptic terminal not only affects the post-synaptic terminal but also the peri-synaptic component, the astrocytes, inducing an intracellular Ca^{2+} rise. In return, astrocytes release gliotransmitters that can exert its effect onto the post-synaptic terminal or can feedback onto the pre-synaptic component. Image from Allen & Barres (2009).

1.2.1 Ca^{2+} signalling and gliotransmission

As astrocytes were shown to present Ca^{2+} oscillations, an entire new Ca^{2+} excitable mechanism was unveiled. Now it is know that astrocytes release signalling molecules, gliotransmitters, such as glutamate, GABA, ATP, adenosine and D-serine, in response to mechanical or neurotransmitter stimuli (Hamilton & Attwell, 2010). Inversely,

gliotransmitters modulate neuronal excitability and synaptic transmission both onto the pre- and post-synaptic terminals (Figure 1.2) (Perea & Araque, 2010).

Gliotransmission is prompt by rapid [Ca^{2+}] rise in the citosol, which is a consequence of membrane receptor activation, such as, purinergic ATP receptors (Fields & Burnstock, 2006), as will be discussed later. This pathway is activated via membrane metabotropic receptors associated to G proteins, which stimulate phospholipase C (PLC) and formation of inositol (1,4,5)-triphosphate (IP_3) and consequently Ca^{2+} release from the endoplasmic reticulum. Ionic channels are also activated, allowing direct Ca^{2+} entry from the extracellular milieu (reviewed by Scemes & Giaume (2006)).

In physiological conditions, cytosolic [Ca^{2+}] is maintained at low levels (≈ 100 nM) compared to [Ca^{2+}] in intracellular storages, which can reach hundreds of mM (Barhoumi *et al.*, 2010). The concentration of this intracellular second messenger is tightly regulated in time and space within the cell. Perturbations of intracellular Ca^{2+} homeostasis normally lead to cellular dysfunction and cytotoxicity (Verkhratsky *et al.*, 1998).

The rapid and brief rise in $[Ca^{2+}]_i$, in response to an external stimulus, triggers gliotransmission and many other cellular processes that derive from Ca^{2+} signalling. Although the molecular mechanisms are not fully comprehended, Ca^{2+} signalling seems to be a specific form of cellular excitability that can be compared to electrical responses in neurons (Scemes & Giaume, 2006).

Distinct forms of Ca^{2+} signalling were observed and vary from spontaneous Ca^{2+} oscillations in individual cells to coordinated forms as intracellular Ca^{2+} waves that propagate throughout the brain (Scemes & Giaume, 2006). Depending on the level of neuronal activity, Ca^{2+} response remains restricted to one cell or propagates to other glial cells (Fellin & Carmignoto, 2004). Due to this fast mechanism of propagation of Ca^{2+} response, astrocytes were proposed to modulate and synchronize neuronal activity in large areas of the brain (Fellin *et al.*, 2004; Halassa *et al.*, 2006). Therefore, Ca^{2+} signalling can be seen as a non-synaptic type of communication between distant neurons. Interestingly, astrocytes can also initiate Ca^{2+} transients in the absence of neurons, which

suggests that this phenomenon has other roles beyond transmission of neuronal information throughout the glial network (Aguado *et al.*, 2002; Nett *et al.*, 2002).

There is little evidence to suggest the actual existence of Ca^{2+} waves in intact tissues '*in situ*' or '*in vivo'* during physiological levels of activity (Agulhon *et al.*, 2008). Nevertheless, spontaneous Ca^{2+} variations and neurotransmitter-induced Ca^{2+} oscillations were detected in vivo (Hirase *et al.*, 2004). Furthermore, Ca^{2+} elevations were observed in response to whisker stimulation, a physiological sensory stimulus (Wang *et al.*, 2006). These results highly support the idea that neuron-astrocyte communication via Ca^{2+} signalling is present *in vivo*.

The molecular mechanisms underlying gliotransmitter release from astrocytes are not well understood. Transporters, hemichannels, volume-activated channels and exocytosis are few of the mechanisms proposed (Hamilton & Attwell, 2010). Furthermore, evidences indicate that exocytosis depends on Ca^{2+} and SNARE proteins (Araque *et al.*, 1998b), involves vesicles (Bezzi *et al.*, 2004) and lysosome exocytosis (Zhang *et al.*, 2007). Nevertheless, very recently, Agulhon et al. (2010) demonstrated that astrocytic modulation of hippocampal plasticity is not dependent on Ca^{2+}-mediated gliotransmitter release mechanisms. Overall, it is very likely that several of these mechanisms co-exist, undergoing differential activation under distinct situations.

1.2.2 Neuron-Astrocyte bidirectional communication

Although, the nature of the mechanisms underlying gliotransmission remain controversial, it was proven that astrocytes control neuron-astrocyte communication, namely synaptic transmission and plasticity, through gliotransmission (Perea & Araque, 2010). Synaptic modulatory effects were both demonstrated at pre- and post-synaptic levels (Fiacco & McCarthy, 2004; Gordon *et al.*, 2005). Modulation of synaptic transmission, by astrocytes, was observed in co-cultures of neurons and astrocytes (Parpura *et al.*, 1994; Araque *et al.*, 1998a; Araque *et al.*, 1998b), as well as, in brain slices (Pasti *et al.*, 1997; Kang *et al.*,

1998). This phenomenon was also demonstrated on other preparations, such as, the retina (Newman & Zahs, 1998) and the neuromuscular junction (Robitaille, 1998; Rochon *et al.*, 2001).

Neuronal plasticity is a well described phenomenon, important in processes underlying learning and memory. Long-lasting changes in astrocytic Ca^{2+} oscillations, induced by neuronal activity, were proposed (Pasti *et al.*, 1995). However, the existence of an astrocytic plasticity *in vivo* is still a controversial subject.

It is common knowledge that neurons exert their excitatory/inhibitory tonus using mostly glutamate/GABA neurotransmitters. Astrocytes also release glutamate as excitatory gliotransmitter but ATP, which is hydrolyzed into adenosine, is the inhibitory molecule (Halassa *et al.*, 2006).

Exciting results indicate that astrocytes not only detect synaptic information but also process it, producing a nonlinear response that is transmitted to adjacent synapses (Perea & Araque, 2006). Moreover, it was not only demonstrated that astrocytes discriminate different neurotransmitters from the same synaptic pathway (Araque *et al.*, 2002), but also that they distinguish different synaptic pathways that use the same neurotransmitter (Perea & Araque, 2005). The fact that astrocytes recognize, internalize and release neurotransmitters seems to indicate that they are able to detect, integrate and respond according to neuronal activity. Therefore, for their importance in the process, transfer and storage of information in the nervous system, some authors suppose that astrocyte deregulation might contribute to an imbalance of neuronal excitability and ultimately to the development of disorders, such as epilepsy (Fields & Burnstock, 2006; Halassa *et al.*, 2006; Sebastião & Ribeiro, 2009b).

These recent discoveries related to astrocytes are revolutionizing the way brain function is perceived and the classical paradigm that it results exclusively from neuronal activity is being questioned. Now we understand that brain function depends on concerted activity of a neuron-glia network, in which intra- and intercellular Ca^{2+} signalling in astrocytes are key elements.

1.3 Purinergic signalling in neuron-glia networks

The word “purinergic” was firstly introduced in the 1970s by Geoffrey Burnstock, who advanced the concept of ATP as a neurotransmitter and a co-transmitter (Burnstock, 1972). Few years later, 2 subtypes of purinergic receptors were proposed based on different ligands, adenosine (P1 receptors) and ATP/ADP (P2 receptors) (Burnstock, 1976). Afterwards it was proposed the separation of P1 (Van Calker *et al.*, 1979) and P2 (Burnstock & Kennedy, 1985) receptor families into subfamilies, which will be discussed below.

Purines have long been recognized as extracellular messengers, mediating communication with the vascular network (Drury & Szent-Györgyi, 1929) but more recently they were also associated to heterotypic communication, between neurons and astrocytes (Koizumi *et al.*, 2003; Zhang *et al.*, 2003), as well as, to homotypic communication, among astrocytes (Guthrie *et al.*, 1999).

Purines also act as an intracellular messenger, regulating a broad scope of phenomena, such as, glial growth, proliferation, motility, survival and differentiation (Fields & Burnstock, 2006). Purines play a preponderant role in stress situations, when their extracellular concentration rises abruptly (Frenguelli *et al.*, 2007). Evidences even suggest that astrocytes sense the severity of damage by the amount of ATP released from damage cells (Fields & Burnstock, 2006).

Purinergic signalling is far more complex than any other neurotransmitter, as ATP degradation produces other purines, namely ADP and adenosine, which can further activate P2R and P1R, respectively (Fields & Burnstock, 2006). From ATP release and enzymatic degradation to purinoceptor activation, different patterns of purinergic signalling can arise.

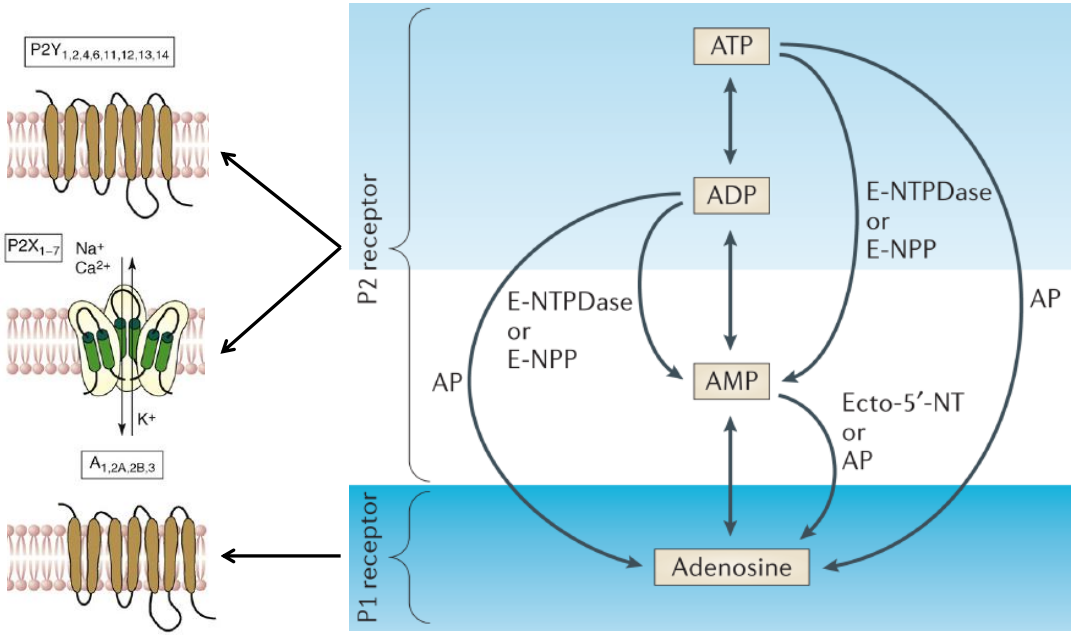

Figure 1.3 – ATP is enzymatically hydrolysed to ADP, AMP and adenosine. P2R (P2Y and P2X) bind to ATP and ADP whereas P1R (A_1, A_{2A}, A_{2B} and A_3) bind to adenosine. The metabolism of extracellular ATP is regulated by several ectonucleotidases, including members of the ENTPDase (ectonucleoside triphosphate diphosphohydrolase) and the E-NPP (ectonucleotide pyrophosphatase/phosphodiesterase) families. Ecto-5'-nucleotidase (Ecto-5'- NT) and alkaline phosphatase (AP) catalyse the nucleotide degradation into adenosine. Adapted from Fields & Burnstock (2006) and Abbracchio *et al.* (2009).

1.3.1 Purinergic receptors

1.3.1.1 P2 (ATP) receptors

In the 1990s, Abbracchio & Burnstock (1994) coined the current nomenclature of purinoceptors - metabotropic P2Y (P2YR) and ionotropic P2X (P2XR) receptors. G-protein-coupled P2YR induce Ca^{2+} release from intracellular store compartments through PLC/IP_3 pathway. P2XR are cationic ligand-gated nonspecific channels that once activated allow the entrance of Ca^{2+} from the extracelular milieu and also the inward Na^+ current, which

depolarizes cell membrane and opens voltage-gated Ca^{2+} channels (Fields & Burnstock, 2006).

P2YR comprise two subgroups, $P2Y_{1,2,4,6,11}$ and $P2Y_{12,13,14}$, based on their phylogenetic similarity and G protein preference (Figure 1.3). The first group corresponds to the group described in the previous paragraph and mediates Ca^{2+} release from the endoplasmic reticulum via G_q/G_{11} proteins. The second group almost exclusively couples to $G_{i/o}$ proteins, which inhibits adenylate cyclase (AC) and modulates ion channels (Abbracchio *et al.*, 2009). Concerning P2XR, seven receptor subtypes were identified ($P2X_{1-7}$), but $P2X_7R$ seem to contribute more for Ca^{2+} entry. This receptor is activated at high ATP concentrations (100-1000 μM) while the others are activated at lower ATP concentrations (1-10 μM) (Abbracchio *et al.*, 2009). As $P2X_7R$ are activated at extremely high ATP levels, it seems probable that they are associated with astroglial responses to brain lesions (Abbracchio *et al.*, 2009).

Currently, several P2YR ($P1Y_{1,2,4,6,12,13,14}$) and P2XR ($P2X_{1-7}$) subtypes have already been identified by western blot and immunocytochemistry, in primary rat cortical astrocytes (Fumagalli *et al.*, 2003; Fischer *et al.*, 2009). In astrocytes, the $P2Y_1R$ and $P2X_7R$ seem to play a major role in Ca^{2+} signalling and Ca^{2+} wave propagation (Fumagalli *et al.*, 2003; Fischer *et al.*, 2009).

1.3.1.2 P1 (ADO) receptors

There are 4 types of G-protein-coupled P1 receptors (GCPR): A_1, A_{2A}, A_{2B} and A_3 (Figure 1.3) (reviewed by Sebastião & Ribeiro (2009a)). All the receptors are present both in neurons and glial cells. High affinity A_1 (A_1R) and A_{2A} ($A_{2A}R$) receptors are probably the most important both in physiology and pathology. Low affinity A_{2B} ($A_{2B}R$) and high affinity A_3 (A_3R) receptors are present in low density in most tissues. A_1R are widely present in the central nervous system, namely in the cerebral cortex, cerebellum and hippocampus. $A_{2A}R$ are mainly present in the striatum, nucleus accumbens and olfactory bulb (Ribeiro *et al.*,

2003). It was also documented that $A_{2A}R$ are present in other brain areas although in lower levels when compared to the striatum (Sebastião & Ribeiro, 1996). A_3R are moderately present in the cerebellum and hippocampus and in lower density in the rest of the brain (Ribeiro *et al.*, 2003).

Remarkably, adenosine can mediate opposite effects, stimulating via $A_{2A}R$ and $A_{2B}R$ and inhibiting via A_1R and A_3R (Fredholm *et al.*, 2001). A_2R are positively coupled to adenylyl cyclase (AC) through 'stimulatory' G_s-proteins, increasing cyclic AMP (cAMP) levels and activating PKA, which stimulates gliotransmitter release (Nishizaki, 2004). A_1R and A_3R are negatively coupled to AC (Peakman & Hill, 1996) through 'inhibitory' $G_{i/o}$-proteins, and probably inhibit gliotransmission.

A_1R and $A_{2A}R$ subtypes are those that are most likely activated by physiological adenosine levels. All adenosine receptors (ADOR) subtypes are known to be present in astrocytes. Again A_1R are highly present and A_2R and A_3R are present in lower quantities and therefore are difficult to detect (Fields & Burnstock, 2006).

1.3.2 ATP, key signalling molecule

ATP is no longer seen as a mere intracellular energy source, it is now seen as a dominant extracellular signalling molecule (Khakh & Burnstock, 2009). After the initial skepticism that such a ubiquitous molecule could perform such a specific role, it was shown that ATP acts as a neurotransmitter, neuromodulator and co-modulator (Abbracchio *et al.*, 2009). It is released and recognized by membrane receptors, both by neurons and astrocytes, in physiological and pathological conditions. ATP is also a key messenger of intercellular communication, enabling glia to detect neuronal activity and communicate to other glial cells by ATP release (Scemes & Giaume, 2006).

An apparent universal property of astrocytes throughout the central nervous system is their responsiveness to ATP. This purine, which is released and co-released along with other neurotransmitters from synaptic vesicles, triggers Ca^{2+} signalling that is the

substrate for astrocytic excitability and intercellular communication (Neary *et al.*, 1988; Pearce *et al.*, 1989). In addition, astrocytes store ATP in vesicles and release it in a regulated-way in response to Ca^{2+} signalling (Coco *et al.*, 2003).

Apart from signalling to neurons, astrocytic released ATP, also signals to other glial cells. ATP was demonstrated to mediate Ca^{2+} wave propagation throughout the glial syncytium via P2R (Guthrie *et al.*, 1999). Initially, gap-junction communication was seen as the sole responsible for wave propagation, allowing direct transference of IP_3 and Ca^{2+} between adjacent cells (Sáez *et al.*, 1989; Finkbeiner, 1992 ; Venance *et al.*, 1997). Then ATP was shown to act as a diffusible sign that is recognized by membrane receptors in nearby cells, actively participating in Ca^{2+} wave spreading (Hassinger *et al.*, 1996).

ATP activates P2R, which then induce further release of ATP, initiating a positive-feedback mechanism that is the basis of Ca^{2+} waves (Scemes & Giaume, 2006). This mechanism allows glia to detect synaptic activity, propagating synaptic information through the complex web of glial cells, and finally influencing neuronal function at remote sites (Halassa *et al.*, 2006).

In astrocytes, prolonged ATP stimulus (≥ 20 seconds) induces a biphasic Ca^{2+} response consisting of an initial peak followed by a sustained plateau. The transient component is evoked by metabotropic P2YR activation and consequent release of Ca^{2+} from the endoplasmic reticulum. The sustained phase is mediated by ionotropic P2XR activation and consequent Ca^{2+} entry from the extracellular medium (Nobile *et al.*, 2003 ; Alloisio *et al.*, 2004).

Unlike classic neurotransmitters, ATP is not removed from the synaptic cleaf. It is enzymatically hydrolyzed to ADP, AMP and finally adenosine by ectonucleotidases. Therefore it plays a dual role because it can directly activates P2R and, after its breakdown into ADP and adenosine, further activates P2R and P1R, respectively, prolonging ATP action (Fields & Burnstock, 2006). The potential for ATP to be sustained at low levels in the pericellular space is also very important, allowing temporal coding of ATP elevation into astrocytic Ca^{2+} signals.

1.3.3 Adenosine, ubiquitous modulator

Adenosine is a ubiquitous modulator and its receptors are present in both neuronal and glial cells throughout the brain. It is not a neurotransmitter since it is neither stored in vesicles nor released as classical neurotransmitters (Sebastião & Ribeiro, 2000). However, adenosine modulates brain functioning, acting as modulator of modulators (e.g. ATP) (Sebastião & Ribeiro, 2009a). This purine controls synaptic activity by acting independently on the three levels of tripartite synapses. Presynaptically, regulating neurotransmitter release, postsynaplically, modulating neurotransmitter actions, and perisynaptically, affecting neurotransmitter uptake and release from astrocytes (Nishizaki *et al.*, 2002; Sebastião & Ribeiro, 2009a; Cristóvão-Ferreira *et al.*, 2011).

This purine is produced intra- and extracellularly by ectoenzymes. Intracellular generated adenosine is released via specific bi-directional nucleoside transporters that tend to even adenosine levels across the cellular membrane (Fredholm *et al.*, 2001). Extracellular conversion of released adenine nucleotides into adenosine through a series of ectoenzymes is also an important mechanism as referred earlier (see Figure 1.3).

Adenosine exerts a dual control upon neuronal excitation and synaptic transmission via inhibitory-A_1 and excitatory-A_{2A} receptors, which initially puzzled the scientific community. The potential for a dual-modulatory action of adenosine was first reported by chance by Ginsborg & Hirst (1971; 1972) using a single synapse model in the neuromuscular junction. They intended to evaluate the relation between cAMP and neurotransmitter release, using adenosine as a pharmacological tool to increase cAMP and NT release but surprisingly adenosine decreased NT release.

Now, adenosine is seen as a complex modulator, rich in shades of regulation that involve cooperation of adenosine receptors and other neurotransmitter receptors (Sebastião & Ribeiro, 2000; Sebastião & Ribeiro, 2009b). More interesting is that both A_1R and A_{2A}R are co-localized in nerve terminals (Correia-de-Sá *et al.*, 1991), exerting a balanced inhibitory/excitatory modulation over synaptic activity, which seems to depend on extracellular adenosine levels. At low concentrations, adenosine acts mostly on high

affinity A_1R (Fredholm *et al.*, 2001). On the contrary, at slightly higher levels adenosine acts predominantly on $A_{2A}R$ (Correia-de-Sá & Ribeiro, 1996). Moreover, cooperation among adenosine receptors leads to a direct modulation of the effects mediated by the other adenosine receptors, e.g., $A_{2A}R$ activation attenuates A_1R mediated inhibition and vice-versa (Sebastião & Ribeiro, 2000). Position cooperativity between A_1 and A_{2A} receptors also occur, namely, in astrocytes (Cristóvão-Ferreira *et al.*, 2011) an issue that will be addressed in later sections of the Introduction.

In glial cells, adenosine dual modulation role was first proposed by van Calker et al. (1979), who showed that adenosine modulates cAMP accumulation differently, via distinct receptors. These authors proposed that A_1R mediate the inhibitory effect and A_2R the facilitatory effect. Later, Porter and McCarthy (1995) documented that adenosine also induces increases in astrocytic $[Ca^{2+}]_i$. Around the same time it was shown that adenosine-elicited Ca^{2+} responses in acutely isolated cortical astrocytes were mediated via $A_{2B}R$ (Pilitsis & Kimelberg, 1998).

Through astrocytes, adenosine, indirectly modulates the neuronal network. This purine modulates gliotransmission thought A_1R and A_2R, controlling the release and uptake of signalling molecules, such as, glutamate (Nishizaki *et al.*, 2002) and GABA (Cristóvão-Ferreira *et al.*, 2011).

As adenosine receptors exert a fine modulation over a broad range of neurotransmitters, gliotransmitters and modulators, abrupt variation of extracellular adenosine levels might interfere in neuronal activity and synaptic transmission, possibly leading to pathological situations (Ribeiro *et al.*, 2003).

1.3.3.1 Ca^{2+} signalling modulation by adenosine

Adenosine is frequently designated as a neuromodulator, but recent evidences indicate that this purine is a more general modulator, as Ca^{2+} excitation in astrocytes is also a

modulation target. As a product of ATP hydrolysis by ectoenzymes, adenosine is rapidly formed in the extracellular space when ATP is released (≈ 200 msec) (Dunwiddie *et al.*, 1997). Thus adenosine and ATP co-exist in the extracellular medium for a brief period of time. It is, therefore, plausible that adenosine, as a ubiquitous modulator, regulates ATP-triggered Ca^{2+} signalling events, a hypothesis that prompted the present work. In addition, $P2Y_1R$ and A_1R are co-localized and present a functional cross-talk in glutamatergic synapses and astrocytes (Tonazzini *et al.*, 2007). These receptors can further heteromerize (Yoshioka *et al.*, 2002), which represents an intimate cross-talk between nucleotide and nucleoside receptors. $P2Y_2R$ can also form herero-oligomers with A_1R in various regions of the rat brain (Namba *et al.*, 2010).

A_1R were shown to potentiate astrocytic Ca^{2+} responses induced by metabotropic glutamate receptor (mGlutR) activation, a process that involves $G_{i/o}$ proteins (Ogata *et al.*, 1994; Toms & Roberts, 1999; Cormier *et al.*, 2001) and potentiation of cAMP levels, which depends on A_1/A_{2A} receptor cooperation (Ogata *et al.*, 1996). A similar modulatory role of adenosine, via A_1R, was observed in Ca^{2+} signalling induced by muscarinic acetylcoline receptors activation (Ferroni *et al.*, 2002).

ATP-mediated Ca^{2+} signalling is potentiated by adenosine, via $A_{2B}R$, in the cortex (Alloisio *et al.*, 2004) and the cerebellum (Jiménez *et al.*, 1999), which implies G_s-protein activation and consequent rise of cAMP levels. Several studies also demonstrated that adenosine modulates Ca^{2+} response triggered by ATP in other cell models, namely, cell lines (Gerwins & Fredholm, 1992; Fredholm *et al.*, 2003), tracheal smooth-muscle cells (Michoud *et al.*, 1999) and rat thyroid FRTL-5 cells (Vainio & Tornquist, 2000).

Alloisio et al. (2004) reported a differential modulatory role of A_1R and $A_{2B}R$ on biphasic Ca^{2+} transients (see section 1.3.2). $A_{2B}R$ activation potentiates the initial Ca^{2+} peak and A_1R activation downregulates the sustained response. No information was reported about the possible dual-modulatory role of adenosine receptors upon the initial transient Ca^{2+} peak, an issue that is included in the scope of this project.

1.3.3.2 Cooperation between ADOR

The presence of overlapping tissue distribution of adenosine receptors raises questions about the functional significance of their co-localization and most importantly the possible interactions between these receptors (Fredholm *et al.*, 2011). This is of particular importance because adenosine mediates both inhibitory and excitatory effects through A_1R and $A_{2A}R$, respectively.

Evidences have been accumulated for functional cross-antagonism interactions between A_1R and $A_{2A}R$ in glutamate release modulation in the striatum and hippocampus (O'Kane & Stone, 1998; Lopes *et al.*, 2002). A_1R and $A_{2A}R$ homomers were detected both in HEK293 and CHO transfected cells (Fredholm *et al.*, 2011). In addition, the co-localization and heterodimerization of A_1R-$A_{2A}R$ was demonstrated in co-transfected HEK cells and striatal glutamatergic nerve terminals (Ciruela *et al.*, 2006). Moreover, this heteromers regulate differential glutamate release from presynaptic nerve terminals via A_1R and $A_{2A}R$. This modulation seems to depend on synaptic adenosine levels, working as a "concentration-dependent switch", which fine-tunes modulation of striatal glutamatergic neurotransmission.

In non-transfected primary cortical astrocytes, A_1R and $A_{2A}R$ were shown to cooperate in GABA uptake modulation (Cristóvão-Ferreira *et al.*, 2011). Moreover, these receptors are physically linked in the cellular membrane as a heterotetramer - A_1R- A_1R-$A_{2A}R$-$A_{2A}R$. On the one hand, the A_1R homodimer mediates inhibition of GABA transport and, on the other hand, the $A_{2A}R$ homodimer facilitates its transport. Each homodimer is coupled to the respective $G_{i/o}$ or G_s-protein and both proteins have to be activated in order for the modulation to occur. A_1R-$A_{2A}R$ differential activation also depends on extracellular adenosine concentration, resulting in differential GABA uptake modulation under distinct physiological situations. At relatively low adenosine levels A_1R are preferentially activated and as adenosine levels rise, $A_{2A}R$ activation overcomes the previous one and A_1R affinity for agonist is decreased.

2 Aims

Adenosine is a potent neuromodulator, acting directly onto neurons, but now we are unveiling indirect neuromodulation via astrocytes. Although evidences indicate that adenosine modulates Ca^{2+} signalling triggered by neurotransmitters, namely ATP, it is not clear what is/are the adenosine receptor(s) with a preponderant role in this modulation. In addition, A_1R and $A_{2A}R$ cooperate in GABA uptake modulation in cortical astrocytes. Nonetheless, nothing is known about a possible similar cooperation mechanism between adenosine receptors to modulate Ca^{2+} signalling and consequent gliotransmitter release.
Overall, the aims of this project were to evaluate the role of adenosine receptors, mainly $A_{2A}R$, in ATP-induced Ca^{2+} signaling and to explore the possible cross-talk between A_1R and $A_{2A}R$ in this modulation.

The specific aims of this work were:

1. To develop and optimize a Ca^{2+} imaging protocol to study Ca^{2+} response modulation by adenosine;
2. To characterize the adenosine receptors involved in the modulation of Ca^{2+} responses in cortical astrocytes;
3. To study if cooperation and/or interaction between high affinity adenosine receptors, primarily A_1R and $A_{2A}R$, is required or not for the modulation effect;
4. To characterize cortical astrocytic primary cultures by,
   4.1 Quantifying different cell populations, namely astrocytes, neurons and microglial cells and;
   4.2 Demonstrating the presence of ATP ($P2Y_1R$) and adenosine (A_1R and $A_{2A}R$) receptors.

3 Methods

3.1 Primary enriched-astrocytic cultures

Cortical astrocytes were obtained from 0-2 days old (P0-P2) Wistar pups, purchased from Harlan Interfauna Iberia (Barcelona, Spain). The procedure was carried out as previously described by Cristóvão-Ferreira et al. (2011). Animals were handled according to the Portuguese law on Animal Care and European Union guidelines (86/609/EEC).

Pups were killed by decapitation and the heads were sterilized by sequential submersion on alcohol. Inside the laminar flow, heads were transferred to a phosphate buffered saline (PBS) solution (in mM: 137 NaCl; 2.11 KCl, 1.8 KH_2PO_4; 10 NaH_2PO_4, pH 7.4), where they were dissected. After opening the skin and skull, the brain was detached, the cerebellum was removed and the two hemispheres of the brain were separated. With the help of a dissecting microscope, the white matter, hippocampus and meninges were removed and then the cortex was mechanically dissociated, with a 10 mL pipette, in Dulbecco's Modified Eagle's Medium (DMEM) (Gibco/Invitrogen®) supplemented with 2mM glutamine, 10% (v/v) fetal bovine serum (FBS) (both from Gibco®) and Antibiotic/Antimicotic solution (100 U/mL penicillin, 0.25 µg/mL anphotericin B and 100 µg/mL streptomycin) (Sigma®). Then followed two filtrations, firstly with a 230µm pore and secondly with a 70µm pore. After each filtration cells were centrifuged at 200g for 10 minutes, the supernatant was discarded and the pellet was resuspended in 10 mL of DMEM supplemented medium. After the last centrifugation the pellet was resuspended for the final volume of 10 mL of DMEM supplemented medium for each cortex. Cells were plated in T-75 (75 cm^2) culture flasks, for Ca^{2+} imaging and immunocytochemistry, or in 100-mm-diameter petri dishes, for western blot. Cells were plated at a density of $38x10^4$ cells/mL (n = 4 independent cultures). Cultures were maintained in a humidified incubator with 5% CO_2 at 37°C. Cell counting was performed in 75% trypan blue cellular solution using a hemacytometer.

After 6 days in culture (DIC 6), cells in the T-75 culture flasks were shaken for 4-5h at 37°C, the supernatant was removed and DMEM supplemented medium was added. At DIC 7, the T-75 culture flasks were shaken again for 2-3 hours at 37°C, the supernatant containing mostly microglia was removed and then cells were washed once with PBS. The adherent astrocytes were enzymatically dispersed (trypsin-EDTA 0.025%) under agitation 1-2 minutes at 37 °C. The enzymatic reaction was stopped by adding excess of DMEM supplemented medium. Cells were diluted in DMEM supplemented medium (1:7) and seeded over γ-irradiated glass bottom microwell dishes (glass thickness: 0.16-0.19mm, glass diameter: 14mm, MatTek®) for imaging experiments or over glass coverslips placed in 24-well plates for immunocytochemistry. Glass coverslips were previously incubated with poli-L-lysine (0,01 mg/mL) for 1 hour and afterwards washed with sterile water, to improve cell adhesion. For Ca^{2+} imaging experiments, cells were used from DIC 9 to DIC 14, similar to what was previously described by *Alloisio et al.* (2004) (DIC 10-15).

The shaking procedure was applied to obtain cultures with a higher percentage of astrocytes in relation to other cell populations, namely microglial cells. The latter cells grow upon astrocytes and for this reason are easy to detached and discard with the supernatant (Jiménez *et al.*, 1999; Du *et al.*, 2010).

3.2 Ca^{2+} Imaging experiments

3.2.1 Technical Approach

The development of optical probes and non-invasive methods to study the dynamics of intracellular ions in living cells provided the technological tools to further explore astrocyte functions, unveiling their Ca^{2+} excitable mechanism. The Ca^{2+} imaging technique allows to follow variations of free Ca^{2+} ions in the cytoplasmic and organellar compartments, using sensitive Ca^{2+} probes to define spatial and temporal patterns of Ca^{2+} behavior.

3.2.1.1 Ca^{2+} indicators

Ca^{2+} sensitive probes are molecules from the family of BAPTA (1,2-bis(o-aminophenoxy)ethane-N,N,N',N'-tetraacetic acid), a relative of the ion chelator – EGTA (Ethyleneglycol bis(β-aminoethylester)-N,N,N',N'-tetraacetate), which bind selectively to free Ca^{2+} ions, forming reversible complexes. These sensors are fluorochromes that undergo a conformational change and consequently a variation in its fluorescence properties when bounded to Ca^{2+}. The most common differences are in the excitation and/or emission of light (Rudolf *et al.*, 2003).

The first fluorescence Ca^{2+} probe for intracellular use was sintetized by Roger Tsien and collaborators in the late 1970s (Tsien, 1980). Currently, several indicators are available with different dissociation constants (K_d), which corresponds to different affinities for Ca^{2+} ions. Therefore, when accessing Ca^{2+}, the probe should be compatible with the $[Ca^{2+}]_i$ range of interest. Higher $[Ca^{2+}]_i$ require a probe with smaller affinity, which means a higher K_d (Paredes *et al.*, 2008).

There are two main groups of Ca^{2+} sensitive dyes:

Non-ratiometric dyes

These are single-wavelength fluorophores, which allow determining relative $[Ca^{2+}]_i$ by relative increase in the fluorescence intensity. There is no shift in excitation or emission wavelength. Disadvantages are susceptibility to variations in dye concentration, photobleaching or leakage from the cell (Johnson & Spence, 2010).

Ratiometric dyes

These fluorochromes do not measure $[Ca^{2+}]_i$ directly, instead the indicator monitors the amount of free and complexed probe. There are two subgroups of ratiometric dyes: dual emission and dual excitation, as the emission or excitation wavelength varies in the bounded/unbounded forms. $[Ca^{2+}]_i$ is determined by the ratio of fluorescence emission or excitation at distinct wavelengths (Johnson & Spence, 2010).

Fura-2, which was used in this project, is the most widely used ratiometric probe and was firstly synthesized in the 1980s by Tsien's group (Grynkiewicz *et al.*, 1985). Its absorbance peak shifts from 380 nm (F380) in the Ca^{2+}-free state to 340 nm (F340) in the Ca^{2+}-bounded state (Figure 3.1). The emission wavelength is maintained at 510 nm. In this case, the F340/F380 fluorescence ratio is used to access variations in $[Ca^{2+}]_i$.

In addition, ratiometric dyes present a series of advantages as they allow correcting for uneven dye loading, dye leakage, photobleaching, dye concentration and changes in cell volume. Furthermore, measurements with these dyes can be performed over a period of one hour without significant loss of fluorescence (Johnson & Spence, 2010).

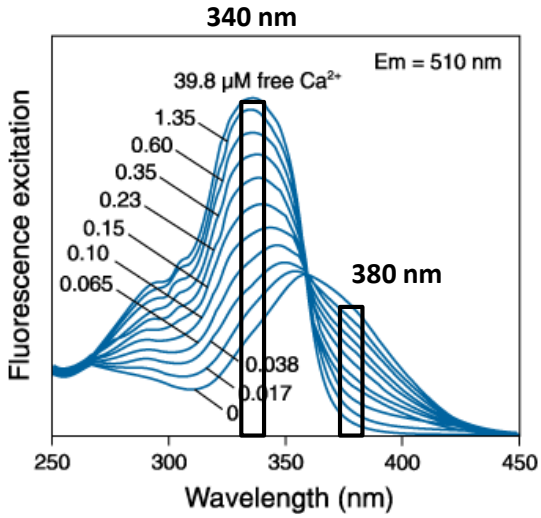

Figure 3.1 – Fluorescence excitation spectra of Fura-2 in solutions containing increasing levels of free Ca^{2+} (0-39.8 µM). 380 nm – maximum fluorescence emission in Ca^{2+}-free medium; 340 nm – maximum fluorescence emission in Ca^{2+}-saturated medium. Image from Johnson & Spence (2010).

The fluorochrome used here, Fura-2, has affinity for Ca^{2+} (K_d) of approximately 224 nM (Grynkiewicz *et al.*, 1985), which means that, theoretically, it is suitable for measuring $[Ca^{2+}]_i$ between 22.4 nM - 2240 nM (0.1* K_d – 10* K_d) (Paredes *et al.*, 2008). In practice, Fura-2 is generally used to detect $[Ca^{2+}]_i$ below 1 µM.

The bulk Ca^{2+} baseline level for all the primary astrocytes studied here was estimated to be approximately 93.05 ± 5.60 nM (n = 247 cells from 62 independent experiments). This value is consistent with the normal cytosolic Ca^{2+} levels ≈ 100 nM (Knot *et al.*, 2005; Barhoumi *et al.*, 2010). Furthermore, the amplitude of Ca^{2+} transients ($\Delta[Ca^{2+}]_i$) presented here goes up to a maximum of about 500 nM. Therefore, the interval of $[Ca^{2+}]_i$ evaluated in the present work was below 1 µM and for this reason, Fura-2 is appropriate to detect this interval of $[Ca^{2+}]_i$.

If saturating $[Ca^{2+}]_i$ levels were reached for Fura-2 ($[Ca^{2+}]_i$ > 1 µM), the fluorophore loses its capacity to accurately report ion concentration. In this case, another indicator would have to be chosen, such as, Mag-FURA-2 that has a higher K_d value (25 µM). This fluorochrome avoids early saturation due to its low Ca^{2+} binding affinity and therefore it can be used to detect a range of higher $[Ca^{2+}]_i$ (1-100 µM). Mag-FURA-2 is also a ratiometric dye and presents excitation and emission wavelengths similar to FURA-2, which makes it appropriate to substitute our dye.

Cell loading can be achieved through several different techniques, such as, microinjection, diffusion from patch clamp pipettes, electroporation, hypoosmotic shock and, the non invasive, AM ester loading (Paredes *et al.*, 2008). The latter technique, was firstly described in the 1980s (Tsien, 1981) and depends on acetoxymethyl esters (AM) groups that are part of the fluorophore molecule and confer a general neutral charge, allowing passive diffusion across the cellular membrane. Once inside, the AM groups are cleaved by cellular enzymes – esterases – so the fluorochrome becomes charged and is trapped inside the cell. This loading technique is simple, requires no previous expertise and is highly effective. Moreover, it allows the simultaneous loading of an entire population of cells. For all the reasons presented above, Fura-2AM was the Ca^{2+} indicator of choice.

3.2.1.2 Experimental apparatus

In this project, it was used a high intensity light source, xenon arc lamp, which emits uniformly across the entire UV spectrum. A set of specific excitation interference filters (340 nm and 380 nm), with a band-pass filter system, select the appropriate wavelength (Figure 3.2). Follows a dichroic mirror that produces a light cone to focus excitation light into the preparation.

As astrocytes, during experiments, were alternately irradiated at two UV wavelengths (340 and 380 nm), it is important to alternate irradiation as fast as possible. For that, the irradiation time at each wavelength was decreased to the minimum so that one can obtain more values and therefore gain sensitivity to detect the maximum of the peak. 100 ms is the minimum technically possible and therefore the light source was programmed for this duration.

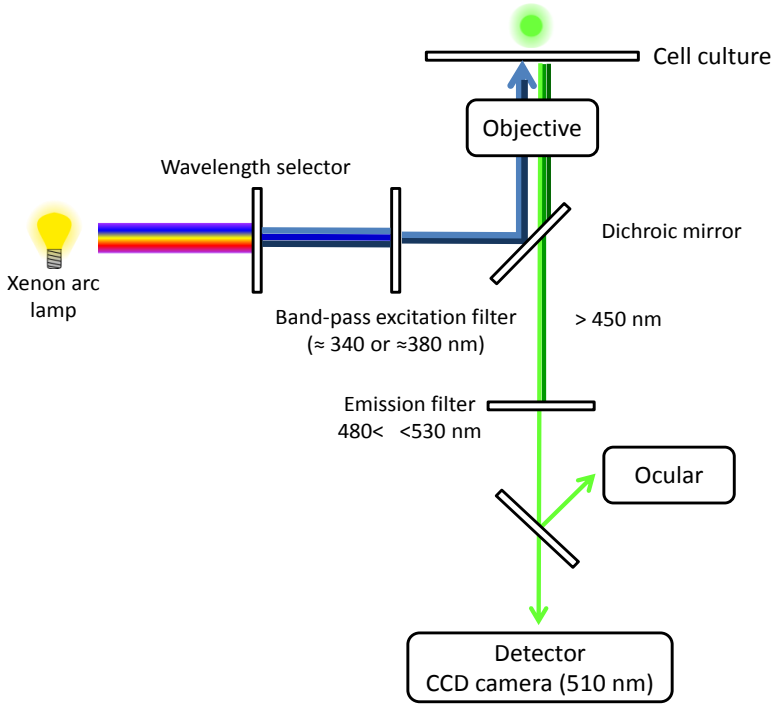

Figure 3.2 – Light path in an inverted epifluorescence microscope.

To image cultured cells, an inverted epifluorescence microscope was used, where the excitation light passes from below, through the objective lens and onto the cells. The light emitted by cells, at a higher wavelength, goes to the detector in the lower part of the apparatus (Figure 3.2).

An additional dichroic mirror followed by an emission filter is used, between the objective and the detector, to filter the fluorescent light, selecting the emission wavelength of the emitted light that goes into the detector. The detector is a CCD camera, which rapidly integrates data, enabling several measurements per second (Figure 3.2).

3.2.2 Ca^{2+} experiments

Fluorescence measurements were performed by Ca^{2+} imaging technique, at room temperature (RT) (22 ^{o}C), using the fluorescent Ca^{2+} dye, Fura-2AM. Prior to each experiment, cells were incubated with 5 µM Fura-2AM in HEPES buffer (in mM: 125 NaCl; 3 KCl; 1.25 NaH2PO4; 10 glucose; 10 HEPES; 2 CaCl; 2 MgSO4; pH ~ 7.38) (Rose *et al.*, 2003) for 45 minutes at 37 ^{o}C. Previously and after fluorochrome incubation, cells were gently washed with HEPPES buffer (2-3x). The glass bottom microwell dish (glass thickness: 0.16-0.19mm, glass diameter: 14mm, MatTek®) was placed on the stage of an inverted epifluorescence microscope (Axiovert 135TV, Zeiss®) with a 60x objective, equipped with a high speed multiple excitation fluorimetric system (Lambda DG-4, Sutter Instruments®, with a 175W Xenon arc lamp). Data was recorded by a CCD camera (Photometrics® CoolSNAP fx). The perfusion medium was activated using a rotating pump system (Mini PULS3, GILSON®) and cells were left for temperature stabilization for about 15 minutes in the beginning of each experiment. This stabilization period also assures complete de-esterification of the dye. Cell cultures were continuously perfused throughout experiments with HEPES buffer at a rate of approximately 1.5mL/minute. This rapid flow prevents the accumulation of ATP, adenosine or any other compound secreted by cells (Jiménez *et al.*, 1999). Special care was taken regarding the volume of buffer in the perfusion chamber. It is of utmost importance that the volume is maintained constant

during the entire experiment because slight variations influence enormously the signal response.

Stimulation by 10 µM ATP, for 200 miliseconds, was achieved through a glass electrode (1.5 mm OD x 0.86 mm ID, Harvard Apparatus®) coupled to a micromanipulator (InjectMan® IN2) and a pressurized system (injection pressure of 15 psi) (FemtoJet®, Eppendorf®). Once an optimal position of the glass electrode was defined in the beginning of the experiment, it was very important to maintain it invariable throughout the experiment, since variations in its position affect enormously cellular response. This was achieved by holding the glass electrode firmly with a micromanipulator.

Drug treatment was applied through the perfusion medium, for at least 15-20 minutes, followed by a washout period with HEPES buffer or further treatment with a drug mixture. Exchange between perfusion mediums was efficiently achieved with a semi-automatic tap system in a fast, non-destabilizing manner.

Fura-2 AM loaded astrocytes were continuously and sequentially excited both at 340nm and 380nm, for 100 ms at each wavelength, and the emission fluorescence was recorded at 510nm. Background fluorescence and autofluorescence were automatically subtracted by the MetaFluor® software. The software also calculated and reported, in real-time, the fluorescence ratio F340/F380 and this parameter was used to monitor $[Ca^{2+}]_i$ changes. The calculus to convert fluorescence ratio into $[Ca^{2+}]_i$ are presented below (see section 3.2.4).

Experiments were performed on cells with a baseline fluorescence ratio around 2, which corresponds approximately to a $[Ca^{2+}]_i$ of about 100 nM, the normal $[Ca^{2+}]_i$ (Knot *et al.*, 2005; Barhoumi *et al.*, 2010). Cells with a baseline fluorescence ratio above 3 were discarded for experiment.

3.2.2.1 Drugs

Drug concentration was chosen so that it acts selectively in the target receptor and does not desensitize it (Table 3.1), similar to drug concentration previously used by Cristóvão-Ferreira *et al.* (2011).

Table 3.1 – Drugs used in Ca^{2+} imaging experiments, the effect they mediate and respective concentrations.

Drug	Mediated effect	Concentration (nM)	Brand
CADO	blanket ADOR agonist	1000	C-5134 – SIGMA®
CGS 21680	$A_{2A}R$ agonist	30	1063 – Tocris®
SCH 58261	$A_{2A}R$ antagonist	50	2270 – Tocris®
DPCPX	A_1R antagonist	50	0439 – Tocris®

CADO has a dissociation constant (K_d) of 9.3 nM for A_1R and of 63 nM for $A_{2A}R$ (Fredholm *et al.*, 2001). The selectivity ratio for the two receptors is lower than 10 and for this reason CADO is considered and used as a non-selective adenosine receptor agonist. On the contrary, CGS 21680 has a K_d of 22 nM for $A_{2A}R$ and the K_d for A_1R is higher than 1 μM, being, therefore, considered as an $A_{2A}R$ selective agonist (Fredholm *et al.*, 2001). Similarly, SCH 58216 has a K_d of 2.3 for $A_{2A}R$ and 120 nM for A_1R and, therefore, is considered as an $A_{2A}R$ selective antagonist. On the contrary, DPCPX has a K_d of 0.3 for A_1R and 340 nM for $A_{2A}R$ and, therefore, is considered as an A_1R selective antagonist (Fredholm *et al.*, 2001).

The drug application and incubation period are also fundamental in pharmacological studies. Drugs were applied through the perfusion medium for at least 15-20 minutes. The incubation time is important to allow drug binding to receptors and the detection of its effect. In some experiments, this time was prolonged because the effect onset varied from cell to cell. Other authors described topical and brief drug application, simultaneously to the ATP stimulus (Alloisio *et al.*, 2004), or a brief 3 minute incubation (Jiménez *et al.*, 1999). This short period of incubation might not lead to total activation of selective receptors.

3.2.3 Recording and analysis of Ca^{2+} transients

For the recording of Ca^{2+} transients, a specific cell was chosen from the culture and it was pressure stimulated with 10 μM ATP (200 ms) every 5 minutes throughout the experiment (Figure 3.3). Its response, as well as, the responses of surrounding cells were recorded for

about 40 seconds every 5 minutes (see Figure 3.3). The stimulus was applied 10 seconds after the beginning of the recording and the transient lasted for about 20 seconds, varying from cell to cell, until the Ca^{2+} basal levels were reached again. Preferentially, cells should be irradiated for the shortest period possible (≈ 40 seconds) to prevent fluorescence bleaching, since the experiments are long and they are irradiated several times throughout the experiment.

The initial idea was to work on single-cell experiments, because the response observed in surrounding cells might be affected by the propagation of the Ca^{2+} wave and not only by the test drug itself. Nevertheless, when results were analyzed, considering whether the cell had been directly stimulated or not, it was concluded that responses from cells that were close to the stimulated cell do not differ from the latter. For this reason, results presented here take into account not only the stimulated cell (depicted with a red circle, Figure 3.3) but also those cells that were directly surrounding the stimulated cell (depicted with blue and green circles, Figure 3.3), since they seem to have responded by direct ATP stimulation.

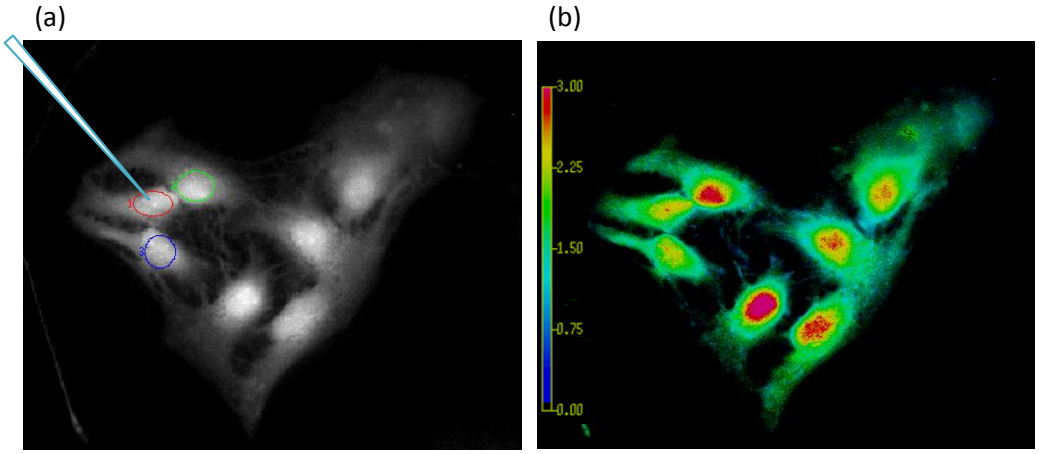

Figure 3.3 – Representative images of a Ca^{2+} imaging experiment. (a) Fluorescence image of primary astrocytes (excitation 340nm, emission 510nm) – schematic representation of a glass electrode. The circles represent the regions of interest (ROI). (b) Image representing F340/F380 ratio, where the color scale corresponds to fluorescence ratio (F340/F380), allowing to evaluate variations in $[Ca^{2+}]_i$.

Initially, HEPES buffer was applied in the perfusion medium and cell response to 10 μM ATP (200 ms) was recorded in the absence of drugs (Figure 3.4). After the first three or four ATP stimuli, when the cellular response was fairly stable, the perfusion medium was changed for the test drug diluted in HEPES buffer and cell response was recorded for at least 15-20 minutes. After this period, the medium was changed again for HEPES buffer, for washout, or for the appropriate drug mixture and cell response was recorded again for at least 15-20 minutes. In few individual cases this period had to be extended, specifically with CGS 21680, an $A_{2A}R$ selective agonist, because it is difficult to washout due to its lipofilic characteristics. At the end of every experiment, maintaining the previous perfusion medium (HEPES buffer or test drug mixture), the maximal cellular response was recorded applying a maximal stimulus with 100 μM ATP (200 ms).

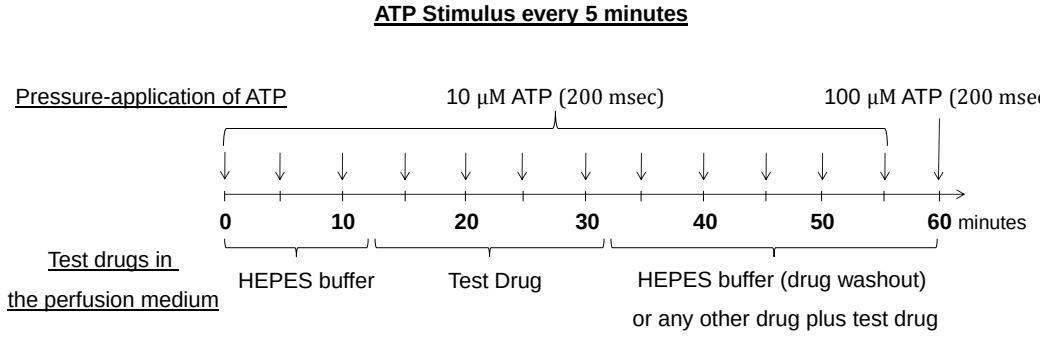

Figure 3.4 – Timeline for stimulation and drug application of a typical Ca^{2+} experiment. Each arrow corresponds to a stimulus, applied every 5 minutes. Above are presented the ATP concentrations values used as stimulus and below are the solutions applied through the perfusion medium.

In very few experiments, particularly those where an agonist and an antagonist of the ADOR were applied together to revert agonist action, cell response to 100 μM ATP was not increased in comparison to 10 μM ATP. In these cases, cells were submitted to a 20 minute washout with HEPES buffer, as they continued to be stimulated with 10 μM ATP every 5 minutes. After this period, cells were stimulated again with 100 μM ATP and response amplitude was considered as maximal. This protocol was not applied to all

experiments, because it was observed that in most cases the maximal cell response previously and after this washout period were not markedly different as can be seen in Figure 3.5.

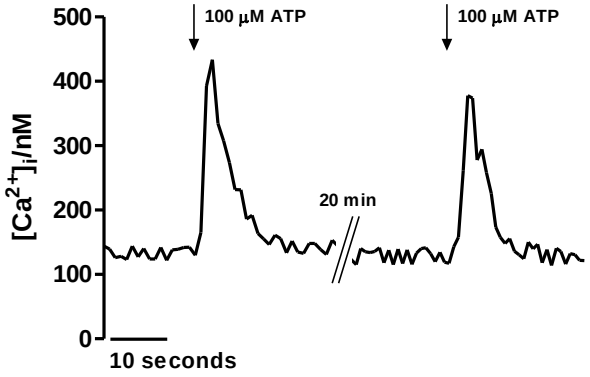

Figure 3.5 – Representative Ca^{2+} mediated responses to 100 μM ATP (200 ms), previously and after the extra 20 minutes washout step with HEPES buffer.

To estimate the amplitude of a Ca^{2+} transient, the mean of the first ten values (10x200ms) recorded before stimulation was calculated and it was taken as the baseline Ca^{2+} level. Then the amplitude was calculated by the difference between the highest value recorded for the Ca^{2+} transient and the baseline Ca^{2+} level. The amplitude of the **control response**, in the absence of any drug, was considered as the mean amplitude obtained for the transients at 5 and 10 minutes (identified in Figure 3.6). Usually, at this point cell response was fairly stable but if this was not the case, stimulation was continued, still with HEPES buffer in the perfusion medium, until the cell response was stable. Then control response was considered as the mean amplitude of the two last transients with HEPES buffer in the perfusion medium.

For the magnitude of **drug response** it was considered the largest change in the Ca^{2+} transient (maximal effect), which occurred 10 to 25 minutes after the beginning of drug perfusion. It was not possible to impose a determined period of time because each cell responds differently, therefore some cells would respond rapidly and other would take longer to respond to the drug. Some cells did not respond to drugs at all, especially those

that already presented considerable large Ca^{2+} transients in the absence of the drug. Data from these cells was also considered to calculate the average. Drug perfusion time could not be further increased because after a long experiment, with repeated stimulations, there is a tendency for a spontaneous decrease of ATP-induced Ca^{2+} transients, even in the absence of drugs. It was considered as drug response only the amplitude of one transient and not the average of two transients because responses were very different in amplitude as this parameter was increased by drug effect (see Figure 3.6).

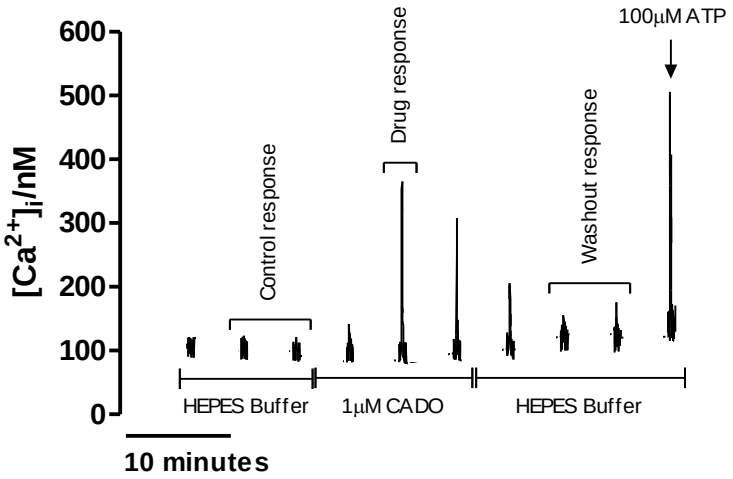

Figure 3.6 – Time course of Ca^{2+} response of a typical Ca^{2+} imaging experiment. Ca^{2+} peaks represent cell response upon ATP stimulation. All stimulations were performed with 10 μM ATP, except for the last one, indicated with an arrow, in which 100 μM ATP was used. 1 μM CADO was applied through the perfusion medium.

Concerning the final step to revert drug effect, with HEPES buffer or an agonist/antagonist drug mixture, the **washout response** was taken as the average of the two last transients before the maximal stimulus. The amplitude of **maximal response** was calculated as stated previously when cells were stimulated with a supramaximal ATP concentration (100 μM).

3.2.4 Calibration procedure

$[Ca^{2+}]_i$ was calculated from fluorescence ratio (F340/F380) using the classical equation developed by Tsien's group (Equation 3.1) (Grynkiewicz *et al.*, 1985). The K_d is the dissociation constant of Fura-2 AM to Ca^{2+}, R is the fluorescence ratio (F340/F380) value, Rmax is the R value at saturating extracellular $[Ca^{2+}]$ ($[Ca^{2+}]_{free}$ = 2 x 10^{-3} M), Rmin is the R value at low extracellular $[Ca^{2+}]$ ($[Ca^{2+}]_{free}$ = 4.172 x 10^{-9} M), A2 is the fluorescence emitted at 510 nm when cells are irradiated at 380 nm at low extracellular $[Ca^{2+}]$ and B2 is the fluorescence emitted at 510 nm when cells are irradiated at 380 nm at saturating extracellular $[Ca^{2+}]$.

Equation 3.1

$$[Ca^{2+}]_i = K_d \times \frac{Rrest - Rmin}{Rmax - Rrest} \times \frac{A2}{B2}$$

Fura-2 AM, the Ca^{2+} probe used, has a K_d of 224 nM for a solution with 1 mM of Mg^{2+} (Grynkiewicz *et al.*, 1985). All the other parameters of the equation were experimentally determined using a calibration procedure according to Benech et al. (2000). In these experiments cells were not stimulated with ATP, only the basal $[Ca^{2+}]_i$ were recorded for about 30 seconds, every 5 minutes.

Firstly, the basal $[Ca^{2+}]_i$ were recorded with HEPES buffer in the perfusion medium. The average of all the values recorded is the resting Ca^{2+} level for that specific cell, **Rrest** (see

Figure 3.7 and Figure 3.8 (a)). Then the perfusion medium was changed for a low-Ca^{2+} HEPES buffer (EGTA 10 mM - in mM: 125 NaCl; 3 KCl; 1.25 NaH2PO4; 10 glucose; 10 HEPES; 0.5 CaCl; 1.5 MgCl2; 2 MgSO4; 10mM EGTA pH ~ 7.38), which mimics an extracellular low-Ca^{2+} situation ($[Ca^{2+}]_{free}$ = 4.172 x 10^{-9} M, at 22°C and pH 7.38, calculated using MaxChelator® tool at maxchelator.stanford.edu). Followed by the addition of 1µM ionomycin free-acid (Ascent®) to the medium. This ionophore complex with Ca^{2+} and carries it across lipophilic membranes. Here it is responsible for the leak of Ca^{2+} from the

citosol of the cell to the extracellular medium, since the $[Ca^{2+}]_i$ is about 100 x 10^{-9} M, and consequent total depletion of intracellular Ca^{2+} storages. For this reason the cellular basal $[Ca^{2+}]_i$ decreases to a minimum, **Rmin**. This parameter is the average of all values recorded during the 30 seconds that cells were irradiated (≈ 5 values are recorded per second). Usually, Rmin is reached after the medium transition for regular HEPES buffer with Ca^{2+}, right before the basal $[Ca^{2+}]_i$ increases (see Figure 3.8 (a)). EGTA should be kept in perfusion for the shortest period of time possible because the lack of Ca^{2+} can lead to cell detachment from the glass coverslip. Then the perfusion medium was changed for HEPES buffer (still with 1 μM ionomycin). This medium, with Ca^{2+} ($[Ca^{2+}]_{free}$ = 2 x 10^{-3} M), leads to an increase in the $[Ca^{2+}]_i$ and consequent dye-saturation. The maximal level represents **Rmax** (see Figure 3.8 (a)). Keeping ionomycin present at this point allows the cells to reach higher basal $[Ca^{2+}]_i$.

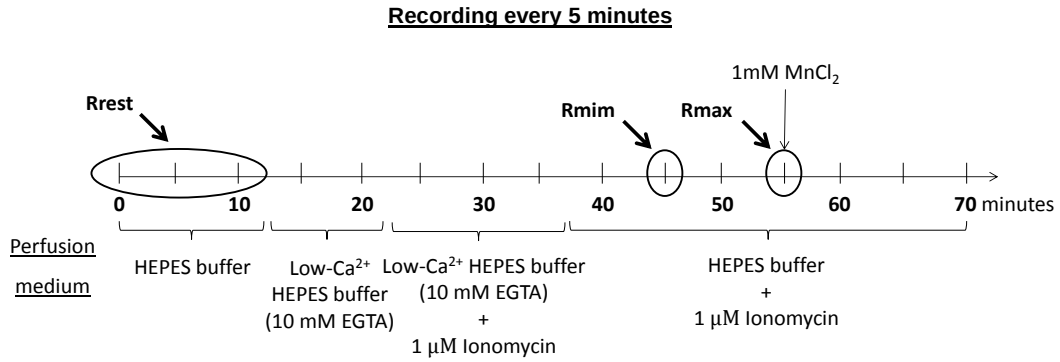

Figure 3.7 – General scheme of a typical calibration procedure experiment. Each vertical line corresponds to the recording of cellular response for 30 seconds. Below are the solutions applied through the perfusion medium. Arrows represent the values that were used to calculate Rrest (0-10 minutes), Rmin (45 minutes) and Rmax (55 minutes).

Once reached the maximal $[Ca^{2+}]_i$, 1mM $MnCl_2$ is added topically and carefully to the perfusion chamber with a pipette. $MnCl_2$ extinguishes the fluorescence from the fluorochrome leaving only the cellular autofluorescence, **Rzero** (Figure 3.8 (a)). In most

experiments, the values of Rmax and Rmin were very similar because the computer software automatically subtracted the background fluorescence and autofluorescence.

A2 and B2 were determined from the emission fluorescence at 510 nm when cells were irradiated at 380 nm, corresponding to the emission of the unbound dye (Figure 3.8 (b2)). A2 is the fluorescence emitted when $[Ca^{2+}]$ in the medium is minimal, corresponding to Rmin in the fluorescence ratio. B2 is the fluorescence emitted when external $[Ca^{2+}]$ is maximal, corresponding to Rmax in the fluorescence ratio.

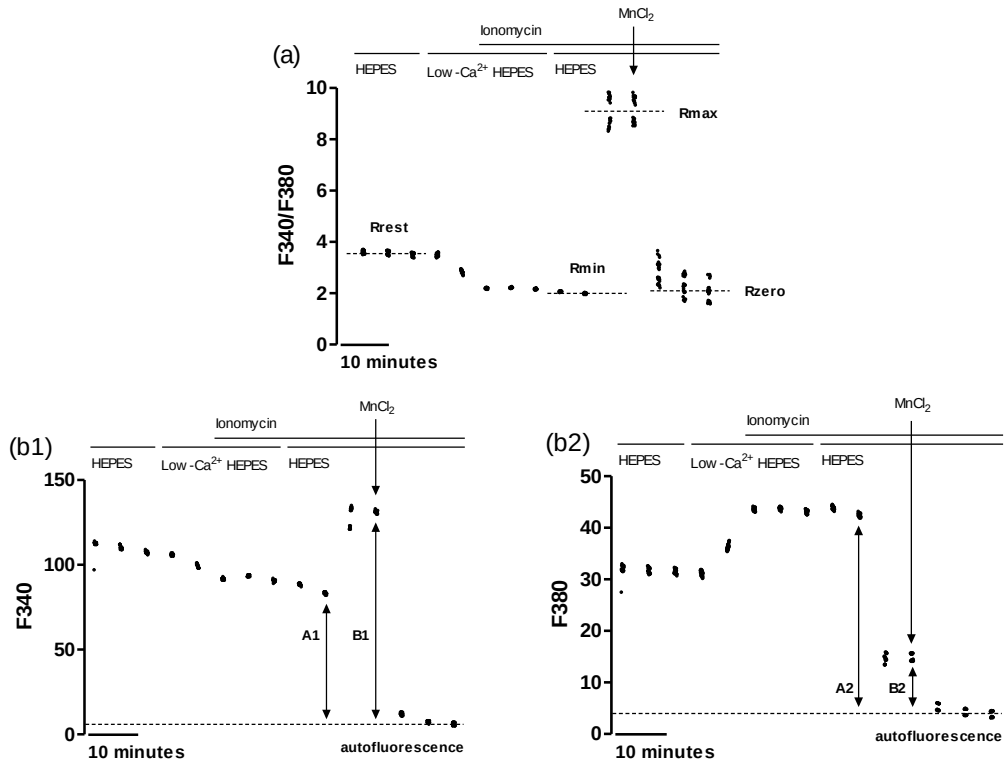

Figure 3.8 – Representative fluorescence of Ca^{2+} mediated responses for a calibration procedure. (a) Fluorescence ratio (F340/F380), (b1) fluorescence at 340 nm and (b2) fluorescence at 380 nm. Solutions applied through the perfusion medium are indicated.

The calibration protocol to convert fluorescence ratio (F340/F380) into $[Ca^{2+}]_i$ should be, ideally, performed in the end of each and every experiment, since the parameters determined are specific of each cell. However, at the end of long experiments, such as

these, cells would respond differently to the protocol compared to their typical response. Moreover, not all the drugs used are easily washed out from cells, which would certainly affect cell response. For these reasons, it was decided to perform separate experiments, in which designated batches of cells were used to apply the calibration procedure. The previous parameters were calculated taking into account cell responses from these experiments.

5 independent experiments were performed and each one of the specific parameters (Rrest, Rmin, Rmax, A2 and B2) was determined for each cell. Then, from the average of the parameters estimated for all the cells of one experiment, the $[Ca^{2+}]_i$ was calculated using the equation of Grynkiewicz *et al.* (1985) (Equation 3.1). Then, the values of $[Ca^{2+}]_i$ *vs.* mean values of F340/F380 were plotted (Figure 3.9). Appling the equation determined by the linear regression of the points ($[Ca^{2+}]_i$ = 73.796 x F340/F380 – 26.494), it was possible to convert the fluorescence ratio of all the other experiments into $[Ca^{2+}]_i$.

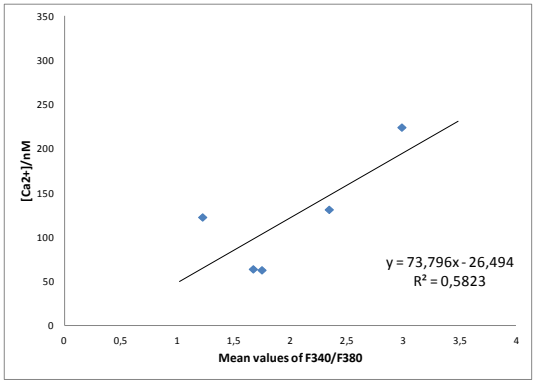

Figure 3.9 – Plot of $[Ca^{2+}]_i$ (nM) vs. mean value of fluorescence ratio (F340/F380) and respective linear regression equation. Each value represents the average of the values calculated for cells of one experiment.

3.3 Optimization of Ca^{2+} imaging experiments

The experimental protocol, to study Ca^{2+} transient modulation by adenosine, described in the previous section was developed and conditions, such as the interval between stimuli,

ATP concentration, stimulation length, rate of the perfusion medium and incubation and perfusion temperatures were optimized. Experimental approach and conditions, inspired in previous works (Jiménez *et al.*, 1999; Alloisio *et al.*, 2004), were improved to fulfill the aims of this project.

3.3.1 Interval between stimuli

The initial idea was to obtain a cellular response for each of the experimental conditions, in the absence of drug, in the presence of the test drug and after the washout. In early experiments, cells were stimulated with ATP every 20 minutes, which is coincident with the minimum period of time for the ADOR ligands to be effective, when applied through the perfusion medium. This was the type of approach used by Alloisio et al. (2004) and Jimenez et al. (1999). However, obtaining just one response per condition was not a good approach due to the slight oscillations in cellular response throughout experiments. This variability was observed not only within cell population but also for each cell in particular. Therefore, in order to accurately differentiate slight drug effects it was important to obtain several measures for each condition so that an average response could be estimated. For this reason, it was decided to decrease the interval between stimulations.

Experiments were performed using 2 minute intervals between stimuli but it seemed that the interval was too short. Cells did not have enough time to recover, probably to refill the internal Ca^{2+} storages, and therefore Ca^{2+} response amplitude decreased throughout experiments.

Subsequently, experiments were performed using 5 minute intervals between stimuli. This seemed to be an ideal protocol because it allowed cells to recover from the continuous stimulation and also the recording of several cellular responses for each condition. However, with this protocol, the length of the experiment increased and cells were continuously exposed to UV light. A natural concern was whether cells would continue to respond or not. It was experimentally confirmed that cells were able to maintain their response for more than one hour.

3.3.2 ATP concentration

It was highly important to determine the ATP concentration to be used as stimulus. To study the potential effect, potentiation or inhibition, of drugs on Ca^{2+} transients it is imperative to obtain a response that is significant but that is not maximal.

For this purpose, cumulative concentration-response experiments were performed. Cells were sequentially stimulated with increasing ATP concentrations (in μM: 0.1, 0.5, 1, 5, 10, 50, 100, 500, 100) every 5 minutes. For each concentration, 2 responses were recorded and the average was estimated. For the total pool of cells studied (n=20), 10 μM ATP, seems to be a good stimulus because it elicits a significant signal response, compared to lower concentrations, nevertheless it does not equals cell maximal response (Figure 3.10 (a)). Surprisingly, maximal response is observed for 50 μM ATP and it is not overcome for higher ATP concentrations. This result could be due to desensitization of ATP receptors to higher agonist concentrations. However, an individual analysis of cellular responses showed that this was a heterogeneous cell population, in which two different cellular behaviors can be distinguished for responses to high ATP concentration stimulation. On the one hand, some cells are able to respond to high concentrations and it is seen that a plateau is reached for ATP concentrations equal or higher than 50 μM (Figure 3.10 (b1)). On the other hand, few cells clearly present a diminished response capacity as the concentration of ATP stimulus was increased (Figure 3.10 (b2)). It is noteworthy that the latter population of cells presents a higher mean response to 10 μM ATP. From this individual analysis, because the decay in cell response is not common to all cells, it can be proposed that this effect is not due to receptor desensitization but due to repetitive cell stimulation, which leads to progressive lost of response capacity.

The lost of response capacity is indeed one of the disadvantages of cumulative concentration-response studies, where the same target cell is used throughout the experiment. Another shortcoming is that results obtained do not correspond to the real maximal cell response as cells saturate. Nevertheless, they are a good approach for the

present purpose of finding an optimal ATP concentration since we do not have the problem of variability in cell response associated to different cells.

50 µM ATP and higher concentrations are supramaximal, meaning that the cell response obtained upon stimulation is maximal. For this reason, 100 µM ATP was used to measure the maximal response of each cell to ATP stimulation.

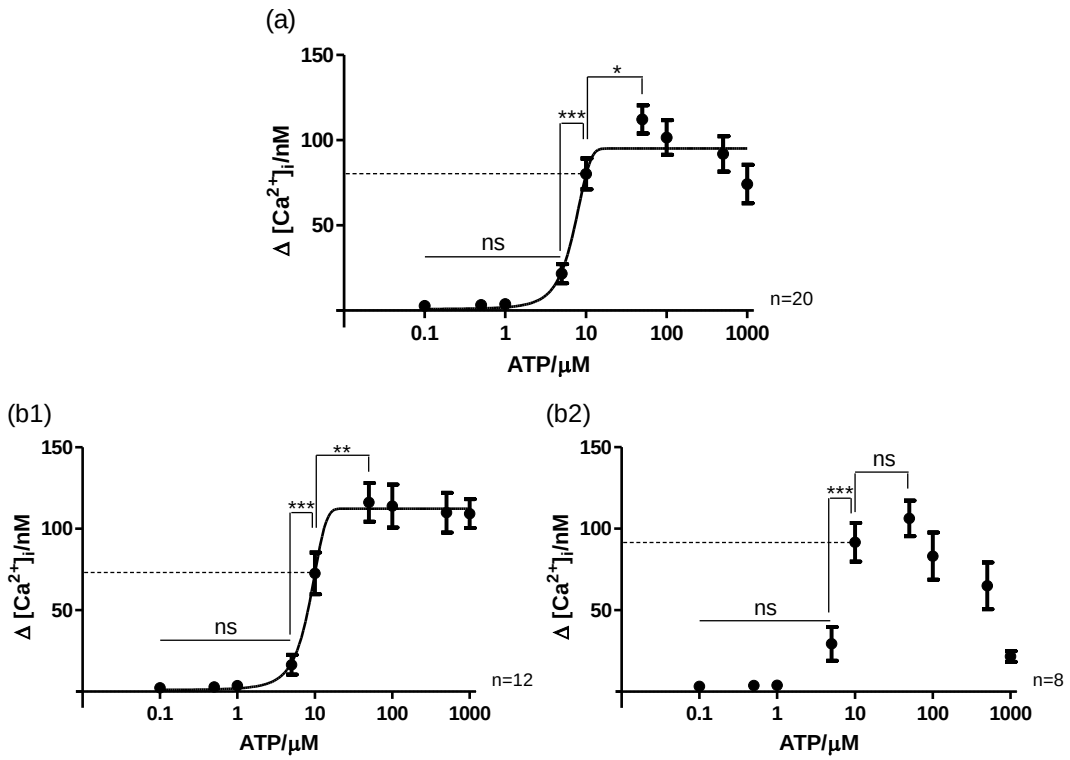

Figure 3.10 – Mean amplitude of Ca^{2+} transients upon stimulation with increasing ATP concentrations with the fitting of a cumulative Gaussian curve. (a) Total pool of cells studied (R^2 = 0.953). (b1), (b2) Cell populations with different responses within the total pool of cells ((b1) R^2 = 0.998). Results are presented as mean of n cells.

3.3.3 Stimulation length

As previously stated in the Introduction, the duration of the stimulation with ATP is an important factor that determines which ATP receptors are preferentially activated, P2YR

or P2XR. As I was particularly interested in studying the effect of adenosine modulation upon the initial transient peak, mediated mostly by P2YR, the stimulation length should be as small as possible. 100 ms is the minimum technically possible due to limitations of the injector, nevertheless, the response elicited using 10 µM ATP (100 ms) is mostly inexistent or undetectable. For this reason, 200 ms of stimulation were used for all experiments. This stimulus (10µM ATP for 200 ms) triggers a small but visible Ca^{2+} peak, in which drug effects could be discerned.

Experimental conditions determined, so far, are close to the physiological situation because stimulation was achieved with a low ATP (10 µM) concentration for a brief (200 ms) period of time, when compared to previous works. Alloisio et al. (2004) used a stimulus of 0.3 µM or 10 µM of ATP with a duration up to hundreds of seconds (50 – 400 seconds). In this case stimulus length is too long and cell response might reach saturation, which would not allow evaluation of signal modulation.

The optimized conditions (10 µM ATP for 200 ms) allowed to perform repeated stimulations for a considerable period of time (≈ 60 minutes) so that different pharmacological situations could be tested. This is advantageous because it allowed direct comparison of amplitudes of peaks obtained in the presence and absence of test drugs for the same cell and also direct comparison of results from different pharmacological approaches.

3.3.4 Rate of the perfusion medium

Throughout experiments, cells were continuously perfused with HEPES buffer or the test drug at a rate of approximately 1.5mL/minute. This rate is similar to what was used by other authors, 1-1.5 mL/minute (Jiménez *et al.*, 1999) and 2.5 mL/minute (Alloisio *et al.*, 2004).

In initial experiments, the medium flow was stopped before stimulation, and different intervals of time were tested. By stopping the flow, the medium stabilized before the stimulus was applied and therefore did not influence cell response. Nonetheless, using

this approach, cell response was extended because ATP and consequently adenosine were not instantly washed out. This was a disadvantage because it easily saturates cell response, masking drug effect. For this reason, it was decided to keep the perfusion medium always on, so that the rapid flow prevents ATP accumulation. Furthermore, constant buffer flow did not appreciable affect the stability of cell response.

3.3.5 Incubation and perfusion temperatures

Temperature is an important factor in any cellular experiment because it directly influences cell activity and consequently cell response. In this particular case, both incubation and perfusion temperatures are important. Cells were incubated at 37°C in an incubator, with controlled conditions, in order to maintain cell viability for a longer period of time. Initially, cells were incubated at RT (22°C) and no appreciable differences in their responses seem to occur, when compared to cells incubated at 37°C. However, by direct cell observation, it appeared that cells were not so intensively fluorescent. This is probably due to less uptake of fluorochrome at lower temperatures, although to confirm this idea the actual emitted fluorescence had to be quantified. For these reasons, cells were incubated at 37°C as previously described by several authors (Jiménez *et al.*, 1999; Alloisio *et al.*, 2004; Fischer *et al.*, 2009).

The incubation period should not be too long to avoid compartmentalization of the indicator dye in intracellular compartments, therefore cells were incubated for 45 minutes as described by Alloisio et al. (2004) rather than for 60 minutes (Jiménez *et al.*, 1999). Incubating cells for less than 45 minutes is not a good option because internalized dye might not underwent complete removal of AM ester groups and therefore the fluorochrome might leak from the cell.

Concerning the temperature of the perfusion medium, experiments were performed both at RT (22°C) and at 30°C. The major difference was that, at 30°C, the basal $[Ca^{2+}]_i$ and transient amplitude to ATP stimulation were augmented. This increase is probably due to higher cellular activity and is not favorable because it approximates cell response to its

maximum. Furthermore, technically, to ensure that this high temperature (30°C) was maintained when changing the medium, through a semi-automatic tap system, was difficult. As slight changes in temperature are a source of destabilization it was decided to perform all experiments at RT (22°C).

It is likely that temperature also affects the characteristics of the Ca^{2+} probe employed, such as, the fluorescence and the K_d. Nonetheless, in the particular case of Fura-2 it was reported that the florescence does not vary significantly over a broad range of temperatures (0°C-40°C) in the hour following solution preparation (Oliver *et al.*, 2000). Furthermore, since Fura-2 is a ratiometric dye, both bound and unbound forms of the dye are affected equally, concealing the destabilization in the final ratio value.

3.4 Culture characterization

3.4.1 Immunocytochemistry

Cell population was characterized by immunocytochemistry using specific antibodies for GFAP (Glial Fibrillary acidic protein), an astrocytic masker, MAP2, a neuronal marker, and CD11b, a microglial cell marker. DIC 14 cortical astrocytes in 24-well plates were washed with PBS (2x5minutes), to remove DMEM medium, and then fixed with 4% paraformaldehyde (PFA) in PBS for 20 minutes. Cells were washed again with PBS (2x5minutes) and then kept with this medium in the fridge (4°C). These cells could be used up to one month after the fixation process. DIC 14 was chosen for fixation because it corresponds approximately to the time period of Ca^{2+} experiments (DIC 9 – DIC 14). The PFA reagent used here establishes cross-link bridges between cytoskeleton proteins, preserving almost intact the cellular architecture.

At the day of the experiment, cells were firstly permeabilized with 0.05%Triton, a nonionic detergent, for 10-15 minutes followed by a washing step with PBS (2x5minutes). Blockade was successfully achieved by 30 minute incubation with 0.25% gelatin in PBS, for MAP-2/GFAP staining, or 10% goat serum/0.03% triton in PBS, for CD11b/GFAP staining. Gelatin and goat serum interact with possible epitopes increasing binding competition and

consequently decreasing nonspecific binding. Primary antibodies were incubated overnight at 4°C, with agitation. Secondary antibodies were incubated for 1 hour at RT, also with agitation. Both primary and secondary antibodies were diluted in 0.1% gelatin or 10% goat serum/0.03% triton in PBS for MAP-2/GFAP and CD11b/GFAP staining, respectively. Nuclei were stained with DAPI (4',6-diamidino-2-phenylindole, 1:15000), which binds strongly to DNA, for 5 minutes. After antibody incubation, cells were washed with 0.05% PBS-Tween-20 (PBS-T) (3x5minutes). Tween-20 is a detergent used to wash unbounded or nonspecific bounded antibodies, decreasing nonspecific binding. After 1 last wash with Mili-Q water, coverslips were mounted in Mowiol anti-fade mounting medium (Sigma®) and were let to dry for one day at RT. Afterwards the slides were kept in the fridge (4°C) for subsequent microscopic analysis.

Results were analyzed through an epifluorescence microscope (Axiovert 200, Zeiss®) equipped with 10x and 40x amplification objectives. To detect fluorescence at different wavelengths specific filters were used: DAPI (blue), YFP (green) and Rhodamine (red). For cell count, the ImageJ® 1.44p software was used.

Table 3.2 - Primary and secondary antibodies used in immunocytochemistry experiments to target different cell populations: astrocytes, microglial cells and neurons.

Cell type	Target protein	Primary antibody	Animal	Dilution	Secondary antibody	Dilution
Astrocytes	GFAP	SIGMA®	Rabbit	1:100	goat anti-rabbit Alexa 568, Invitrogen®	1:500
		Chemicon®	Mouse	1.100	goat anti-mouse Alexa 488, Invitrogen®	
Microglial cells	CD11b	Serotec®	Mouse	1:500		
Neurons	MAP-2	Chemicon®	Mouse	1:200	Goat anti-mouse Alexa 568, Invitrogen®	

3.4.2 Western blot and protein quantification

The expression of purinergic ATP ($P2Y_1$) and adenosine (A_1 and A_{2A}) receptors in primary astrocytic cultures was detected by western blot technique using specific antibodies for each receptor. Firstly, I applied the lysis buffer method to detect these proteins in DIC 14

cultures and later the sucrose buffer method was applied to detect $A_{2A}R$ in DIC14 and DIC21 cultures.

Lysis buffer method – $P2Y_1R$, A_1R and $A_{2A}R$

DIC 14 cortical astrocytes plated in 100-mm-diameter glass bottom microwell dishes were washed twice with cold PBS (in mM: 137 NaCl; 2.1 KCl, 1.8 KH_2PO_4; 10 NaH_2PO_4) and then lysed by adding 2.5 mL of lysis buffer (in mM: 25 Tris base at pH 7.5, 150 NaCl, 1 EDTA, 1% Triton X-100 plus EDTA-free protease inhibitors cocktail (Roche®) and also 5 mM *N-Ethylmaleimide* (NEM) (Sigma®) and 0.2 mM *Phenylmethylsulfonyl fluoride* (PMSF) (Sigma®)). After 30 minute incubation in ice, cellular membranes were mechanically dissociated by pipetting through a P1000 tip, followed by 10-15 minutes incubation in the fridge with agitation. After 15 minute centrifugation (25,000g) at 4°C, the supernatant was transferred to an eppendorf and frost (-20°C) for later protein quantification and western blot.

Prior to western blot, protein denaturation was achieved using sample buffer (70 mM Tris-HCl, 6% glycerol, 2% SDS, 120 mM dithiothreitol, 0.0024% Bromophenol Blue, pH 6.8) for 10 minute, at 70°C. Tris-glycine SDS-polyacrylamide gel for electrophoresis was prepared using 10% resolving gel and 5% stacking gel. The apparatus was mounted with running buffer (25 mM Tris, 192 mM glycine, 0.1% SDS) and equal volumes of all the samples were loaded into the gel (20 μg of protein) (see
Table 3.3). Samples were stacked by running at 80 V and resolved at 140 V.

Proteins were transferred from the gel into the *polyvinylidene difluoride* (PVDF) membrane at maximum current for about 1h30min. Membranes were previously activated with methanol for about 15 seconds. For the transference, transfer buffer was used (24 mM Tris, 182 mM glycine, 15% methanol). Afterwards, membranes were washed in 0.05% PBS-T, followed by blockage with 5% non-fat powered milk (w/v) in 0.05% PBS-T for 1 hour at RT. During blockage and until the end of the experiment membranes were constantly shaken. Then again membranes were washed with 0.05% PBS-T (3x5minutes).

Membranes were incubated overnight at 4°C with primary antibodies, diluted in 0.02% NaN_3/3% BSA solution in 0.05% PBS-T (

Table 3.3). Then membranes were washed with 0.05% PBS-T (3x5minutes). Followed secondary antibody incubation for 1 hour at RT. The secondary antibodies were diluted in 5% non-fat powered milk (w/v) in 0.05% PBS-T. Again membranes were washed with 0.05% PBS-T (4x10minutes) and one last time with PBS. For protein detection the ECL plus WB detection reagent (GE Health Care®) was used. This reagent will luminesce when exposed to the reporter on the secondary antibodies and the chemiluminescence emitted is detected by the X-Ray film (Fugifilm®).

Sucrose buffer method - A_1R, $A_{2A}R$

DIC 14 and DIC 21 cortical astrocytes plated in 100-mm-diameter glass bottom microwell dishes were washed twice with cold PBS and then lysed by adding 800 µL of 0.32M sucrose buffer with 50 mM Tris plus protease inhibitors cocktail (ROCHE®), pH 7.6. Then cells were mechanically dissociated by rapidly scraping the plate with a cell scraper and pipeting with a syringe. After 10 minute centrifugation (1000g) at 4°C, the supernatant was transferred to an eppendorf and frost (-20°C) for later protein quantification and western blot. Protein concentration was achieved at 70°C in a water bath. Once again, DIC 14 was chosen and also DIC 21 because at 3 weeks, cells are more confluent and the total amount of $A_{2A}R$ is higher, which supposedly makes it easier for detection.

Prior to the western blot, protein denaturation was achieved using sample buffer for 30 minute, at 37°C. Sample loading (125 µg of protein) and running were performed as previously described. Protein transference into the PVDF membrane and blockade in 5% non-fat powdered milk (w/v) in Tris Buffered Saline (TBS) (in mM: 0.2 Tris, 137 NaCl) with 0.1% Tween-20 (TBS-T), were performed as described for the lysis buffer method. In the presence of constant shake, membranes were washed with 0.1% TBS-T (3x5minutes).

Membranes were incubated overnight at 4°C with primary antibodies, diluted in 0.02% NaN_3/3% BSA solution in 0.1% TBS-T (

Table 3.3). Membranes were washed with 0.1% TBS-T (4x10minutes). Followed secondary antibody incubation for 1 hour at RT. The secondary antibodies were diluted in 5% non-fat powdered milk (w/v) in 0.1% TBS-T. Again membranes were washed with 0.1% TBS-T (4x10minutes) to remove nonspecific bonded antibodies and one final time with TBS. Proteins were detected as described previously.

Table 3.3 - Protein loading, primary and secondary antibodies used in western blot to detect P2 ($P2Y_1$) and P1 (A_1 and A_{2A}) receptors and α-tubulin, an internal control.

Protein	**DIC**	**Lysis method**	**Protein Loading (µg)**	**Primary Antibody**	**Animal**	**Dilution**	**Secondary Antibody**	**Dilution**
$P2Y_1R$	14	Lysis Buffer	20	Alamone labs® (APR-009)	Rabbit	1:200	goat anti-rabbit (sc-2004) goat anti-mouse (sc-2005) Santa Cruz Biotechnology®	1:10000
A_1R	14	Lysis Buffer	20	Affinity BioReagents® (PA1-041A)	Rabbit	1:1000		1:15000
	14	Sucrose Buffer	125					
	21	Sucrose Buffer	125					
$A_{2A}R$	14	Lysis Buffer	20	Upstate® (05-717)	Mouse	1:2000		1:5000
	14	Sucrose Buffer	125					
	21	Sucrose Buffer	125					
α-Tubulin	-	-	-	Abcam® (ab4074)	Rabbit	1:5000		1:10000

Protein Quantification

Total protein quantification was performed according to the Bradford method assay (Bradford, 1976) using the Bio-Rad® Protein assay kit. Different BSA concentrations (in mg/mL: 0, 0.05, 0.1, 0.2, 0.3, 0.4, 0.5, 0.6, 0.7, 0.8, 0.9, 1) were used as standard. Results of absorbance at 750 nm (Abs 750 nm) vs. [BSA] are plotted in Figure 3.11. The equation from the linear regression was used to calculate the concentration of each sample from

their Abs 750 nm and therefore determine the volume that corresponds to either 20 or 125 µg of protein.

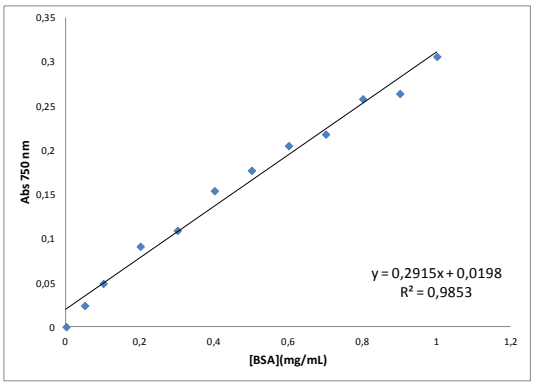

Figure 3.11 - Graphic representation of the variation of absorbance at 750 nm for various BSA solutions of known concentration.

3.5 Statistical Analysis

Bar plots represent mean ± standard error mean (s.e.m.). Statistical significance of differences between mean values was evaluated using a parametric test, one-way ANOVA for repeated measures, with a post-Bonferroni test to compare all pairs of columns (95% confidence interval). Differences were regarded as statistically significant for $p < 0.05$. For fold increase values, statistical analysis was performed using a one-way analysis of variance with a post-Dunnett test to compare all columns *vs.* a control column (fold increase = 1, which represents no variation of cell response upon drug perfusion). When comparing statistical significance, the following code was used: ns – non significant; * $p < 0.05$; ** $p < 0.01$; ***$p < 0.0001$.

4 Results

4.1 ATP induces Ca^{2+} signalling

A brief stimulation of P2R with 10 μM ATP (0.2 seconds) induced a sharp and fast Ca^{2+} peak (Figure 4.1; Figure 4.2). The $[Ca^{2+}]_i$ returned to the basal levels approximately 20 seconds after the stimulus. Signal transients induced by a prolonged 10 μM ATP stimulus (≥ 20 seconds) presented a biphasic behavior constituted by an initial large transient peak followed by a smaller sustained phase (Figure 4.1). As the aim of this project was to study the modulation of the initial Ca^{2+} peak, mediated mostly by P2YR (Alloisio *et al.*, 2004), it was decided to use a brief stimulus (0.2 seconds) in all experiments.

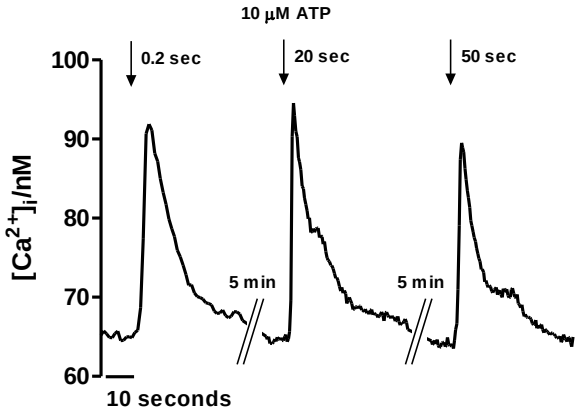

Figure 4.1 – Representative Ca^{2+}-mediated responses elicited by 10 μM ATP for different stimulus length (0.2, 20 and 50 seconds). Cells were perfused only with HEPES buffer, no pharmacological treatment was applied.

When perfusing cells with a low-Ca^{2+} HEPES buffer, the amplitude of the transients decreased throughout the time, nevertheless, cells continued to respond. Adding Ca^{2+} to the perfusion medium was enough to completely reverse the effect observed (Figure 4.3). These observations indicate that both metabotropic P2YR and ionotropic P2XR contribute to the cytoplasmic Ca^{2+} rise induced by ATP.

A decrease in the baseline $[Ca^{2+}]_i$ was observed in the presence of low-Ca^{2+} medium, which is promptly reverted when Ca^{2+} is added to the medium, reinforcing the idea that external Ca^{2+} entry is important to maintain $[Ca^{2+}]_i$ stable.

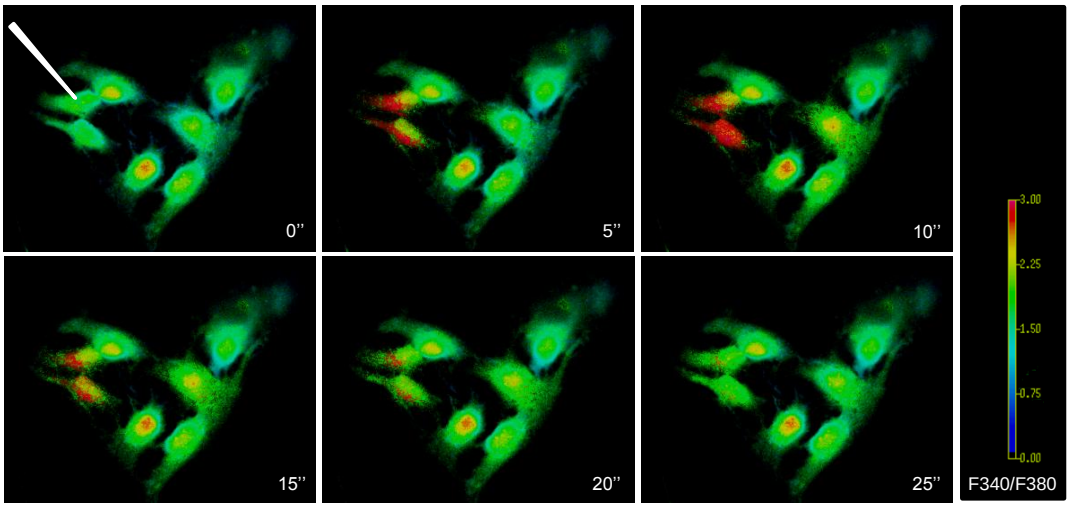

Figure 4.2 – Representative sequence of images of a Ca^{2+} transient. The color scale corresponds to fluorescence ratio (F340/F380), which allows to evaluate variations in $[Ca^{2+}]_i$.

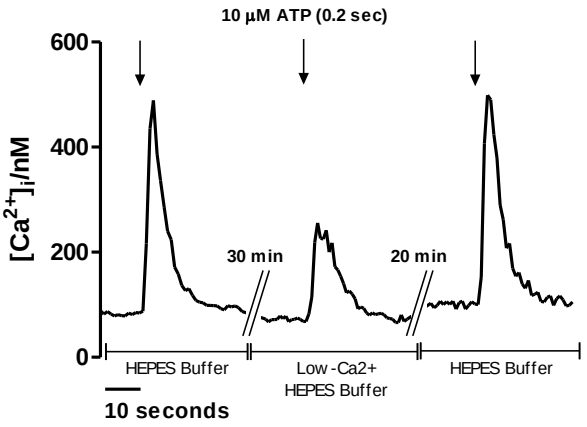

Figure 4.3 – Representative Ca^{2+}-mediated responses to 10 µM ATP (0.2 seconds) for a low-Ca^{2+} medium experiment. The perfusion medium was changed from the initial HEPES buffer with Ca^{2+} ($[Ca^{2+}]_{free}$ = 2 x 10^{-3} M) to low-Ca^{2+} HEPES buffer ($[Ca^{2+}]_{free}$ = 1.6 x 10^{-7} M) and back again to regular buffer for the washout. Cells were continuously stimulated with ATP every 5 minutes.

4.2 Ca^{2+} signalling modulation by adenosine

4.2.1 Modulation by ADOR activation

To evaluate the role of adenosine receptors, particularly $A_{2A}R$, in Ca^{2+} signalling modulation, an adenosine analogue - 2-chloro-adenosine (1µM CADO), which binds unselectively to adenosine receptors, was used. CADO presents a high structural similarity to adenosine but is resistant to metabolization by ectoenzymes or uptake by cells. An $A_{2A}R$ selective agonist, CGS 21680 (30 nM), was also used.

The adenosine analogue, 1 µM CADO, markedly enhanced the signal response induced by 10 µM ATP (fold increase: 3.19 ± 0.30, n = 73 cells, $p < 0.0001$) (Figure 4.4 (a); Figure 4.5 (a)). The magnitude of the effect corresponds to the ratio between the amplitude of the transient obtained in the presence of the agonist and the amplitude of the transient obtained in the absence of the agonist, for each cell. The $A_{2A}R$ selective agonist, 30 nM CGS 21680, mimicked the facilitatory effect (fold increase: 2.92 ± 0.32, n = 80 cells, $p < 0.0001$) (Figure 4.4 (a); Figure 4.5 (a)). This result indicates the involvement of $A_{2A}R$ in the modulatory effect.

In the presence of higher stimuli (50 µM and 100 µM of ATP) there was no significant potentiation of Ca^{2+} responses to the agonists, 1 µM CADO and 30 nM CGS 21680 (data not shown).

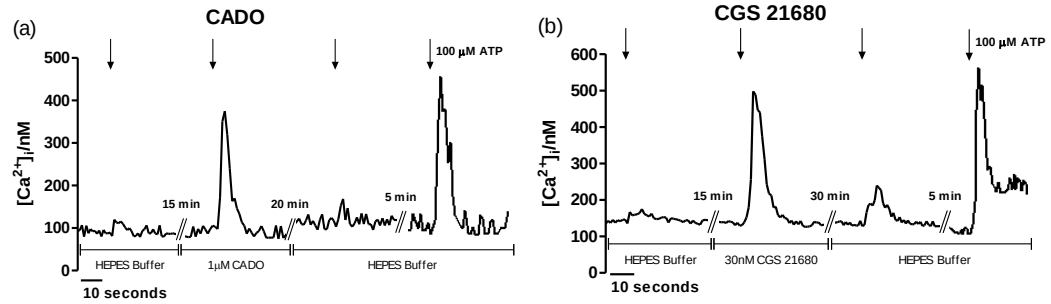

Figure 4.4 - Representative Ca^{2+} mediated responses to 10 µM ATP (200 ms) for experiments with (a) 1 µM CADO and (b) 30 nM CGS 21680. For each experiment is presented a response in the presence of HEPES buffer, test drug, after the washout with HEPES buffer and triggered by 100 µM ATP.

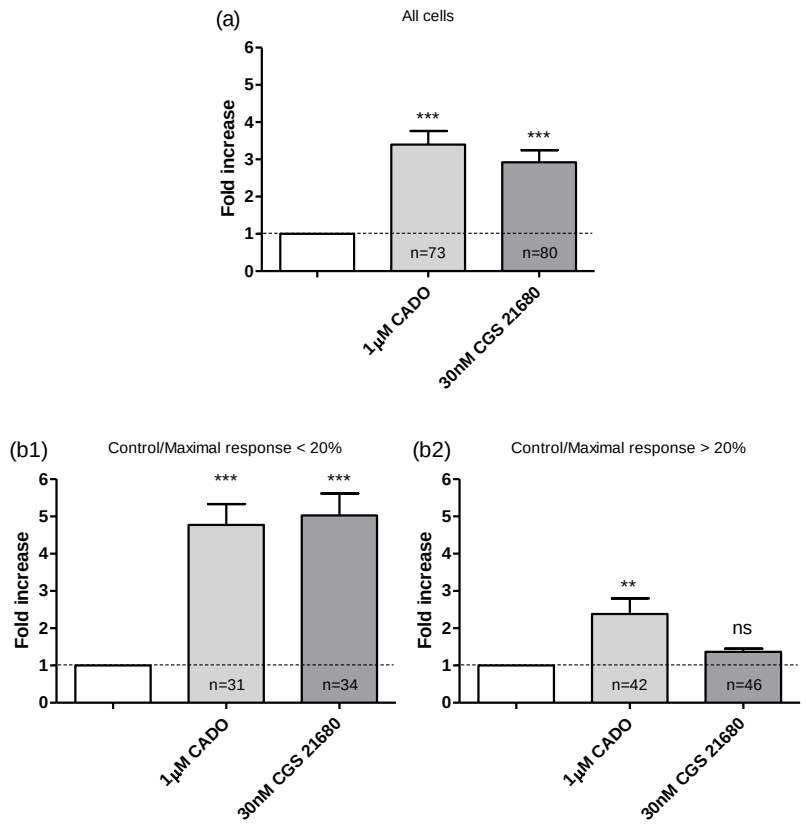

Figure 4.5 – Fold increase of 10 µM ATP-induced responses, observed in the presence of 1 µM CADO and 30 nM CGS 21680. (a) Mean values from the entire pool of cells studied (CADO, n = 73 cells, 19 experiments; CGS 21680, n = 80 cells, 24 experiments). (b1) Mean values considering only those cells that presented a control/maximal response < 20% (CADO, n = 31 cells, 12 experiments; CGS 21680, n = 34 cells, 16 experiments). (b2) Mean values considering only those cells that presented a control/maximal response > 20% (CADO, n = 42 cells, 17 experiments; CGS 21680, n = 46 cells, 24 experiments). Statistical significance: ns – non significant, ** $p < 0.01$, *** $p < 0.0001$.

Another parameter calculated was the percentage of control/maximal response. This parameter is the ratio between the amplitude of the transient triggered by 10 µM ATP stimulation and the amplitude of the transient triggered by 100 µM ATP, in the absence of test drugs. When plotting the fold increase *vs.* control/maximal response to all the cells

studied for CADO and CGS 21680, separately, an interesting correlation between this parameter and the effect of CADO and CGS 21680 was evident (Figure 4.6 (a) and (b)).

Cells that presented a smaller control/maximal response, in particular those under 20%, underwent a higher increase in response in the presence of the agonists, and therefore presented a higher fold increase (CADO 4.77 ± 0.56, n = 31 cells, $p < 0.0001$; CGS 21680 5.03 ± 0.59, n = 34 cells, $p < 0.0001$) (Figure 4.5 (b1); Figure 4.6 (a) and (b)). That is to say that, cells presenting a small control response to 10 µM ATP underwent a markedly potentiation in Ca^{2+} response in the presence of the adenosine receptors agonist (Figure 4.6 (a1) and (b1)). The potentiation induced by the adenosine receptor agonist decreased as control/maximal response increased, meaning that cells presenting a higher control response to 10 µM ATP are characterized by a smaller fold increase value caused by adenosine receptor stimulation (CADO 2.39 ± 0.42, n = 42 cells, $p < 0.01$; CGS 21680 1.37 ± 0.08, n = 46 cells, non significant)) (Figure 4.5 (b2); Figure 4.6 (a2) and (b2)). These observations clearly show the heterogeneity in cell response within the cell population.

To analyse cell response to drugs throughout experiments, bar plots were made to represent the mean of Ca^{2+} transient amplitude in the absence and in the presence of the agonist, after the washout with HEPES buffer and also the maximal response triggered by 100 µM ATP (Figure 4.7). The mean amplitude of Ca^{2+} transients was presented for the entire pool of cells (Figure 4.7 (a) and (b)) and separately for cells that had control/maximal response under 20% (Figure 4.7 (a1) and (b1)) and above 20% (Figure 4.7 (a2) and (b2)). As shown, the facilitatory effect upon ATP-induced Ca^{2+} signals mediated by both agonists (1 µM CADO and 30 nM CGS 21680) was reverted by washout with HEPES buffer (Figure 4.7 (a) and (b)). This indicates that the effect was due to the agonist perfusion and not caused by any other interference. For CADO, the unselective agonist, the potentiation was completely reverted during washout while for CGS 21680, the $A_{2A}R$ selective agonist, the reversion was not so effective.

The amplitude of Ca^{2+} responses in the presence of CGS 21680 (30 nM) represented 66% of the maximal response amplitude (100 µM ATP), which indicates that the saturation plateau was not reached with CGS 21680 perfusion (Figure 4.7 (b)). On the contrary, the

amplitude of Ca^{2+} responses in the presence of CADO (1 µM) represented 94% of the maximal response amplitude (100 µM ATP), which means that the saturation plateau was reached with the perfusion of CADO (Figure 4.7 (a)). Therefore in the case of CADO, the ceiling effect may camouflage the magnitude of the effect. For this reason, lower concentrations of CADO need to be tested in the future to compare the efficacy of both CADO and CGS 21680 to enhance ATP-induced Ca^{2+} signals in astrocytes.

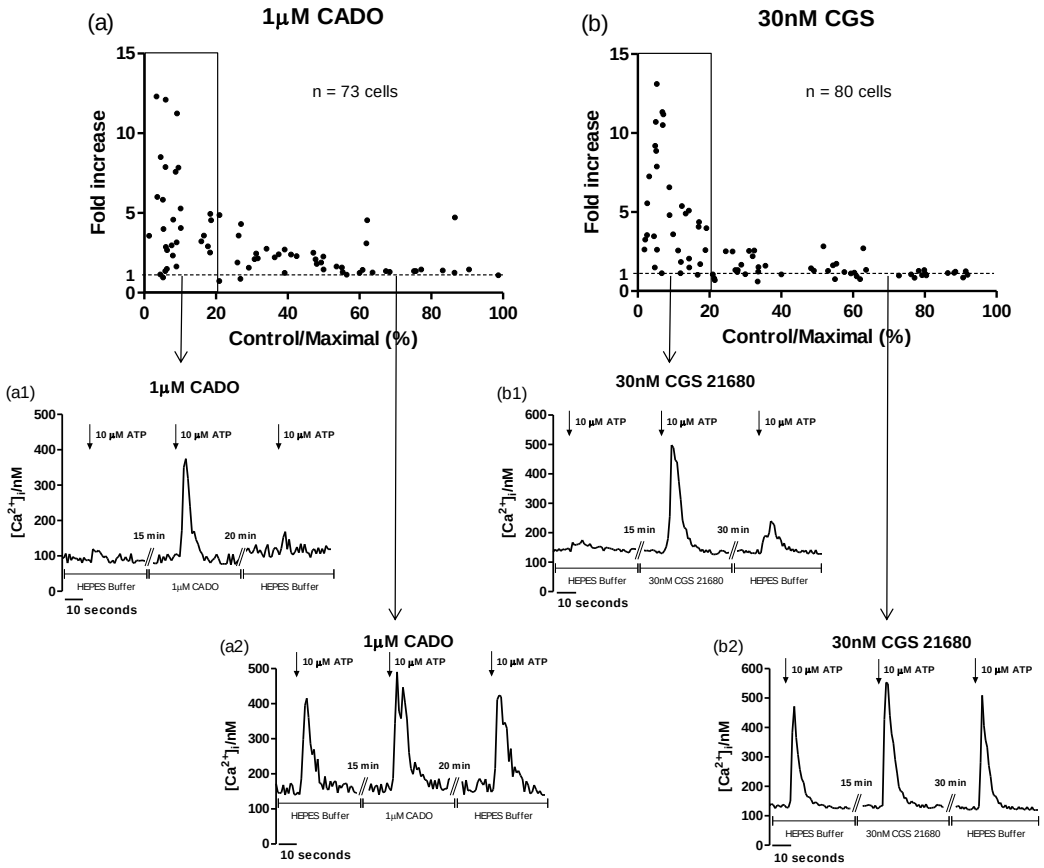

Figure 4.6 – Cell distribution for values of fold increase vs. control/maximal values for (a) 1 µM CADO and (b) 30 nM CGS 21680. Representative Ca^{2+} mediated responses to 10 µM ATP (200 ms) for experiments with 1µM CADO or 30nM CGS 21680, which presented control/maximal response < 20% ((a1) and (b1)) or > 20% ((a2) and (b2)). For each experiment is presented a response in the presence of HEPES buffer, test drug (CADO or CGS 21680) and after the washout with HEPES buffer.

When comparing the Ca^{2+} response obtained for the entire pool of cells (Figure 4.7 (a) and (b)) with Ca^{2+} response obtained for those cells that presented control/maximal response under 20% (Figure 4.7 (a1) and (b1)), it can be seen that the amplitude of ATP-induced Ca^{2+} transients (as $\Delta[Ca2+]_i$) in the presence of the agonist is similar (CADO – (a) 342.80 ± 50.05, n = 11 cells vs. (a1) 272.80 ± 99.39, n = 5 cells); CGS 21680 – (b) 229.30 ± 33.12, n = 13 cells vs. (b1) 219.70 ± 57.15, n = 7 cells). Therefore, the higher values of fold increase observed previously for cells with control/maximal response under 20% (Figure 4.5 (b1)) are probably not due to a higher amplitude of drug response but can be explained by a smaller amplitude of the control response in the absence of the test drug (Figure 4.7 (a1) and (b1)).

By analysing the results obtained for cells that presented control/maximal response above 20% (Figure 4.7 (a2) and (b2)), one can observe that CGS 21680 did not induced a significant increase in cell response. CADO potentiated Ca^{2+} response but the fold increase was small when compared to the other groups of cells (Figure 4.5).

Prior to 10 μM ATP stimulation, the basal $[Ca^{2+}]_i$ of cells for these two groups (control/maximal response < 20% vs. control/maximal response > 20%) were not significantly different ($p < 0.05$) (data not shown).

In spite of all the clear differences between the two populations of cells, when pooling all data together (Figure 4.7 (a) e (b)) the effect of CADO and CGS 21680 remained clear. Therefore, from now on, data will be presented as amplitude of Ca^{2+} responses for the entire pool of cells studied.

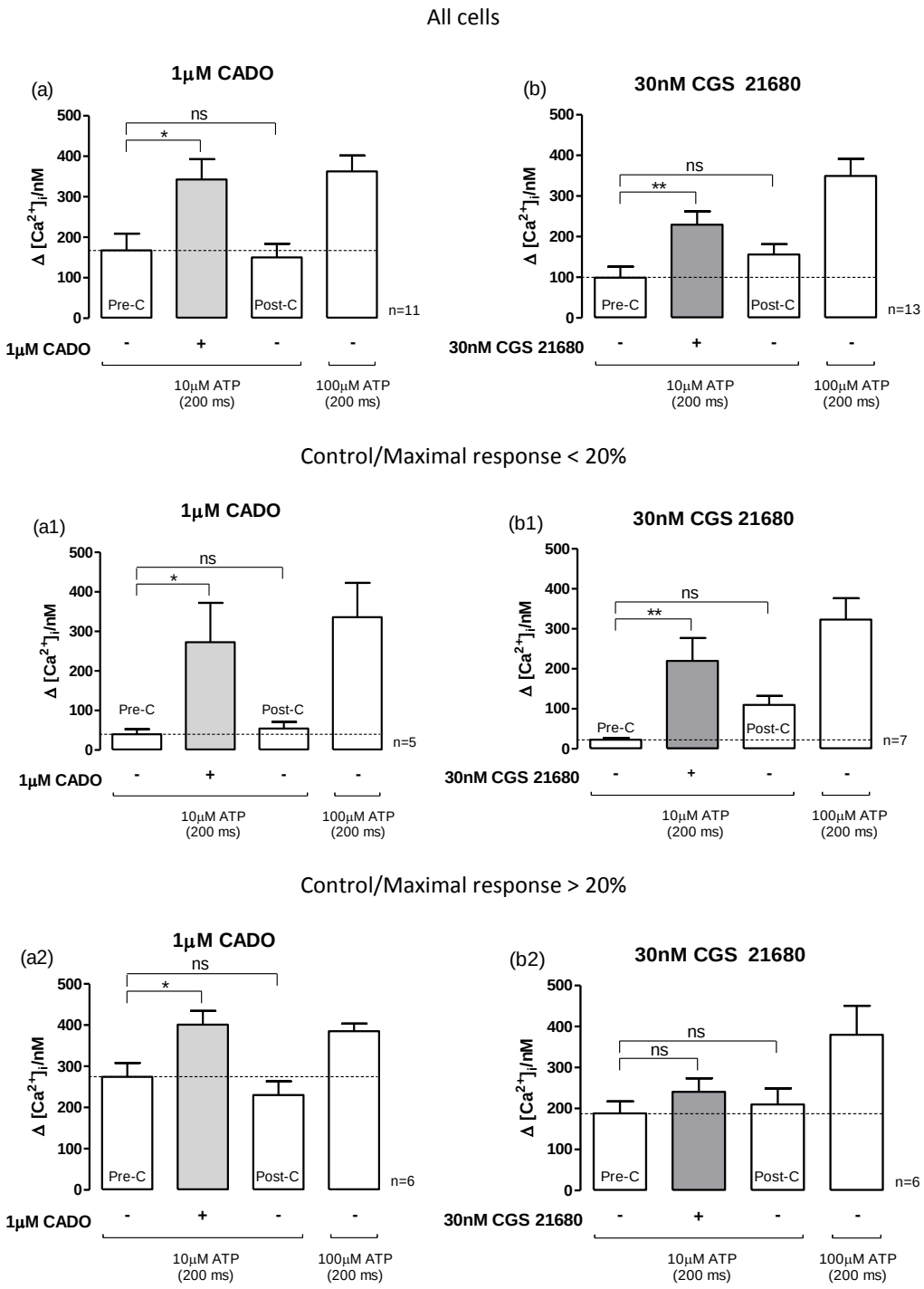

Figure 4.7 – Amplitude of Ca^{2+} transients elicited by 10 µM ATP for control, drug, washout and maximal responses (100 µM ATP) for 1 µM CADO and 30 nM CGS 21680. Plots (a) and (b) present →

mean values for the entire pool of cells. Plots (a1), (b1) and (a2), (b2) present mean values for cells that presented control/maximal response < 20% and > 20%, respectively. In each plot is discriminated the drug applied through the perfusion medium, 1 µM CADO or 30 nM CGS 21680, and the stimulus applied, 10 µM or 100 µM of ATP. (a) n = 11 cells, 4 experiments; (b) n = 13 cells, 6 experiments; (a1) n = 5 cells, 2 experiments; (b1) n = 7 cells, 4 experiments; (a2) n = 6 cells, 2 experiments; (b2) n = 6 cells, 4 experiments. Statistical significance: ns – non significant, * $p < 0.05$, ** $p < 0.01$.

4.2.2 Modulation by ADOR blockade

The effect of an $A_{2A}R$ selective antagonist (SCH 58216) and an A_1R selective antagonist (DPCPX) in Ca^{2+} signalling modulation were also studied. Data analysis similar to the one presented previously for the effect of agonists was performed. Neither the $A_{2A}R$ antagonist (50 nM SCH 58261), nor the A_1R antagonist (50 nM DPCPX) influenced ATP-induced Ca^{2+} responses, and therefore no significant variations on fold increase were obtained (Figure 4.8; Figure 4.9).

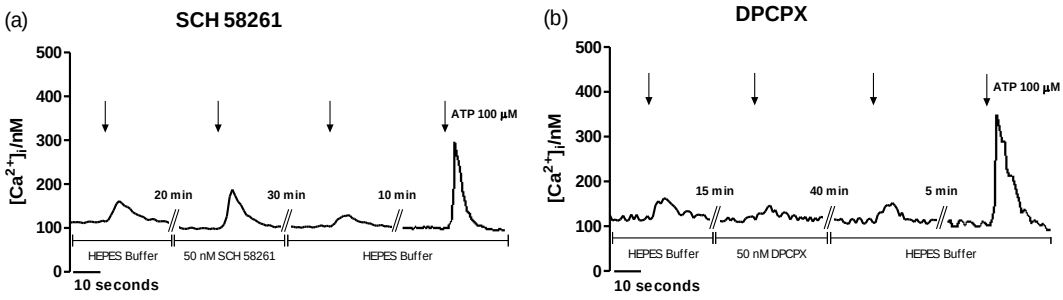

Figure 4.8 - Representative Ca^{2+} mediated responses to 10 µM ATP (200 ms) for experiments with (a) 50 nM SCH 58261 and (b) 50 nM DPCPX. For each experiment is presented a control response in the presence of HEPES buffer, test drug, after the washout with HEPES buffer and triggered by 100 µM ATP.

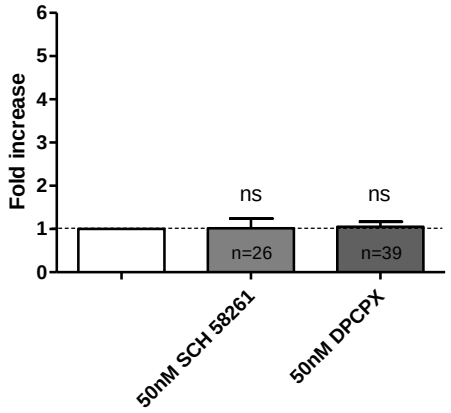

Figure 4.9 - Fold increase of 10 µM ATP-induced responses, observed in the presence of 50 nM SCH 58261 and 50 nM DPCPX. Mean values are presented for the entire pool of cells studied (SCH 58261, n = 26 cells, 7 experiments; DPCPX, n = 39 cells, 7 experiments). Statistical significance: ns – non significant.

Also, the plot of fold increase *vs.* control/maximal response did not present the correlation observed earlier for the two agonists, which was expected since the antagonists induced no variations in Ca^{2+} response (Figure 4.10).

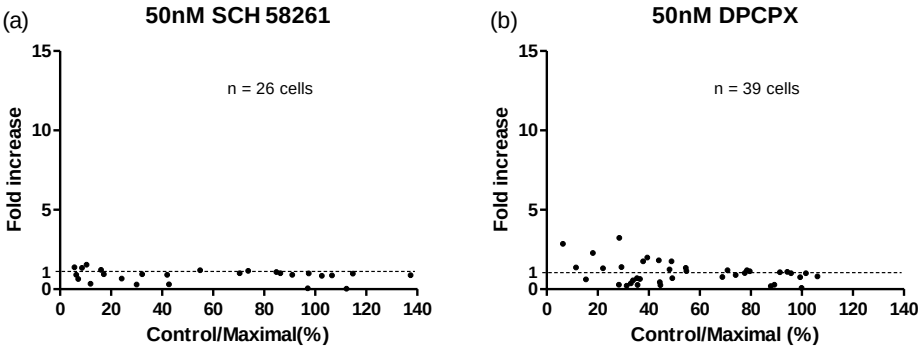

Figure 4.10 – Cell distribution for values of fold increase vs. control/maximal values for (a) 50 nM SCH 58261 and (b) 50 nM DPCPX. Percentage values of control/maximal response above 100% correspond to those cells that had a maximal response (100 µM ATP) smaller than the control response (10 µM ATP).

Comprehensive analysis of cell response to adenosine receptors antagonists throughout experiments confirmed that both $A_{2A}R$ and A_1R antagonists did not affect Ca^{2+} transient amplitude in a statistical significant way (Figure 4.11). Surprisingly, for DPCPX there was a significant decrease in the amplitude of ATP-induced Ca^{2+} transients after the washout, for which I have no possible explanation yet (Figure 4.11 (b)).

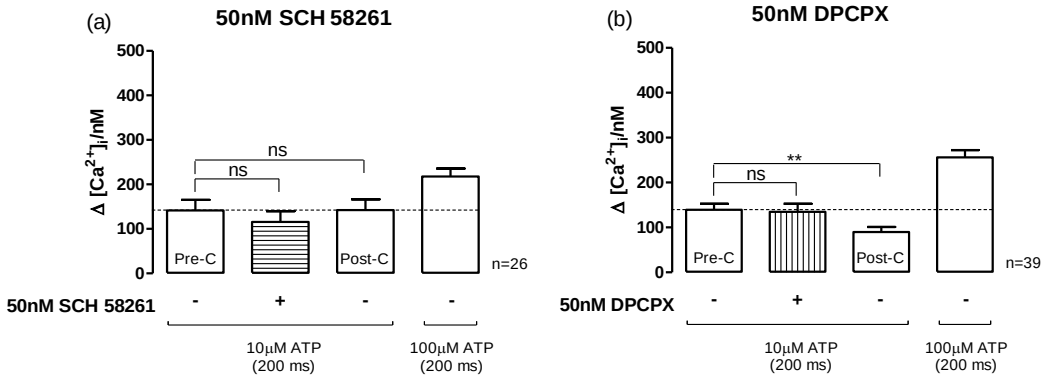

Figure 4.11 – Amplitude of Ca^{2+} transients elicited by 10 μM ATP for control, drug, washout and maximal responses (100 μM ATP) for 50 nM SCH 58261 and 50 nM DPCPX. Both plots present mean results from the entire pool of cells studied. In each plot is discriminated the drug applied through the perfusion medium, 50 nM SCH 58261 or 50 nM DPCPX, and the stimulus applied, 10 μM or 100 μM of ATP. (a) n = 26 cells, 7 experiments; (b) n = 39 cells, 7 experiments. Statistical significance: ns – non significant, ** $p < 0.01$.

4.2.3 Ca^{2+} signalling modulation via $A_{2A}R$

Results reported above for the effect of CGS 21680 indicate the contribution of $A_{2A}R$ in Ca^{2+} signalling potentiation. To confirm $A_{2A}R$ involvement, experiments were performed where the potentiation of Ca^{2+} response was first induced, applying either CADO or CGS 21680, and then the perfusion medium was changed to a mixture of the agonist and the $A_{2A}R$ selective antagonist (SCH 58261).

The facilitatory effect mediated by the unselective (1 μM CADO) and $A_{2A}R$ selective (30 nM CGS 21680) agonists was completely reverted by blockade of $A_{2A}R$, using a selective

antagonist (50 nM SCH 58261) (Figure 4.12; Figure 4.13). These results clearly show that the potentiation mechanism is mediated by $A_{2A}R$.

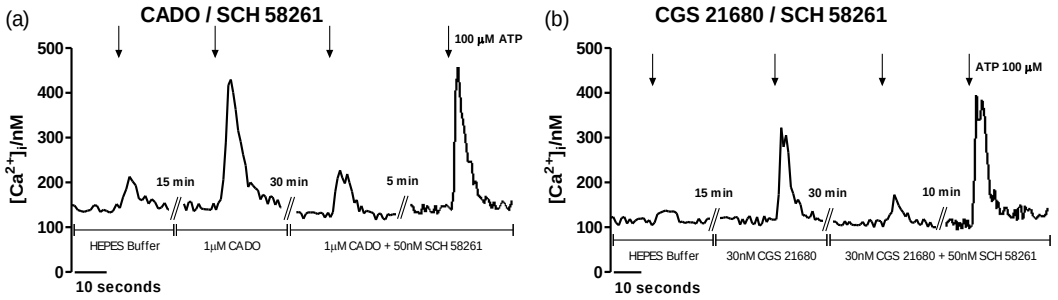

Figure 4.12 - Representative Ca^{2+} mediated responses to 10 µM ATP (200 ms) for experiments with (a) 1µM CADO / 50nM SCH 58261 and (b) 30nM CGS 21680 / 50nM SCH 58261. For each experiment is presented a response in the presence of HEPES buffer, test drug (CADO or CGS 21680), agonist/antagonist mixture and triggered by 100 µM ATP.

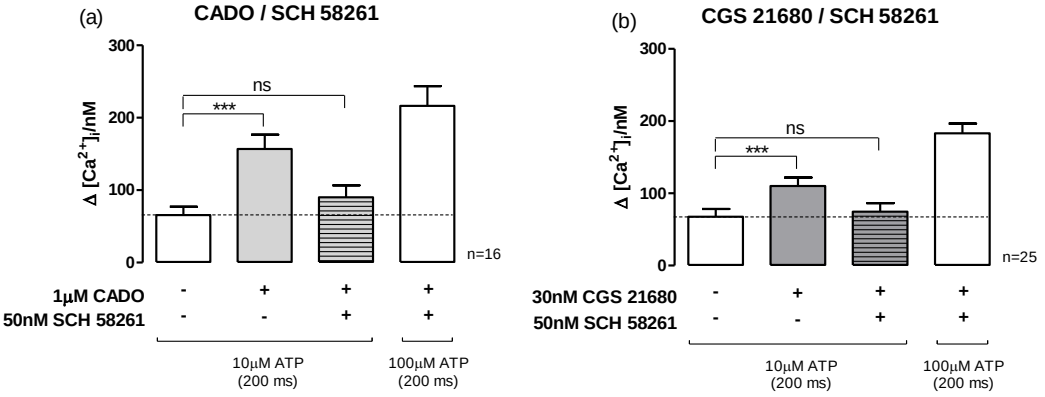

Figure 4.13 – Amplitude of Ca^{2+} transients elicited by ATP for control, drug, washout and maximal responses using agonists (1µM CADO or 30nM CGS 21680) and antagonist (50 nM SCH 58261). Plots present mean results from the entire pool of cells studied. In each plot is discriminated the drug mixture applied through the perfusion medium and the stimulus applied, 10 µM or 100 µM of ATP. (a) n = 16 cells, 5 experiments; (b) n = 25 cells, 7 experiments. Statistical significance: ns – non significant, *** $p < 0.0001$.

4.3 A_1R-$A_{2A}R$ cooperation in Ca^{2+} signalling modulation

In order to test if the adenosine modulation over ATP-induced Ca^{2+} signalling was dependent on A_1R-$A_{2A}R$ cooperation, an A_1R selective antagonist, DPCPX, was used. Unexpectedly, the potentiation mediated by the unselective (1 μM CADO) and $A_{2A}R$ selective (30 nM CGS 21680) agonists was completely reverted by blockade of A_1R, using a selective concentration (50 nM) of DPCPX) (Figure 4.14; Figure 4.15). Overall, results reported in the prior section (4.2.3) and here indicate that the activation of both A_1R and $A_{2A}R$ is required for adenosine to mediate the facilitation of ATP-induced Ca^{2+} responses, a mechanism that denotes A_1R-$A_{2A}R$ cooperation.

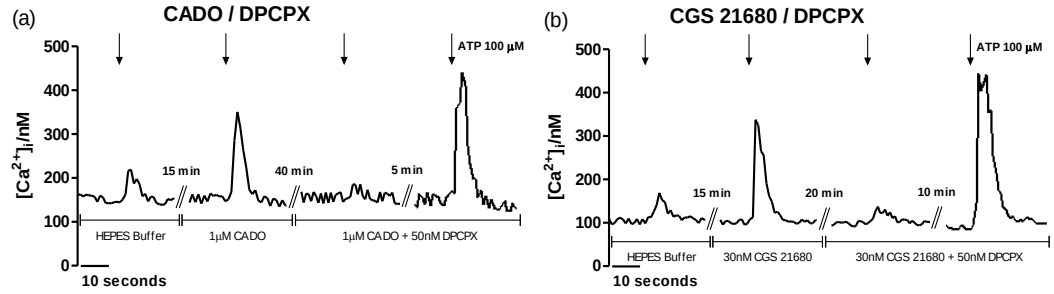

Figure 4.14 - Representative Ca^{2+} mediated responses to 10 μM ATP (200 ms) for experiments with (a) 1μM CADO/ 50nM DPCPX and (b) 30nM CGS 21680 / 50nM DPCPX. For each experiment is presented a response in the presence of HEPES buffer, test drug (CADO or CGS 21680), agonist/antagonist mixture and triggered by 100 μM ATP.

Averaged analysis showed that DPCPX, the A_1R selective antagonist, reverted the facilitatory effect towards and even below the control levels, obtained prior to CADO or CGS 21680 perfusion (Figure 4.15 (a) and (b)).

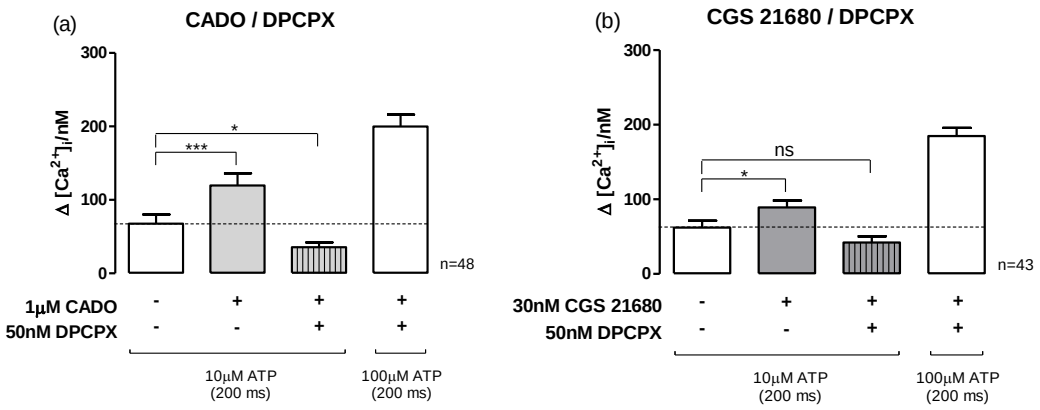

Figure 4.15 – Amplitude of Ca^{2+} transients elicited by ATP for control, drug, washout and maximal responses using agonists (1μM CADO or 30nM CGS 21680) and antagonist (50 nM DPCPX). Plots present mean results from the entire pool of cells studied. In each plot is discriminated the drug mixture applied through the perfusion medium and the stimulus applied, 10 μM or 100 μM of ATP. (a) n = 48 cells, 10 experiments; (b) n = 43 cells, 11 experiments. Statistical significance: ns – non significant, * $p < 0.05$, *** $p < 0.0001$.

4.4 Culture Characterization

Relevant for this project was the characterization of the astrocytic primary cultures used in Ca^{2+} imaging experiments. Firstly, the percentages of different cell populations present in culture were determined by immunocytochemistry. Then the presence of A_1R, $A_{2A}R$ and $P2Y_1R$ was confirmed by western blot.

4.4.1 Cell counting by Immunocytochemistry

Astrocytic primary cultures, at 14 days in culture (DIC14), are mainly constituted by astrocytes (> 90%) and few microglial cells (Figure 4.16) and therefore, according to Saura (2007), are designated enriched primary astrocytic cultures. Neurons are very rare, two or three per vision field (mean total of 600 cells per vision field) (Figure 4.17) due to the protocol applied, namely culture medium composition, and because after birth (P0-P2)

neuronal precursor cells have already differentiated into neurons, in contrast, astrocyte precursor cells are still present at P0-P2, giving rise to the astrocytic population. For this reason, it was assumed that to calculate the percentage of astrocytes and microglial cells, neurons could be disregarded. Therefore the number of astrocytes was considered as the difference between the total number of cells, given by nuclei count, and the number of microglial cells.

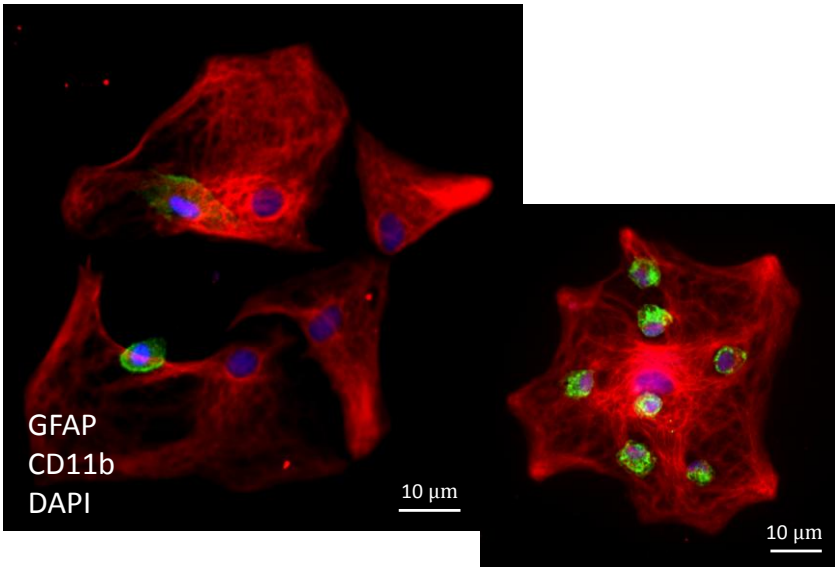

Figure 4.16 - Immunofluorescence images, obtained with a epifluorescence microscope, representing astrocytes (red), microglial cells (green) and nuclei (blue), from a culture at DIC 14 (40x amplification lens).

Microglial cells are known to express a plethora of P2 and P1 receptors and have a Ca^{2+} excitable mechanism similar to astrocytes (Verkhratsky *et al.*, 1998; Abbracchio & Ceruti, 2006; Butt, 2011). For these reasons, it was considered relevant to evaluate the degree of microglia contamination.

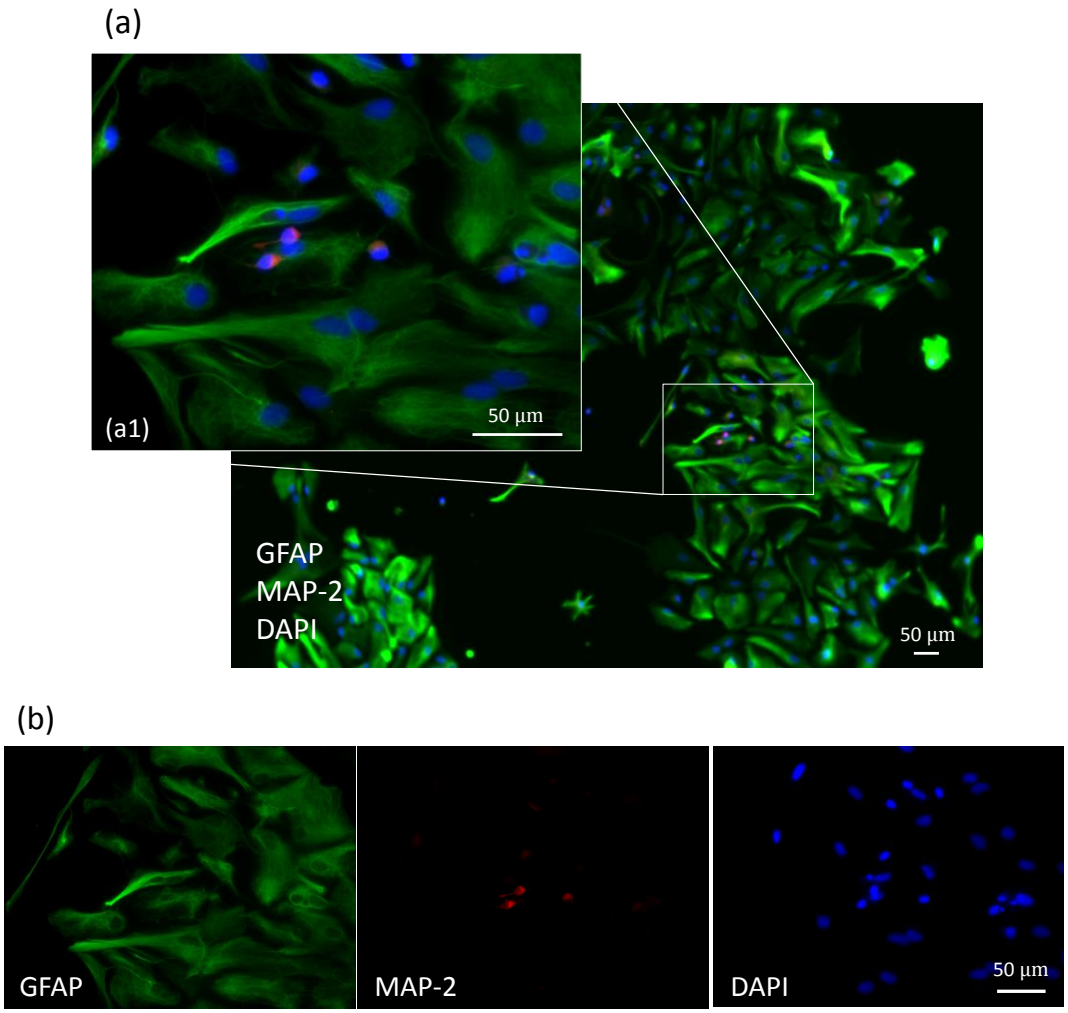

Figure 4.17 - (a) Immunofluorescence image, obtained with a epifluorescence microscope, representative of a primary culture (10X amplification lens). (a1) Enlarged image representing astrocytes (green), neurons (red) and nuclei (blue) (40x amplification lens). (b) Immunofluorescence images representing culture amplification (40x) for each fluorescence filter.

To minimize microglia contamination, an extra 5h cellular shake at DIC6, the day before cell replating, was added to the primary culture protocol that was previously applied in the host laboratory (previously described by Biber *et al.* (1997)). According to several authors (Jiménez *et al.*, 1999; Du *et al.*, 2010), culture shaking followed by supernatant

removal is a good method to remove microglia and to obtain enriched astrocytic cultures. As microglial cells grow mostly on top of astrocytes, they are not attached to the bottom of the flask and therefore are easier to detach by shaking. To test if this also applied to our culture conditions, two different cell batches were prepared from the same culture. One of them underwent this extra shake (4-5 hours at DIC 6) and the other did not. The purpose was to calculate the percentage of microglial cells for both cell batches in order to understand if there was less microglia in cultures that underwent the extra shaking period.

Primary cultures that were not submitted to the extra 5h shake are mainly constituted by astrocytes (≈ 95%) and microglial cells (Table 4.1). The percentage of astrocytes after the extra 5h shake was higher (≈ 98%), which indicates that more microglial cells were discarded during the extra shaking step. The increase in astrocyte percentage observed here is similar to the one observed by Du *et al.* (2010) between shaken once (94.8±1.325%) and shaken twice (96.5±1.080%) cultures.

Table 4.1 - Results from cell counting. Mean total number of cells, percentage of astrocytes and of microglial cells for two independent cultures, applying the two different protocols.

Treatment	Culture	Mean total number of cells per vision field	Astrocytes (%)	Microglial cells (%)
No shake	1	688	97.33	2.67
	2	209	92.06	7.94
	Mean	-	**94.7**	**5.3**
5h shake	1	875	99.31	0.69
	2	619	95.59	4.41
	Mean	-	**97.5**	**2.5**

Overall, results indicate that adding a 5h shaking step to the protocol produces cultures with higher percentage of astrocytes and therefore this new step was added to the protocol. Besides, Ca^{2+} imaging experiments performed with cultures that underwent these two different treatments did not presented significant changes in Ca^{2+} signalling (data not shown).

Other alternatives that could also be used are laminin that inhibits microglial growth and promotes astroglial growth or ARA-C, a mitotic inhibitor, that is added to stop mitosis after astrocytes have reached confluence (Saura, 2007). Given the high enrichment of the cultures in astrocytes, I decided not to use growth inhibitors.

Astrocytes are a very heterogeneous cell population and it is possible to visually distinguish different types of astrocytes. Although, it was not performed any immunocytochemistry for specific astrocytic markers, because it was beyond the scope of this project, it appeared that Type-I and Type-II astrocytes were present in cultures (Figure 4.18). These two types of cells can be easily differentiated by their shape as explained earlier (see section 1.1.1, in Introduction). Nevertheless, differences between this two types of astrocytes, at the molecular level, are not well characterized and most of the work published was performed on Type-I astrocytes. For these reasons, Ca^{2+} imaging experiments presented here were performed using, presumably, Type-I astrocytes that can be visually differentiated because they are bigger in size.

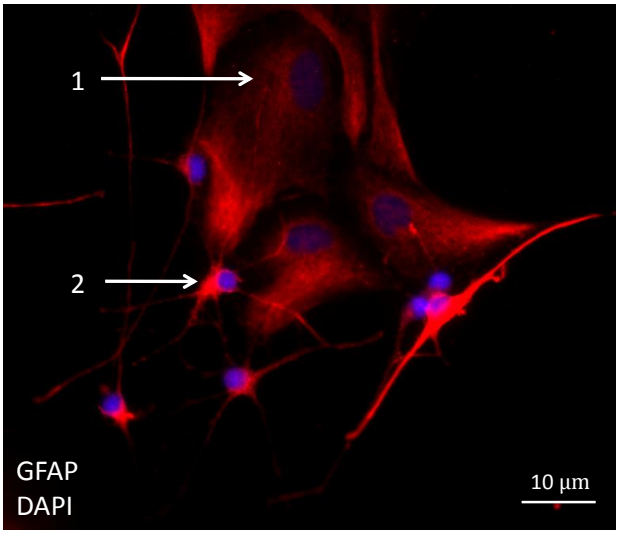

Figure 4.18 - Immunofluorescence image of a primary astrocytic culture. Type-I (1) and Type-II (2) astrocytes (red), nuclei (blue). This image is not representative of Type-I/Type-II astrocytes percentages in cultures.

4.4.2 Western blot analysis of $P2Y_1$, A_1 and A_{2A} receptors

Western blot analysis of primary cultures using the lysis buffer method showed the presence of $P2Y_1R$ (42 kDa) and A_1R (37 kDa) in cultures at DIC 14 (Figure 4.19). However, with this method, it was not possible to detect $A_{2A}R$ (43 kDa). The unspecific bands present at higher molecular weight (≈ 50-60 kDa) do not correspond to $A_{2A}R$ but are always present when this antibody is regularly used in the laboratory. These receptors are difficult to detect because they are present at very low density in the cortex compared to other brain regions, such as, the striatum (Ribeiro *et al.*, 2003). For this reason, in the following experiments, a sample of striatum was used as positive control for $A_{2A}R$.

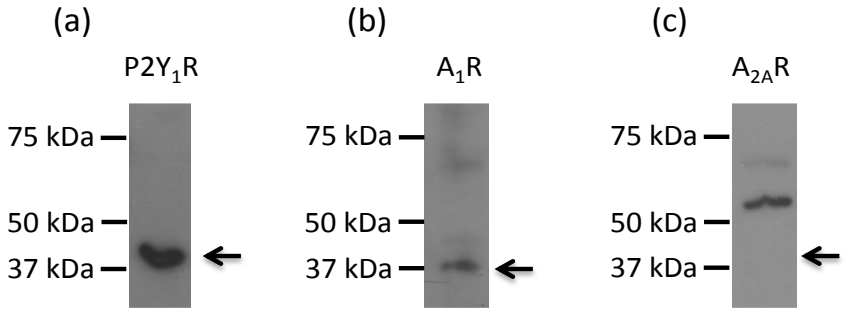

Figure 4.19 - Results of western blot experiments using lysis buffer method for astrocytes at DIC 14 (Protein leading: 20 μg). (a) $P2Y_1R$ (42 kDa), (b) A_1R (37 kDa) and (c) no visible band corresponding to $A_{2A}R$ (43 kDa).

Western blot was repeated applying the sucrose buffer method to detect A_1R and $A_{2A}R$. Sucrose buffer allows a milder lysis compared to lysis buffer. Protein loading was increased for 125 μg of protein in wider lanes and samples at DIC 14 and DIC 21 were applied. In spite of being interested in detecting $A_{2A}R$ proteins at DIC 14, i.e. at the period when Ca^{2+} experiments were performed (DIC 9-14), once $A_{2A}R$ are difficult to detect, it was also used a sample of cells at DIC 21. At 3 weeks, cultures are more confluent and

therefore samples are expected to have a higher quantity of $A_{2A}R$, which should be easier to detect.

Again, A_1R (37 kDa) were detected both at DIC 14 and DIC 21, as well as tubulin (50 kDa), used as an internal control (Figure 4.20 (a)). Still, it was not possible to detect $A_{2A}R$ (43 kDa) in any of the samples, only in striatum, the positive control (Figure 4.20 (b)). This could be due to the very low density of $A_{2A}R$, which are undetectable by western blot, or these proteins were degraded during the lysis process. Therefore, the protocol needs further optimization.

Nevertheless, Cristovão-Ferreira *et al.* (2011) already observed, in cortical astrocytes, relatively low expression of $A_{2A}R$ at DIC 14, as well as, functional effects of the receptors on GABA transport. Furthermore, in Ca^{2+} imaging experiments presented here, cells responded to $A_{2A}R$ selective activation and blockade. For these reasons, it can be concluded that $A_{2A}R$ are present in these samples. In the future, RT-PCR technique can be used to amplify mRNA levels present in samples and quantify them. However, it should always be kept in mind that the presence of mRNA does not necessarily indicate the presence of functional proteins.

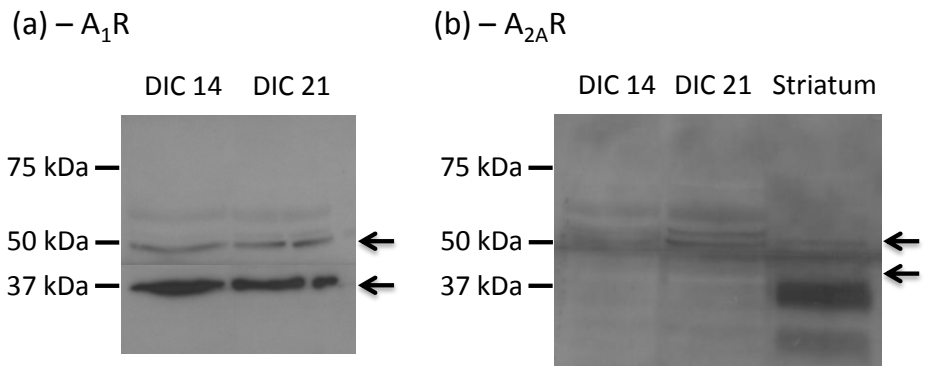

Figure 4.20 - Results of western blot experiments using sucrose lysis method (Protein leading: 125 µg). (a) A_1R (37 kDa) from samples at DIC 14 and DIC 21; (b) $A_{2A}R$ (43 kDa) from samples at DIC 14, DIC 21 and striatum.

5 Discussion

A brief stimulation with ATP induces a sharp and fast Ca^{2+} transient in cortical astrocytes. The work now reported clearly shows that adenosine potentiates ATP-induced Ca^{2+} transients, via $A_{2A}R$ activation. Furthermore, it was demonstrated that the cooperation between A_1R and $A_{2A}R$ is essential for Ca^{2+} signalling modulation.

5.1 ATP induces Ca^{2+} signalling

Astrocytic Ca^{2+} responses can be seen as a measure of cellular response to an external stimulus and therefore it allows to evaluate cellular communication. Here, it has been shown that a brief stimulus (10 μM ATP for 0.2 seconds) induces a sharp and fast Ca^{2+} transient. Results presented confirm that Ca^{2+} responses elicited by a prolonged stimulus (10 μM ATP for ≥ 20 seconds) present a biphasic behavior, an initial large transient peak followed by a smaller sustained phase, as previously seen by other authors (Nobile *et al.*, 2003 ; Alloisio *et al.*, 2004). These authors also described that the Ca^{2+} influx observed in these two phases is mediated by different P2R subtypes. The initial peak corresponds to the release of Ca^{2+} from intracellular storages, via P2YR activation, namely $P2Y_1R$, whose presence was confirmed here by western blot. The plateau is maintained by Ca^{2+} influx through ionotropic P2XR, namely $P2X_7R$. Nevertheless, results obtained here disprove these previous observations by showing that both metabotropic (P2Y) and ionotropic (P2X) ATP receptors contribute to the Ca^{2+} rise when cells are activated by a brief ATP stimulus (10 μM ATP for 0.2 seconds).

5.2 Ca^{2+} signalling modulation via $A_{2A}R$

The experimental approach developed here uses Ca^{2+} imaging to study which adenosine receptors are involved in Ca^{2+} signalling modulation in primary astrocytes. The use of a

smaller ATP concentration and appropriate concentrations of each test drug, as well as, the stimulation pattern developed, have great advantages when compared to the protocols developed previously (Jiménez *et al.*, 1999; Alloisio *et al.*, 2004).

A stable adenosine analogue, 1 μM CADO, markedly enhanced Ca^{2+} transients induced by 10 μM ATP. Potentiation observed here was completely reversed upon washout. These results are in agreement with previous observations from Alloisio et al. (2004), who saw the potentiation of Ca^{2+} peaks in the presence of CADO (10 μM) and NECA (10 μM), both unselective agonists of adenosine receptors.

Alloisio et al. (2004) provided pharmacological evidence that adenosine can modulate biphasic Ca^{2+} responses differently due to a differential activation of adenosine receptors. $A_{2B}R$ activation potentiates the initial peak and A_1R activation downregulates the sustained response. Therefore, the next step was to characterize the individual role of adenosine receptors, particularly $A_{2A}R$, in Ca^{2+} signaling modulation.

In the present study, the facilitation of ATP-induced Ca^{2+} responses mediated by CADO was mimicked by an $A_{2A}R$ selective agonist, CGS 21680 (30 nM). It was also shown, using a combination of selective agonists and antagonists, that the potentiation observed for both agonists (CADO and CGS 21680), is completely reverted by an $A_{2A}R$ selective antagonist, SCH 58261 (50 nM). Altogether, these results clearly show that the potentiation mechanism is mediated by $A_{2A}R$.

Interestingly, these findings refute results obtained by Alloisio et al. (2004) and Jimenez et al. (1999), who saw no modulation effect on ATP-induced Ca^{2+} responses when an $A_{2A}R$ selective agonist (10 μM CGS 21680) was used. These authors also used primary cultures from cortex and cerebellum, respectively, prepared in similar conditions to the ones used here. Therefore this conflicting data could be due to the unselective agonist concentration used by these authors, 10 μM, contrasting with the 30 nM CGS 21680 solution used here. At micromolar concentration, GCS 21680 not only desensitize $A_{2A}R$ but also activates A_1R, making these high concentration unviable for $A_{2A}R$ identification (Correia-de-Sá *et al.*, 1991).

The observations that in the presence of higher stimuli (50 µM and 100 µM of ATP) there was no significant potentiation of Ca^{2+} responses to the agonists, 1 µM CADO and 30 nM CGS 21680, can be explained due to the fact that these ATP concentrations are supramaximal. When maximal response is reached, a ceiling effect is expected and it might camouflages a drug effect, being it a potentiation or inhibition.

The facilitatory effect mediated by CGS 21680 was not so effectively reverted by HEPES washout, as in the case of CADO. Due to the its liposoluble character, CGS 21680 molecules remain bonded to the lipidic membrane for a longer period of time. Indeed, CADO e much more hydrosoluble than CGS 21680 and, therefore, easier to washout.

$A_{2A}R$ and A_1R selective antagonists, SCH 58261 (50 nM) and DPCPX (50 nM), did not affect Ca^{2+} responses, suggesting that in the culture conditions used neither A_1R nor $A_{2A}R$ are activated by endogenous extracellular adenosine.

In the present study, the relation observed, for CADO and CGS 21680, between fold increase and control/maximal response is very interesting and supports the idea that we are working with a heterogeneous astrocytic cell population (Matyash & Kettenmann, 2010). Cells with high responses to ATP (10 µM) had a smaller potentiation of Ca^{2+} responses, under adenosine modulation, compared to cells with low responses to ATP. These cells not only behave differently when stimulated by ATP but also are modulated in a different way by adenosine. Peakman and Hill (1996) reported a differential segregation of A2R and A_1R to Type-I and Type-II astrocytes, respectively. A possible differential distribution of adenosine receptors in astrocytic cell populations could explain the differential modulation observed. Altogether, it seems to be fundamental to separately dissect the contribution of individual adenosine receptors for Ca^{2+} modulation in Type-I and Type-II astrocytes.

Despite the different cellular behaviors described, it is interesting that these groups of cells (control/maximal response < 20% *vs.* control/maximal response > 20%) present similar basal $[Ca^{2+}]_i$ and reached similar $[Ca^{2+}]_i$ upon ATP stimulation, in the presence of the adenosine receptors agonists, CADO and CGS 21680. The great difference was the

$[Ca^{2+}]_i$ reached upon ATP stimulation in the absence of the adenosine receptor agonists. This can be indicative of some sort of internal cell regulation process that program cells to synchronize their responses and reach certain Ca^{2+} levels upon a given external stimulus in the presence of an adenosine receptor agonist. It could also indicate a physiological limitation, meaning that cells are not capable of reaching higher Ca^{2+} levels. The later hypothesis is very unlikely, at least for cells used in experiments with CGS 21680, because the Ca^{2+} response amplitude obtained in the presence of the $A_{2A}R$ selective agonist is far below the maximal Ca^{2+} response to 100 µM ATP. This is not the case for CADO, since the Ca^{2+} response amplitude obtained in the presence of the unselective agonist is similar to the maximal Ca^{2+} response, which indicates that the saturation plateau was reached. In this situation, the cellular Ca^{2+} response might not be capable to undergo further potentiation induced by CADO, and for this reason the facilitatory effect might be underestimated.

Interestingly, the presence of internal cell regulation that programs cells for a certain response to a determined stimulus is a plausible idea. It is known that astrocytes are capable to integrate and process external inputs (Perea & Araque, 2005). In turn, cells develop a considered Ca^{2+} response and transmit it to other cells. Such mechanisms might be important to synchronize Ca^{2+} response in astrocytic cell populations and consequently in synaptic networks (Halassa *et al.*, 2006).

5.3 A_1R-$A_{2A}R$ cooperation in Ca^{2+} signalling modulation

The second aim of this project was to analyze if cooperation between adenosine A_1R and $A_{2A}R$ is required for Ca^{2+} signalling modulation. Experiments were focused in A_1R and $A_{2A}R$ because these receptors have high affinity for adenosine and it is known that the cooperation between these receptors exists, namely in astrocytes, to modulate GABA uptake (Cristóvão-Ferreira *et al.*, 2011). A similar cooperation mechanism might be involved in Ca^{2+} signalling modulation.

Here it was shown, using a combination of selective agonists and antagonists for adenosine receptors, that the potentiation observed for both CADO, unselective ADOR agonist, and CGS 21680, $A_{2A}R$ selective agonist, is completely reverted not only by SCH 58261 (50 nM), an $A_{2A}R$ selective antagonist, but also by DPCPX (50 nM), an A_1R selective antagonist. This data strongly suggests that the modulation mediated by adenosine, via $A_{2A}R$, is dependent on A_{2A} and A_1 receptor activation, which provides strong evidence for cooperation and/or interaction between these two receptors.

These results indicate a situation of cross-antagonism, where conformational changes induced by one of the A_1R or $A_{2A}R$ antagonists prevent the effect mediated by the complex. Similar results were reported by Cristóvão-Ferreira et al. (2011), where A_1R or $A_{2A}R$ individual blockade completely prevented modulation of GABA uptake by adenosine. The cross-antagonism observed between the two receptors might indicate A_1R-$A_{2A}R$ heteromerization (Ferrada *et al.*, 2009; Moreno *et al.*, 2010; Cristóvão-Ferreira *et al.*, 2011) and should be further explored.

Again, our findings refute results obtained by Alloisio et al. (2004), who saw no inhibition of the facilitatory effect mediated by CADO (10 μM) in the presence of DPX (10 μM), a A_1R selective antagonist. Such contrasts in results might be due to drug application, as these authors described DPX topical application for about 200 seconds, which is very different from the drug perfusion method used here. Beyond all the discrepancies in experimental protocols, it should be kept in mind that the dual-modulatory role of adenosine might account for the variable effects reported under different experimental conditions.

An interesting observation was that DPCPX, an A_1R selective antagonist, seems to be more effective in reverting the $A_{2A}R$-mediated facilitation of Ca^{2+} response, when compared to SCH 58261, an $A_{2A}R$ selective antagonist. These results can be indicative of some kind of modulatory effect that is mediated by A_1R. To further explore this issue more experiments have to be performed in order to understand the role of A_1R in Ca^{2+} signalling modulation and test if the A_1R-mediated modulatory effect is also inhibited when A_1R and $A_{2A}R$ are individually antagonized.

The contribution of other adenosine receptors for this modulatory effect cannot be ruled out and should be evaluated in the future. Low-affinity $A_{2B}R$, similarly to $A_{2A}R$, are also positively coupled to cAMP (Peakman & Hill, 1994). Moreover, these receptors were proposed to mediate potentiation of ATP-induced Ca^{2+} responses in cortical (Alloisio *et al.*, 2004) and cerebellar astrocytes (Jiménez *et al.*, 1999). These two authors also reported no potentiation of Ca^{2+} transients mediated by A_1R. Nonetheless, it is fundamental to dissect the role, possibly inhibitory, of these receptors in Ca^{2+} signalling modulation. A_1R are not only known to mediate an opposite inhibitory effect, mediated by G_i-proteins, but also seem to cooperate with $A_{2A}R$ in modulatory processes, namely, in astrocytes (Cristóvão-Ferreira *et al.*, 2011). A_3R contribution should also be dissected, as in previous works was observed that IB-MECA, an A_3R selective agonist, is responsible for enhancing the ATP-induced Ca^{2+} responses in tracheal smooth-muscle cells (Michoud *et al.*, 1999). Alloisio *et al.* (2004) reported no modulatory effect of A_3R upon the initial Ca^{2+} peak.

In order to understand if the potentiation of Ca^{2+} responses by adenosine is dependent on extracellular Ca^{2+}, further experiments have to be performed. On the one hand, it was already shown that for cortical and cerebellar astrocytes, potentiation of ATP-induced Ca^{2+} responses by CADO and Ap5A (diadenosine pentaphosphate, activates P2R), respectively, is independent on extracellular Ca^{2+}, which indicates a purely metabotropic mechanism (Jiménez *et al.*, 1998; Alloisio *et al.*, 2004). On the other hand, Michoud *et al.* (1999) saw that the facilitation of ATP-induced Ca^{2+} responses by adenosine, in tracheal smooth-muscle cells, depends on extracellular Ca^{2+}.

5.4 Physiological importance of Ca^{2+} signalling modulation by ADOR

Still an unexplored issue is the functional significance, in the brain, of the modulation effect resulting from the cross-talk between nucleotide and nucleoside receptors. The modulatory effect described here might be of particular importance in pathological situations, where both ATP and adenosine accumulate in the extracellular space (Fields &

Burnstock, 2006; Sebastião & Ribeiro, 2009b). Nonetheless, it might also be a significant regulatory mechanism in opposite situations, when the extracellular levels of ATP drop below a certain level. In this case adenosine production might function as a compensating mechanism, sensitizing astrocytes for ATP, and compensating its lower levels.

In astroglial cells, ATP seems to prompt phenomena such as astrogliosis, and consequently cell proliferation or apoptosis, by eliciting a change in the internal cellular Ca^{2+} dynamic (Neary *et al.*, 1996). Adenosine receptors in astrocytes may play a pivotal role in regulating the Ca^{2+} patterning and therefore differential activation of transcriptions factors (Dolmetsch *et al.*, 1997).

Concerning cooperation among adenosine receptors, Cristovão-Ferreira et al. (2011) proposed that the heteromer A_1R-$A_{2A}R$, which mediates both potentiation and inhibition, might operate as a dual amplifier to control GABA levels at synapses. It is structurally advantageous for cells to contain a single complex that mediates both positive and negative modulation, allowing a tight regulation and smooth transition between states. In addition, it would be even more advantageous for cells if the same receptor complex modulates several phenomena, such as, neurotransmitter uptake and gliotransmitter release by astrocytes, the latter via Ca^{2+} signalling modulation, the mechanism disclosed here.

The transition between activation states, mediated by such a complex, was shown to be dependent on adenosine extracellular levels (Ciruela *et al.*, 2006; Cristóvão-Ferreira *et al.*, 2011). This would allow a fine modulation of Ca^{2+} signalling under different physiological situations. For example, adenosine receptors, might mediate differential Ca^{2+} signalling regulation in response to low or high neuronal activity that is sensed via neuronal released-ATP, which is instantaneously converted into adenosine.

Ciruela et al. (2006), have specifically shown that A_1R-$A_{2A}R$ cooperation dual-modulates glutamate release in striatal nerve terminals according to synaptic adenosine levels. In astrocytes, ATP-mediated Ca^{2+} signalling is known to be responsible for triggering glutamate release (Newman, 2003). In addition, adenosine was shown to stimulate astrocytic glutamate release via $A_{2A}R$ in the hippocampus (Nishizaki, 2004), modulating

cellular communication. Now that A_1R-$A_{2A}R$ cooperation in Ca^{2+} signalling modulation in astrocytes was uncovered, we might be unveiling an indirect neuromodulatory mechanism by which adenosine dual-modulates Ca^{2+} signalling, and consequently gliotransmission. The role of A_1R, per se, in Ca^{2+} signalling modulation, as well as, of other adenosine receptors present in astrocytes, namely $A_{2B}R$ and A_3R, needs further elucidation.

As it is now coming to light, communication between cells is very complex. Modulation of Ca^{2+} excitability by adenosine can be envisioned as a way for astrocytes to regulate Ca^{2+} patterning and ultimately cellular communication. Furthermore, the cooperation between adenosine receptors, explored here, adds an extra level of modulation to communication between cells.

6 Conclusions

The work here reported clearly shows that adenosine strongly enhances ATP-induced Ca^{2+} responses and that this effect is mimicked by selective activation of $A_{2A}R$. Furthermore, the potentiation induced by adenosine is completely reverted by $A_{2A}R$ selective blockade. Therefore, it is concluded that adenosine potentiates Ca^{2+} signalling via $A_{2A}R$.
In addition, it was demonstrated that the facilitatory effect mediated by adenosine is also completely reverted by A_1R selective blockade. Altogether, these data suggest that both A_1R and $A_{2A}R$ activation is required for Ca^{2+} signalling modulation by adenosine, providing a strong evidence for A_1R-$A_{2A}R$ cooperation in cortical astrocytes.

Here, a new modulatory mechanism mediated by adenosine was, therefore, characterized. Thus this purine acts not only as a neuromodulator, a well known action of adenosine, but also more broadly as a glial modulator, regulating the astrocytic Ca^{2+} excitable mechanism and consequently gliotransmission and cellular communication. The uncovering of an A_1R-$A_{2A}R$ dual-modulatory complex adds an extra level of complexity to cellular communication, producing new shades of astrocytic responses.

As an overall conclusion, adenosine, through $A_{2A}R$ activation, potentiates ATP-induced Ca^{2+} signalling in primary cortical astrocytes. Furthermore, A_1R-$A_{2A}R$ cooperation is required for this modulation (Figure 6.1).

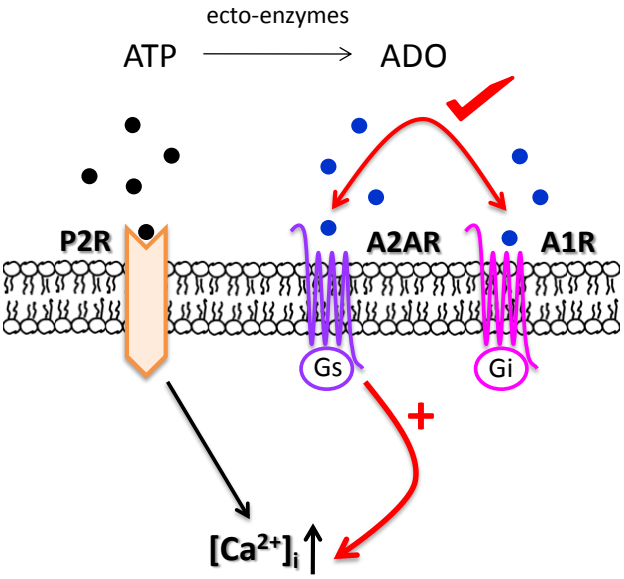

Figure 6.1 – Schematic representation of the mechanisms, here uncovered, involved in Ca^{2+} signalling modulation mediated by adenosine receptors.

Agradecimentos

Gostaria de agradecer ao Professor Joaquim Alexandre Ribeiro por me ter recebido no seu Laboratório de Neurociências, tendo-me possibilitado crescer científica e humanamente nesta equipa fantástica.

Um agradecimento muito especial à Professora Ana Maria Sebastião, minha orientadora, pela oportunidade concedida para iniciar a minha carreira científica em Neurociência. Pelos bons conselhos dados, pela disponibilidade em discutir o meu trabalho e ainda pela confiança transmitida, mesmo nos momentos em que o trabalho não seguia o rumo esperado.

Um agradecimento especial também ao Doutor Pedro Lima, que esteve sempre disponível, tendo contribuído muito mais do que aquilo que compete a um orientar interno. Pelas longas e profícuas discussões sobre a técnica e os inúmeros problemas com que nos deparámos.

Outro agradecimento muito especial à Sandra Vaz, que acabou por se tornar minha orientadora. Pelos ensinamentos e toda a ajuda dada na parte laboratorial, mas sobretudo pela amizade e constante incentivo para seguir em frente.

Ao Joaquim Jacob agradeço toda a paciência em me ensinar e acompanhar nos primeiros passos na técnica de cálcio.

Finalmente, um obrigado muito grande a todos os colegas de laboratório, que desde o primeiro dia se mostraram sempre disponíveis para me ajudar com as minhas pequenas duvidas e problemas. Obrigado, por tornarem este laboratório uma segunda casa maravilhosa, mesmo nos dias longos e intermináveis.

Ao meu pai, por desde sempre me incentivar a seguir o meu caminho e a lutar para ser cada vez melhor e chegar mais longe.

References

Abbracchio M, Burnstock G. (1994) Purinoceptors: are there families of P2X and P2Y purinoceptors? . *Pharmacol Ther* 64: (3) 445-75.

Abbracchio MP, Burnstock G, Verkhratsky A, Zimmermann H. (2009) Purinergic signalling in the nervous system: an overview. *Trends Neurosci* 32: (1) 19-29.

Abbracchio MP, Ceruti S. (2006) Roles of P2 receptors in glial cells: focus on astrocytes. *Purinergic Signalling* 2: 595–604.

Aguado F, Espinosa-Parrilla JF, Carmona MA, Soriano E. (2002) Neuronal activity regulates correlated network properties of spontaneous calcium transients in astrocytes in situ. *J Neurosci* 22: 9430-44.

Agulhon C, Fiacco TA, McCarthy KD. (2010) Hippocampal short- and long-term plasticity are not modulated by astrocyte Ca2+ signaling. *Science* 327: 1250-4.

Agulhon C, Petravicz J, McMullen A, Sweger E, Minton S, Taves S, Casper K, Fiacco T, McCarthy K. (2008) What is the role of astrocyte calcium in neurophysiology? *Neuron* 59: (6) 932-46.

Allen NJ, Barres BA. (2009) Neuroscience: Glia — more than just brain glue. *Nature* 457: 675-7.

Alloisio S, Cugnoli C, Ferroni S, Nobile M. (2004) Differential modulation of ATP-induced calcium signalling by A_1 and A_2 adenosine receptors in cultured cortical astrocytes. *Br J Pharmacol* 141: (6) 935–42.

Araque A, Martín ED, Perea G, Arellano JI, Buno W. (2002) Synaptically released acetylcholine evokes Ca2+elevations in astrocytes in hippocampal slices. *J Neurosci* 22: (7) 2443-50.

Araque A, Parpura V, Sanzgiri R, Haydon P. (1998a) Glutamate-dependent astrocyte modulation of synaptic transmission between cultured hippocampal neurons. *Eur J Neurosci* 10: (6) 2129-42.

Araque A, Parpura V, Sanzgiri RP, Haydon PG. (1999) Tripartite synapses: glia, the unacknowledged partner. *Trends Neurosci* 22: 208-15.

Araque A, Sanzgiri R, Parpura V, Haydon P. (1998b) Calcium elevation in astrocytes causes an NMDA receptor-dependent increase in the frequency of miniature synaptic currents in cultured hippocampal neurons. *J Neurosci* 18: (17) 6822-9.

Barhoumi R, Qian Y, Burghardt RC, Tiffany-Castiglioni E. (2010) Image analysis of Ca2+ signals as a basis for neurotoxicity assays: promises and challenges. *Neurotoxicol Teratol.* 32: (1)

Benech JC, Lima PA, Sotelo JR, Brown ER. (2000) Ca2+ dynamics in synaptosomes isolated from the squid optic lobe. *J Neurosci Res* 62: 840-6.

Bezzi P, Gundersen V, Galbete J, Seifert G, Steinhäuser C, Pilati E, Volterra A. (2004) Astrocytes contain a vesicular compartment that is competent for regulated exocytosis of glutamate. *Nat Neurosci* 7: (6) 613-20.

Biber K, Klotz K-N, Berger M, Gebicke-Harter PJ, Van Calker D. (1997) Adenosine A_1 receptor-mediated activation of phospholipase C in cultured astrocytes depends on the level of receptor expression. *J Neurosci* 17: (13) 4956-64.

Bradford M. (1976) A rapid and sensitive method for the quantitation of microgram quantities of protein utilizing the principle of protein-dye binding. *Analytical Biochemistry* 72: 248-54.

Burnstock G. (1972) Purinergic nerves. *Pharmacol Rev* 24: (3) 509-81.

Burnstock G. (1976) Purinergic receptors. *J Theor Biol* 62: (2) 491-503.

Burnstock G, Kennedy C. (1985) Is there a basis for distinguishing two types of P2-purinoceptor? . *Gen Pharmacol* 16: (5) 433-40.

Butt AM. (2011) ATP: A ubiquitous gliotransmitter integrating neuron–glial networks. *Seminars in Cell & Developmental Biology* 22: 205–13.

Charles A, Merrill J, Dirksen E, Sanderson M. (1991) Intercellular signaling in glial cells: calcium waves and oscillations in response to mechanical stimulation and glutamate. *Glia* 6: (6) 983-92.

Ciruela F, Casado V, Rodrigues RJ, Lujan R, Burgueno J, Canals M, Borycz J, Rebola N, Goldberg SR, Mallol J, Cortes A, Canela EI, Lopez-Gimenez JF, Milligan G, Lluis C, Cunha RA, Ferre S, Franco R. (2006) Presynaptic control of striatal glutamatergic neurotransmission by adenosine A1–A2A receptor heteromers. *J Neurosci* 26: (7) 2080 –7.

Coco S, Calegari F, Pravettoni E, Pozzi D, Taverna E, Rosa P, Matteoli M, Verderio C. (2003) Storage and release of ATP from astrocytes in culture. *J Biol Chem* 278: (2) 1354-62.

Cormier R, Mennerick S, Melbostad H, Zorumski C. (2001) Basal levels of adenosine modulate mGluR5 on rat hippocampal astrocytes. *Glia* 33: (1) 24-35.

Cornell-Bell A, Finkbeiner S, Cooper M, Smith S. (1990) Glutamate induces calcium waves in cultured astrocytes: long-range glial signaling. *Science* 247: (4941) 470-3.

Correia-de-Sá P, Ribeiro J. (1996) Adenosine uptake and deamination regulate tonic A2a receptor facilitation of evoked [3H]acetylcholine release from the rat motor nerve terminals. *Neuroscience* 73: (1) 85-92.

Correia-de-Sá P, Sebastião A, Ribeiro J. (1991) Inhibitory and excitatory effects of adenosine receptor agonists on evoked transmitter release from phrenic nerve ending of the rat. *Br J Pharmacol* 103: (2) 1614-20.

Cristóvão-Ferreira S, Navarro G, Brugarolas M, Pérez-Capote K, Vaz SH, Fattorini G, Conti F, Lluis C, Ribeiro JA, McCormick PJ, Casadó V, Franco R, Sebastião AM. (2011) Adenosine A1R-A2AR heteromers modulate GAT-1- and GAT-3-mediated GABA uptake by astrocytes. *J Neurosci*: (in press).

Dolmetsch R, Lewis R, Goodnow C, Healy J. (1997) Differential activation of transcription factors induced by Ca2+ response amplitude and duration. *Nature* 386: (6627) 855-8.

Drury A, Szent-Györgyi A. (1929) The physiological activity of adenine compounds with special reference to their action upon the mammalian heart. *J Physiol* 68: (3) 213-37.

Du F, Quian Z, Zhu L, Wu X, Qian C, Chan R, Ke Y. (2010) Purity, cell viability, expression of GFAP and bystin in astrocytes cultured by different procedures. *J Cell Biochem* 109: 30-7.

Dunwiddie TV, Diao L, Proctor WR. (1997) Adenine nucleotides undergo rapid, quantitative conversion to adenosine in the extracellular space in rat hippocampus. *J Neurosci* 17: (20) 7673–82.

Fellin T, Carmignoto G. (2004) Neurone-to-astrocyte signalling in the brain represents a distinct multifunctional unit. *J Physiol* 559: 3-15.

Fellin T, Pascual O, Gobbo S, Pozzan T, Haydon P, Carmignoto G. (2004) Neuronal synchrony mediated by astrocytic glutamate through activation of extrasynaptic NMDA receptors. *Neuron* 43: (5) 729-43.

Ferrada C, Moreno E, Casadó V, Bongers G, Cortés A, Mallol J, Canela E, Leurs R, Ferré S, Lluís C, Franco R. (2009) Marked changes in signal transduction upon heteromerization of dopamine D1 and histamine H3 receptors. *Br J Pharmacol* 157: (1) 64-75.

Ferroni S, Marchini C, Ogata T, Schubert P. (2002) Recovery of deficient cholinergic calcium signaling by adenosine in cultured rat cortical astrocytes. *J Neurosci Res* 68: (5) 615-21.

Fiacco T, McCarthy K. (2004) Intracellular astrocyte calcium waves in situ increase the frequency of spontaneous AMPA receptor currents in CA1 pyramidal neurons. *J Neurosci* 24: (3) 722-32.

Fields RD, Burnstock G. (2006) Purinergic signalling in neuron–glia interactions. *Nat Rev Neurosci* 7: (6) 423–36.

Finkbeiner S. (1992) Calcium waves in astrocytes-filling in the gaps. *Neuron* 8: (6) 1101-8.

Fischer W, Appelt K, Grohmann M, Franke H, Norenberg W, Illes P. (2009) Increase of intracelular Ca^{2+} by P2X and P2Y receptor-subtypes in cultured cortical astroglia of the rat. *Neuroscience* 160: 767–83.

Fredholm B, IJzerman A, Jacobson K, Klotz K, Linden J. (2001) International Union of Pharmacology. XXV. Nomenclature and classification of adenosine receptors. *Pharmacol Rev* 53: 527-52.

Fredholm BB, Assender JW, Irenius E, Kodama N, Saito N. (2003) Synergistic effects of adenosine A_1 and P2Y receptor stimulation on calcium mobilization and PKC translocation in DDT1 MF-2 cells. *Cell Mol Neurobiol* 23: (3) 379-400.

Fredholm BB, IJzerman AP, Jacobson KA, Linden J, Muller CE. (2011) International Union of Basic and Clinical Pharmacology. LXXXI. Nomenclature and Classification of Adenosine Receptors—An Update. *Pharmacol Rev* 63: (1) 1–34.

Frenguelli BG, Wigmore G, Llaudet E, Dale N. (2007) Temporal and mechanistic dissociation of ATP and adenosine release during ischaemia in the mammalian hippocampus. *J Neurochem* 101: 1400–13.

Fumagalli M, Brambilla R, D'ambrosi N, Volonte C, Matteoli M, Verderio C, Abbracchio MP. (2003) Nucleotide-mediated calcium signaling in rat cortical astrocytes: Role of P2X and P2Y receptors. *Glia* 43: 218-30.

Gerwins P, Fredholm BB. (1992) ATP and its metabolite adenosine act synergistically to mobilize intracellular calcium via the formation of inositol 1,4,5-trisphosphate in a smooth muscle cell line. *J Biol Chem* 267: (23) 16081-7.

Ginsborg B, Hirst G. (1971) Cyclic AMP, transmitter release and the effect of adenosine on neuromuscular transmission. *Nat New Biol* 232: (28) 63-4.

Ginsborg B, Hirst G. (1972) The effect of adenosine on the release of the transmitter from the phrenic nerve of the rat. *J Physiol* 224: (3) 629-45.

Gordon G, Baimoukhametova D, Hewitt S, Rajapaksha W, Fisher T, Bains J. (2005) Norepinephrine triggers release of glial ATP to increase postsynaptic efficacy. *Nat Neurosci* 8: (8) 1078-86.

Grynkiewicz G, Poenie M, Tsien RY. (1985) A New Generation of Ca2+ Indicators with Greatly Improved Fluorescence Properties. *J Biol Chem* 260: (6) 3440-50.

Guthrie PB, Knappenberger J, Segal M, Bennett MVL, Charles AC, Kater SB. (1999) ATP released from astrocytes mediates glial calcium waves. *J Neurosci* 19: (2) 520–8.

Halassa MM, Fellin T, Haydon PG. (2006) The tripartite synapse: roles for gliotransmission in health and disease. *Trends Mol Med* 13: (2) 54-63.

Hamilton NB, Attwell D. (2010) Do astrocytes really exocytose neurotransmitters? *Nat Rev Neurosci* 11: 227-38.

Hassinger T, Guthrie P, Atkinson P, Bennett M, Kater S. (1996) An extracellular signaling component in propagation of astrocytic calcium waves. *PNAS* 93: (23) 13268-73.

Hirase H, Qian L, Barthó P, Buzsáki G. (2004) Calcium dynamics of cortical astrocytic networks in vivo. *PLoS Biol* 2: (4) 494-9.

James G, Butt AM. (2002) P2Y and P2X purinoceptor mediated Ca^{2+} signalling in glial cell pathology in the central nervous system. *Eur J Pharmacol* 447: 247–60.

Jiménez AI, Castro E, Delicado EG, Miras-Portugal MT. (1998) Potentiation of adenosine 5'-triphosphate calcium responses by diadenosine pentaphosphate in individual rat cerebellar astrocytes. *Neurosci Lett* 246: 109–11.

Jiménez AI, Castro E, Mirabet M, Franco R, Delicado EG, Miras-Portugal MT. (1999) Potentiation of ATP calcium responses by A_{2B} receptor stimulation and other signals coupled to G_s proteins in Type-1 cerebellar astrocytes. *Glia* 26: 119-28.

Johnson I, Spence MTZ, eds. 2010. *Molecular Probes Handbook, A guide to fluorescent probes and labeling technologies*: Molecular Probes

Kang J, Jiang L, Goldman S, Nedergaard M. (1998) Astrocyte-mediated potentiation of inhibitory synaptic transmission. *Nat Neurosci* 1: (8) 683-92.

Kettenmann H, Ransom BR, eds. 2005. *Neuroglia*: Oxford University Press, Inc

Kettenmann H, Verkhratsky A. (2008) Neuroglia: the 150 years after. *Trends in Neurosciences* 31: (12) 653-9.

Khakh BS, Burnstock G. (2009) The double life of ATP *Sci Am* 301: (6) 84-92.

Knot HJ, Laher I, Sobie EA, Guatimosim S, Gomez-Viquez L, Hartmann H, Song L-S, Lederer WJ, Graier WF, Malli R, Frieden M, Petersen OH. (2005) Twenty years of calcium imaging: cell physiology to dye for. *Molecular Interventions* 5: (2) 112-27.

Koizumi S, Fujishita K, Tsuda M, Shigemoto-Mogami Y, Inoue K. (2003) Dynamic inhibition of excitatory synaptic transmission by astrocyte-derived ATP in hippocampal cultures. *PNAS* 100: (19) 11023–8.

Lopes L, Cunha R, Kull B, Fredholm B, Ribeiro J. (2002) Adenosine A(2A) receptor facilitation of hippocampal synaptic transmission is dependent on tonic A(1) receptor inhibition. *Neuroscience* 112: (2) 319-29.

Matyash V, Kettenmann H. (2010) Heterogeneity in astrocyte morphology and physiology. *Brain Research Reviews* 63: 2-10.

Michoud MC, Tao FC, Pradhan AA, Martin JG. (1999) Mechanisms of the potentiation by adenosine of adenosine triphosphate–induced calcium release in tracheal smooth-muscle cells. *Am J Respir Cell Mol Biol* 21: 30–6.

Moreno E, Hoffmann H, Gonzalez-Sepúlveda M, Navarro G, Casadó V, Cortés A, Mallol J, Vignes M, McCormick P, Canela E, Lluís C, Moratalla R, Ferré S, Ortiz J, Franco R. (2010) Dopamine D1-histamine H3 receptor heteromers provide a selective link to MAPK signaling in GABAergic neurons of the direct striatal pathway. *J Biol Chem* 286: (7) 5846-54.

Namba K, Suzuki T, Nakata H. (2010) Immunogold electron microscopic evidence of in situ formation of homo- and heteromeric purinergic adenosine A1 and P2Y2 receptors in rat brain. *BMC Res Notes* 3: (323)

Neary J, Rathbone M, Cattabeni F, Abbracchio M, Burnstock G. (1996) Trophic actions of extracellular nucleotides and nucleosides on glial and neuronal cells. *Trends Neurosci* 19: (1) 13-8.

Neary J, van Breemen C, Forster E, Norenberg L, Norenberg M. (1988) ATP stimulates calcium influx in primary astrocyte cultures. *Biochem Biophys Res Commun* 157: (3) 1410-6.

Nedergaard M. (1994) Direct signaling from astrocytes to neurons in cultures of mammalian brain cells. *Science* 263: (5154) 1768-71.

Nett WJ, Oloff SH, McCarthy KD. (2002) Hippocampal astrocytes in situ exhibit calcium oscillations that occur independent of neuronal activity. *J Neurophysiol* 87: 528-37.

Newman E, Zahs K. (1998) Modulation of neuronal activity by glial cells in the retina. *J Neurosci* 18: (11) 4022-8.

Newman EA. (2003) New roles for astrocytes: Regulation of synaptic transmission. *TRENDS in Neurosciences* 26: (10) 537-42.

Nishizaki T. (2004) ATP- and adenosine-mediated signaling in the central nervous system: Adenosine stimulates glutamate release from astrocytes via A_{2A} adenosine receptors. *J Pharmacol Sci* 94: 100-2.

Nishizaki T, Nagai K, Nomura T, Tada H, Kanno T, Tozaki H, Li X, Kondoh T, Kodama N, Takahashi E, Sakai N, Tanaka K, Saito N. (2002) A new neuromodulatory pathway with a glial contribution mediated via A(2a) adenosine receptors. *Glia* 39: (2) 133-47.

Nobile M, Monaldi I, Alloisio S, Cugnoli C, Ferroni S. (2003) ATP-induced, sustained calcium signalling in cultured rat cortical astrocytes: evidence for a non-capacitative, $P2X_7$-like-mediated calcium entry. *FEBS Lett* 538: 71-6.

O'Kane E, Stone T. (1998) Interaction between adenosine A1 and A2 receptor-mediated responses in the rat hippocampus in vitro. *Eur J Pharmacol* 362: (1) 17-25.

Ogata T, Nakamura Y, Schubert P. (1996) Potentiated cAMP rise in metabotropicallv stimulated rat cultured astrocytes by a Ca2+-related A1/A2 adenosine receptor cooperation. *Eur J Neurosci* 8: 1124-31.

Ogata T, Nakamura Y, Tsuji K, Shibata T, Kataoka K, Schubert P. (1994) Adenosine enhances intracellular Ca2+ mobilization in conjunction with metabotropic glutamate receptor activation by t-ACPD in cultured hippocampal astrocytes. *Neurosci Lett* 170: (1) 5-8.

Oliver AE, Baker GA, Fugate RD, Tablin F, Crowe JH. (2000) Effects of temperature on calcium-sensitive fluorescent probes. *Biophysical Journal* 78: 2116–26.

Paredes RM, Etzler JC, Watts LT, Lechleiter JD. (2008) Chemical calcium indicators. *Methods* 46: (3) 143–51.

Parpura V, Basarsky T, Liu F, Jeftinija K, Jeftinija S, Haydon P. (1994) Glutamate-mediated astrocyte-neuron signalling. *Nature* 369: (6483) 744-7.

Pasti L, Pozzan T, Carmignoto G. (1995) Long-lasting changes of calcium oscillations in astrocytes. A new form of glutamate-mediated plasticity. *J Biol Chem* 270: (25) 15203-10.

Pasti L, Volterra A, Pozzan T, Carmignoto G. (1997) Intracellular calcium oscillations in astrocytes: a highly plastic, bidirectional form of communication between neurons and astrocytes in situ. *J Neurosci* 17: (20) 7817-30.

Peakman M, Hill S. (1994) Adenosine A2B-receptor-mediated cyclic AMP accumulation in primary rat astrocytes. *Br J Pharmacol* 111: 191-8.

Peakman M, Hill S. (1996) Adenosine A1 receptor-mediated inhibition of cyclic AMP accumulation in type-2 but not type-1 rat astrocytes. *Eur J Pharmacol* 306: (1-3) 281-9.

Pearce B, Murphy S, Jeremy J, Morrow C, Dandona P. (1989) ATP-evoked Ca2+ mobilisation and prostanoid release from astrocytes: P2-purinergic receptors linked to phosphoinositide hydrolysis. *J Neurochem* 52: (3) 971-7.

Perea G, Araque A. (2005) Properties of synaptically evoked astrocyte calcium signal reveal synaptic information processing by astrocytes. *J Neurosci* 25: (9) 2192–203.

Perea G, Araque A. (2006) Synaptic information processing by astrocytes. *J Physiol* 99: (2-3) 92-7.

Perea G, Araque A. (2010) Glia modulates synaptic transmission. *Brain Research Reviews* 63: 93-102.

Pilitsis JG, Kimelberg HK. (1998) Adenosine receptor mediated stimulation of intracellular calcium in acutely isolated astrocytes. *Brain Res* 798: 294–303.

Porter J, McCarthy K. (1995) Adenosine receptores modulate [Ca2+]i in hippocampal astrocytes in situ. *J Neurochem* 65: (4) 1515-23.

Porter J, McCarthy K. (1996) Hippocampal astrocytes in situ respond to glutamate released from synaptic terminals. *J Neurosci* 16: (16) 5073-81.

Ribeiro JA, Sebastião AM, de Mendonça A. (2003) Adenosine receptors in the nervous system: pathophysiological implications. *Prog Neurobiol* 68: 377–92.

Robitaille R. (1998) Modulation of synaptic efficacy and synaptic depression by glial cells at the frog neuromuscular junction. *Neuron* 21: (4) 847-55.

Rochon D, Rousse I, Robitaille R. (2001) Synapse-glia interactions at the mammalian neuromuscular junction. *J Neurosci* 21: (11) 3819-29.

Rose CR, Blum R, Pichler B, Lepier A, Kafitz KW, Konnerth A. (2003) Truncated TrkB-T1 mediates neurotrophin-evoked calcium signalling in glia cells. *Nature* 426:

Rudolf R, Mongillo M, Rizzuto R, Pozzan T. (2003) Looking forward to seeing calcium. *Nat Rev Mol Cell Biol* 4: 579-86.

Sáez J, Connor J, Spray D, Bennett MV. (1989) Hepatocyte gap junctions are permeable to the second messenger, inositol 1,4,5-trisphosphate, and to calcium ions. *Proc Natl Acad Sci* 86: (8) 2708-12.

Salm A, McCarthy K. (1990) Norepinephrine-evoked calcium transients in cultured cerebral type 1 astroglia. *Glia* 3: (6) 529-38.

Saura J. (2007) Microglial cells in astroglial cultures: a cautionary note. *J Neuroinflammation* 4: (26)

Scemes E, Giaume C. (2006) Astrocyte calcium waves: what they are and what they do. *Glia* 54: (7) 716–25.

Sebastião A, Ribeiro J. (1996) Adenosine A2 receptor-mediated excitatory actions on the nervous system. *Prog Neurobiol* 48: (3) 167-89.

Sebastião AM, Ribeiro JA. (2000) Fine-tuning neuromodulation by adenosine. *TiPS* 21: 341-6.

Sebastião AM, Ribeiro JA. (2009a) Adenosine receptors and the central nervous system. *Handb Exp Pharmacol* 193: 471-534.

Sebastião AM, Ribeiro JA. (2009b) Tuning and fine-tuning of synapses with adenosine. *Curr Neuropharmacol* 7: 180-94.

Toms N, Roberts P. (1999) Group 1 mGlu receptors elevate [Ca2+]i in rat cultured cortical type 2 astrocytes: [Ca2+]i synergy with adenosine A1 receptors. *Neuropharmacology* 38: (10) 1511-7.

Tonazzini I, Trincavelli ML, Storm-Mathisen J, Martini C, Bergersen LH. (2007) Co-localization and functional cross-talk between A1 and P2Y1 purine receptors in rat hippocampus. *Eur J Neurosci* 26: 890–902.

Tsien R. (1981) A non-disruptive technique for loading calcium buffers and indicators into cells. *Nature* 290: (5806) 527-8.

Tsien RY. (1980) New calcium indicators and buffers with high selectivity against magnesium and protons: design, synthesis, and properties of prototype structures. *Biochemistry* 19: 2396-404.

Vainio M, Tornquist K. (2000) The role of adenosine A1 receptors in the ATP-evoked Ca^{2+} response in rat thyroid FRTL-5 cells. *Eur J Pharmacol* 390: 43–50.

Van Calker D, Müller M, Hamprecht B. (1979) Adenosine regulates via two different types of receptors, the accumulation of cyclic AMP in cultured brain cells. *J Neurochem* 33: 999-1005.

Venance L, Stella N, Glowinski J, Giaume C. (1997) Mechanism involved in initiation and propagation of receptor-induced intercellular calcium signaling in cultured rat astrocytes. *J Neurosci* 17: (6) 1981-92.

Verkhratsky A, Orkand RK, Kettenmann H. (1998) Glial Calcium: Homeostasis and Signaling Function. *Physiological Reviews* 78: (1)

Wang X, Lou N, Xu Q, Tian G, Peng W, Han X, Kang J, Takano T, Nedergaard M. (2006) Astrocytic Ca2+ signaling evoked by sensory stimulation in vivo. *Nat Neurosci* 9: (6) 816-23.

Yoshioka K, Hosoda R, Kuroda Y, Nakata H. (2002) Hetero-oligomerization of adenosine A1 receptors with P2Y1 receptors in rat brains. *FEBS Lett* 531: (2) 299-303.

Zhang J, Wang H, Ye C, Ge W, Chen Y, Jiang Z, Wu C, Poo M, Duan S. (2003) ATP released by astrocytes mediates glutamatergic activity-dependent heterosynaptic suppression. *Neuron* 40: 971–82.

Zhang Z, Chen G, Zhou W, Song A, Xu T, Luo Q, Wang W, Gu X, Duan S. (2007) Regulated ATP release from astrocytes through lysosome exocytosis. *Nat Cell Biol* 9: (8) 945-53.